CHARACTERIZING THE INFLUENCE OF SOIL BULK DENSITY AND CLIMATE FACTORS ON WOOD QUALITY IN DOUGLAS-FIR TREES

A Dissertation

Presented in Partial Fulfillment of the Requirements for the

Degree of Doctor of Philosophy

with a

Major in Natural Resources

in the

College of Graduate Studies

University of Idaho

by

Carl D. Morrow

December 2013

Major Professor: Thomas Gorman, Ph.D.

Authorization to Submit Dissertation

This dissertation of Carl D. Morrow, submitted for the degree of Doctor of Philosophy with a major in Natural Resources and titled “Characterizing the Influence of Soil Bulk Density and Climate Factors on Wood Quality in Douglas-Fir Trees," has been reviewed in final form. Permission, as indicated by the signatures and dates given below, is now granted to submit final copies to the College of Graduate Studies for approval.

Major Professor: _____Date_____
Dr. Thomas Gorman

Committee Members: _____Date_____
Dr. Armando McDonald

_____Date_____
Dr. Steven Shook

_____Date_____
Dr. Mark Coleman

Department Administrator: _____Date_____
Dr. Anthony Davis

Discipline's College Dean: _____Date_____
Dr. Kurt Pregitzer

Final Approval and Acceptance by the College of Graduate Studies:

_____Date_____
Dr. Jie Chen

Abstract

The percentage of an annual ring composed of high density latewood measured using the threshold latewood demarcation method is commonly reported as a descriptor of both the annual ring formation process and the quality of the wood produced. Recently developed methods have been reported to provide more consistent estimates of latewood in trees exhibiting high intra-ring variability; but there is little published regarding the anatomy at the transition from earlywood (EW) to latewood (LW), and the ability of these alternative methods to predict mechanical properties. These alternative measures of latewood may be more consistent, but without an understanding of the anatomy at the EW-LW transition selected by these alternative methods, the interpretation of the latewood percentages returned by these methods is not meaningful. An assessment of the ability of these alternative latewood measures to predict physical and mechanical properties would further define the value of these alternative latewood measurement methods.

In this paper, we compared the threshold latewood method (TLWP), an inflection based latewood method (ILWP), and a polynomial based latewood method (PLWP) in terms of the region selected as the EW-LW transition, how they measured tree response to environment, and how well they predicted mechanical properties.

We found that in mature suppressed Douglas-fir, ILWP and PWLP were not well correlated with average density (AVGDEN), but that the difference between TLWP and ILWP or PLWP was positively correlated with AVGDEN. Microscopy at the EW-LW transition points showed that the threshold method selected a transition point near Mork's definition of latewood and that the inflection and polynomial methods targeted the region in which the cell wall thickness and lumen diameter changed most rapidly, but exhibited a systematic bias in the location chosen based on AVGDEN.

We studied the differences in TLWP, PLWP, ILWP, and AVGDEN between suppressed Douglas-fir growing on low and high bulk density soils. Analyzing the characteristics of the annual rings over 30 years, we found differences between the groups for all measures that were consistent with the hypothesized difference predicted by the Least Limiting Water Range concept. Trees grown on low bulk density soils had significantly higher AVGDEN and latewood using all measures, but all the measures suggested similar differences.

Finally, we studied the ability of AVGDEN, TLWP, PLWP, and ILWP to predict Modulus of Elasticity (MOE) and Modulus of Rupture (MOR) in small clear samples and the matching high grade 2x4s. We found that AVGDEN and TLWP were better predictors for small clear properties, but PLWP and ILWP had some predictive ability. All measures were better predictors of MOR in the small clears and MOE in the 2x4s. The results of the three studies presented form a basis with which to interpret ILWP and PLWP in the context of both tree response to the environment and the mechanical properties of the wood in Douglas-fir.

Acknowledgements

My heartfelt thanks go to Dr. Tom Gorman for his guidance during the course of this research and the personal and professional advice he has shared, Dr. Armando McDonald for dragging me kicking and screaming into an expanded understanding of wood science, Dr Steve Shook for his advice and guidance on this paper and other projects, and Dr. Mark Coleman for helping improve the quality of this document. I am indebted to the Coalition for Advanced Structures for funding this research and my studies at the University of Idaho. I thank the work-studies that helped with this research, and the graduate students of the RMAT program who have been a constant source of inspiration and support. Finally, thanks to my wife, Adrienne, for supporting a deadbeat graduate student without complaint.

Table of Contents

List of Figures

List of Tables

Chapter One
Introduction

Problem statement

Latewood proportion is most frequently reported as the percent of an annual ring that exceeds a given threshold density. Studies reporting latewood period can be broken down into two general groups: 1) Studies that summarize one or more physical properties of the xylem with a single measurement and 2) studies that measure the response of the tree to the environment. Studies reporting the relationship between latewood percentage and mechanical properties focus on latewood percentage as a proxy for density and other correlated characteristics (e.g. maturity or microfibril angle) to predict mechanical properties. To pose this as a question: How does this component of density and other characteristics predict mechanical properties? Studies regarding changes in latewood percentage due to treatments or events use latewood as a proxy measurement to describe the physiological processes at work during xylem formation within the annual ring of the tree. In other words: How did the xylogenic process respond to the stimuli being studied? It is reasonable to ask if these two questions could be answered using the same measure of latewood.

Background

Formation and measurement of latewood

During the xylem formation process in conifers the cambial initials must pass through three steps to become mature xylem: 1) a division step, 2) an enlargement step, and 3) a maturation or densification step (Wilson et al. 1966). Cuny et al. (2012 ; 2013) liken the process to a series of three connected pools in which division, enlargement, and densification occur and the duration a tracheid spends in any pool determines its properties. Upon division from the cambial initial, the newly formed xylem begins the radial enlargement process. The radial diameter of a forming tracheid is determined by the rate and duration of the expansion process. Research in Douglas-fir suggests that

both the rate and duration change seasonally to produce wide tracheids in the early growing season and narrowing tracheids as the season progresses (Dodd and Fox 1990). Densification occurs as the secondary cell walls of the tracheid thicken. The duration of the cell wall thickening stage seems to be the primary determinant of the degree of densification as the rate of cell wall deposition remains relatively constant (Dodd and Fox 1990). The duration of the wall thickening process peaks near the end of the growing season leading to increasing density toward the end of the annual ring. The maturation process ends with the death of the tracheid and assumption of water conduction (Dodd and Fox 1990). The process of tracheid development gives rise to wide and thin-walled earlywood with low density early in the season and narrower thick-walled latewood with higher density later in the season.

The resulting annual ring is therefore a record of the duration and rates of expansion and cell wall deposition that produced an annual ring as well as the external factors that can manipulate them. Precipitation, heat, drought, fertilization, thinning, and a host of other variables can manipulate the tracheid formation process to produce different ratios of earlywood to latewood and rings of varied density (Jozsa and Brix 1989; Antony et al. 2009; Gonzalez-Benecke et al. 2010; Kantavichai et al. 2010). Measures of latewood proportion and the density of the resulting earlywood and latewood can be used to infer timing and intensity of seasonal changes in the xylogenic process.

The terms earlywood and latewood and the point in the annual ring that separates them have no universally accepted definition or standard. Mork's definition (Mork 1928) is one of the most commonly cited, and defines the latewood transition point as the point in the annual ring in which the shared wall of adjacent tracheids is greater than twice their lumen diameter Many variations on Mork's definition have been reported (reviewed in Creber and Chaloner 1984) but they all require extensive microscopic analysis. The introduction of X-ray densitometers opened up a new avenue of annual ring investigation, and was followed quickly with the development of the threshold method. Threshold methods declare the latewood transition to be the point at which the annual ring profile

crosses a set density value, frequently at a density that approximates Mork's definition (Polge 1978). The region of the annual ring that is less dense is considered earlywood, and the region that is denser is considered latewood (Polge 1978, Creber and Chaloner 1984). Whether by exposure of X-ray sensitive film (e.g. Polge 1978) or more modern X-ray detectors (e.g. Clark et al. 2006), the threshold method can be applied quickly and easily, and has been shown to be well correlated to average wood density (Lachenbruch et al. 2010; El-Kassaby et al. 2011).

A presupposition of the use of the threshold latewood method is that the latewood transition occurs at the same density for all trees or rings. This definition may be useful if the latewood percentage is being used as a substitute for density, but may not provide a consistent evaluation of the xylogenic process mentioned previously if the researcher is interested in measuring tree response. As Koubaa et al. (2005) and Antony et al. (2010) have noted for black spruce and loblolly pine, the threshold method might not adequately describe the wood formation process for both juvenile wood and mature wood simultaneously. They demonstrated that two dynamic latewood methods gave more consistent measures of latewood percentage between juvenile and mature wood than the threshold method.

Dynamic latewood methods use changes in the density within rings to determine a point which represents the transition from earlywood to latewood. The method developed by Koubaa et al. (2005) used polynomials to fit a curve to the density/position profile and found the roots of the second derivative that best met a series of selection rules. The inflection method reported by Antony et al. (2010) used smoothed splines fit to the density/position profile and chose the inflection point as the second derivative of the spline crossed through zero during the transition from earlywood to latewood. The use of the slope of the density/position curve in the annual ring density profile makes it possible to identify a latewood transition point regardless of the average density of the species or individual.

Assessing variation in ring characteristics through time

To assess the ability of any of the latewood methods to measure physiological changes in trees due to climate or treatments, the annual ring characteristics of multiple trees must be assessed, preferably over multiple years of growth. The study of serial data collected from the same individuals over time presents a unique set of challenges (Ott and Longnecker 2001). Many of the more commonly used statistical tools require an assumption of independence between samples, in that the results of one sample has no correlation with the results of another sample. In addition, there is an assumption of constant variance between samples, which requires the degree of random variation to remain constant from sample to sample. In the study of annual rings of trees, the independence assumption would equate to the assumption that the events (e.g. climatic, cultural, or biological) in years past had no influence on this year's growth (covariance between years equals zero) or that the events of 100 years ago has the same influence as last year's event (covariance between years equals a constant). The assumption of constant variance would be interpreted to require that the random differences are constant through time and that all years would exhibit the same degree of dispersion (Fitzmaurice et al. 2011). A basic familiarity with tree growth and physiology would suggest that applying these assumptions to serial data would be spurious at best, or even misleading.

Violations of independence and constant variance assumptions can make it difficult to assess the significance of the effects being measured (Oehlert 2000). Violations of the independence assumption lie in the fact that although our estimates of the treatment effect remain unbiased, our estimate of the variation about the averages of the treatments is no longer unbiased. Because the responses of each of our samples are correlated to one another, each additional sample no longer represents a "new" piece of information. The analysis may reveal that there is a numerically large difference between treatments, we are confident in that result, but we can't accurately assess the significance of that difference using standard practices. Violations of the constant variance assumption lead to variation in the rates at which we reject or accept the null especially in

unbalanced datasets. Issues with nonconstant variance stem from the fact that we need to use the same estimate of error variance to test the significance of different groups, so when one small group has a very small associated error and a larger second group has a high degree of error, we overestimate the amount of error for the first group resulting in a conservative test, and underestimate the amount of error in the second group resulting in a liberal test. (Oehlert 2000).

Repeated measures methodologies provide a means to address the violations of independence and constant variance assumptions that are inherent in repeated measures of the same individuals over time. Repeated measures techniques use a much more complicated framework describing variation within (and in some cases between) individuals over time. By allowing observations close in time to be more similar and observations separated by more time to be less similar, repeated measures models can give a more valid estimation of the variation within the samples, and allows more accurate tests for significance. Likewise, allowing the variance within individuals to change through time permits more accurate assessments of significance. However, if accurately modeling the samples through time requires a lot of parameters (i.e. there is no general pattern or it is very complex), when we try to test the significance of elements of our model, we will find that it takes a larger difference in treatments to register the same level of significant difference.

Latewood as a measure of wood quality

Wood quality is a primary driver of the value of a given tree or species and determines the end uses to which it may be applied (Bowyer, 2003). This paper will focus on the quality attributes desirable for structural lumber i.e. strength and stiffness, but other properties may be desirable based on the end use of the product. The numbers of characteristics that determine wood quality are vast and subject to variation at any spatial level from species range down to individual annual rings (Larson et al. 2001). The simultaneous modeling of the entire suite of quality limiting characteristics and the factors that influence them is not currently a realistic proposition. However, researchers may

measure a few key factors associated with wood quality and infer the effect on resulting end products.

One of the earliest and most cited characteristics associated with wood quality is the density of a sample of lumber (Newlin and Wilson 1917; Markwardt and Wilson 1935; Doyle 1968; Lachenbruch et al. 2010). The correlations of density to mechanical properties has been reported frequently and the basis of the correlations stem from the fact that the density of the material comprising the walls of virtually all wood is constant (USDA 2002). The density of a wood sample is therefore a measure of the volume of the sample occupied by solid wood. If a simplified model of wood under bending is used, with tracheids represented by a collection of slender pipes of uniform outside diameter and differences in density are manifested as thicker or thinner pipe walls, engineering mechanics suggest that the thickening cell walls will increase the transformed moment of inertia (Bodig and Jayne 1982). If the Modulus of Elasticity (MOE) and Modulus of Rupture (MOR) of the cell wall material are held constant, greater loads will be required to reach the same midspan displacement and bending stress as density increases. At the macroscopic scale, we will report specimens with higher density as exhibiting higher MOE and MOR. This model can be expanded to incorporate all manner of physical characteristics, but density remains one of the most important properties.

Latewood percentage has also been correlated with mechanical properties (Biblis et al. 2004; Choi 1986; Lachenbruch et al. 2010). The influence of latewood proportion on mechanical properties has at least two components. First, latewood percentage is well correlated with density (Bower et al. 2003; USDA 2002) because latewood percentage (especially threshold latewood percentage) relates the relative amount of high density latewood to the amount of lower density earlywood in the annual ring. The correlation may strengthen or weaken depending on the density of the earlywood and latewood components, but it is one of the primary sources of variability in annual ring density (Lachenbruch et al. 2010). Microfibril Angle (MFA) of the cellulose fibrils in the secondary cell wall

of fibers and tracheids has been shown to be negatively correlated with mechanical properties, especially in juvenile wood (Groom et al. 2002a; 2002b; Hein and Lima 2012; Yang and Evans 2003). Within an annual ring, the MFA of latewood is generally lower than the MFA of earlywood (Lachenbruch et al. 2010, Groom et al. 2002b). The proportion of latewood in an annual ring therefore is related to the average MFA for that ring.

Research Objectives

Chapter Two

There has been little research published concerning the correlations in latewood percentage measured between the threshold, inflection, and polynomial methods with average ring density. There has also been limited research regarding the anatomy of the earlywood/latewood transition point chosen by the inflection and polynomial methods. In order to use the results of the inflection and polynomial methods to predict mechanical properties, a better understanding of their correlations to the threshold method and average density is required. In order to use the inflection and polynomial methods to assess tree response to the environment, the consistency of the anatomy at the latewood transition point assigned by the inflection and polynomial methods must be determined.

Objective 1: Assess the relationship between the inflection and polynomial methods, with threshold latewood percentage and average density.

Objective 2: Assess the anatomy at the latewood transition point identified by the inflection and polynomial methods.

Chapter Three

In a prior paper (Morrow et al. 2013) we found a nondestructive measure of stiffness varied significantly between trees grown on low and high bulk density soils. Based on this result we hypothesized that a specific climate-soil moisture-root relationship could affect the xylogenic

process. In Chapter Three, we used a repeated measures analysis to test for systematic differences in annual ring characteristics between soil bulk density (SBD) groups.

Objective 1: Test for differences between SBD groups using the 1) threshold, 2) inflection, 3) polynomial latewood percentages, and 4) average ring density in a repeated measures analysis.

Objective 2: Determine if annual ring differences between SBD groups were consistent with the a priori hypothesis.

Objective 3: Assess the agreement between latewood measures with respect to differences found between SBD groups.

Chapter Four

We found no data published concerning the correlations between wood quality and the inflection and polynomial latewood methods. In Chapter Four, we compared the abilities of 1) average density, 2) the threshold method, 3) the inflection method, and 4) polynomial methods, and average density to predict the MOE and MOR of small clear samples and their matched high grade 2x4s.

Objective 1: Compare the ability of the inflection and polynomial method to predict mechanical properties with the more commonly used threshold latewood and average density.

Objective 2: Assess the correlation of each wood density measure with MOE and MOR in both small clear samples and full size 2x4s.

References

Antony F, Jordan L, Daniels RF, Schimleck LR, Clark A, 2009. Hall DB. Effect of midrotation fertilization on growth and specific gravity of loblolly pine. Can. J. For. Res. 39(5): 928-935.

Biblis E, Meldahl R, Pitt D, Carino HF. 2004. Predicting flexural properties of dimension lumber from 40-year-old loblolly pine plantation stands. Forest Product Journal 54(12): 109-112.

Bodig J, Jayne B. 1982. Mechanics of Wood and Wood Composites. Van Nostrand Reinhold Company Inc. New York, New York. 712p.

Bowyer JL, Shmulsky R, Haygreen JG. 2003. Forest Products and Wood Science: An Introduction. Iowa State Univeristy Press. Ames, Iowa. 554p.

Choi ASC. 1986. Correlation between mechanical strength of wood and annual ring characteristics of Douglas-fir juvenile and mature wood. Master of Science Thesis. Oregon State University, OR. 1986, 84p.

Clark A, Daniels RF, Jordan L. 2006. Juvenile/mature wood transition in loblolly pine as defined by annual ring specific gravity, proportion of latewood, and microfibril angle. Wood and Fiber Science 38(2): 292-299

Cuny HE, Rathberger CBK, Lebourgeois F, Fortin M, Fournier M. 2012. Life strategies in intra-annual dynamics of wood formation: example of three conifer species in a temperate forest in north-east France. Tree Physiology 32(5): 612-625.

Cuny HE, Rathburger CBK, Kiesse TS, Hatman FP, Barbeito I, Fournier M. 2013. Generalized additive models reveal the intrinsic complexity of wood formation dynamics. Journal of Experimental Botany 64(7): 1983-1994.

Creber GT, Chaloner WG. 1984. Influence of environmental factors on the wood structure of living and fossil trees. Botanical Review 50(4): 357-448

Dodd RS, Fox P. 1990. Kinetics of tracheid differentiation in Douglas-fir. Annals of Botany 65(6): 649-657.

Doyle DV. 1968. Properties of No. 2 dense kiln-dried southern pine dimension lumber. USDA FPL-RP-96. Madison, WI: U.S. Department of Agriculture, Forest Service, Forest Products Laboratory. 24p.

El-Kassaby YA, Mansfield M, Isik F, Stoehr M. 2011. In situ wood quality assessment in Douglas-fir. Tree Genetics and Genomes 7(3): 553-561.

Fitzmaurice GM, Laird NM, Ware JH. 2011.Applied Longitudinal Analysis-2nd ed. John Wiley & Sons Inc., Hoboken, New Jersey. 1211p.

Gonzalez-Benecke CA, Martin TA, Clark A, Peter GF. 2010. Water Availability and genetic effects on wood properties of loblolly pint (*Pinus taeda*). Can. J. For. Res. 40(12): 2262-2277.

Groom L, Mott L, Shaler S. 2002a. Mechanical properties of individual southern pine fibers. PartI. Determination and variability of stress-strain curves with respect to tree height and juvenility. Wood and Fiber Science 34(1): 14-27.

Groom L, Mott L, Shaler S. 2002b. Mechanical properties of individual southern pine fibers. Part III-Global relationships between fiber properties and fiber location within an individual tree. Wood and Fiber Science 34(2): 238-250.

Hein PRG, Lima JT. 2012. Relationships between microfibril angle, modulus of elasticity and compressive strength in *Eucalyptus* wood. Maderas. Ciencia y Tecnologia 14(3):267-274.

Jozsa LA, Brix H. 1989. The effects of thinning on wood quality of a 24-year-old Douglas-fir stand. Can. J. For. Res. 19(9): 1137-1145.

Kantavichai R, Briggs D, Turnblom E. 2010. Modeling effects of soil, climate, and silviculture on growth ring specific gravity of Douglas-fir on a drought-prone site in Western Washington. Forest Ecology and Management 259(6): 1085-1092.

Koubaa A, Zhang SYT, Makni S. 2002. Defining the transition from earlywood to latewood in black spruce based on intra-ring wood density profiles from X-ray densitometry. Ann. For. Sci. 59(5): 511-518.

Larson PR, Kretschmann DE, Clark A, Isebrands JG. 2001. Formation and properties of juvenile wood in southern pine: A synopsis. Gen Tech. Rep. FPL-GTR-129. Madison, WI: U.S. Department of Agriculture, Forest Service, Forest Products Laboratory. 42p

Lachenbruch B, Johnson GR, Downes GM, Evans R. 2010. Relationships of density, microfibril angle, and sound velocity with stiffness and strength in mature wood of Douglas-fir. Can. J. For. Res 40(1):55-64.

Markwardt LJ, Wilson TRC. 1935. Strength and related properties of woods grown in the United States. USDA FPL Tech Bul FPL-TB-479. Madison WI: U.S. Department of Agriculture, Forest Service, Forest Products Laboratory. 115p. Retrieved from http://naldc.nal.usda.gov/download/CAT86200473/PDF.

Morrow CD, Gorman TM, Evans JW, Hatfield CA. 2013. Prediction of wood quality in small-diameter Douglas-fir using site and stand characteristics. Wood and Fiber Science. 45(1):49-61.

Newlin JA, Wilson TRC. 1917. Mechanical properties of woods grown in the United States. USDA FPL-PP-556. Madison WI: U.S. Department of Agriculture, Forest Service, Forest Products Laboratory.47p. Retrieved from http://archive.org/details/mechanicalproper556newl.

Oehlert GW. 2000. A first course in design and analysis of experiments. W.H. Freeman and Company. New York, New York. 659p.

Ott RL, Longnecker M. 2001. An introduction to statistical methods and data analysis-5th edition. Wadsworth Group. Pacific Grove, CA. 1152p.

Polge H. 1978. Fifteen years of wood radiation densitometry. Wood Sci. Technol. 12(3): 187-196.

Wilson BF, Wodzicki TJ, Zahner R. 1966. Differentiation of cambial derivatives: proposed terminology. Forest Science 12(4): 438-440.

Yang JL, Evans R. 2003. Prediction of MOE of eucalypt wood from microfibril angle and density. Eur. J. Wood Prod. 61(6):449-452.

Chapter Two
Comparison of methods to determine latewood percentage in suppressed Douglas-fir

Abstract

Latewood methods such as the threshold or Mork's methods have been used extensively in forest research, but may not provide consistent results in all trees. Alternative methods of latewood measurement have been reported to be more consistent, but the lack of published studies of the anatomy at the earlywood/latewood transition currently limits their interpretation. To assess these alternative methods, radial strips from 45 small-diameter Douglas-fir were analyzed using X-ray densitometry to test the performance of three latewood measurement methods: a static threshold method, a dynamic inflection method, and a dynamic polynomial method. The analysis indicated that the static and dynamic measures seemed to be only moderately correlated ($R^2 \approx 0.5$) , and the difference between methods was correlated to average ring density ($R^2 \approx 0.6$). The threshold measurement was by far the most highly correlated to average ring density ($R^2=0.67$) while the inflection and polynomial methods were poorly correlated with average density ($R^2=0.23$, $R^2=0.16$). Anatomical measurements from a subset of the annual rings indicated the position identified by the 500kg/m^2 threshold measurement was the most consistent, and chose a point very close to Mork's definition of latewood. The ratio of radial lumen diameter to the radial cell wall thickness at the transition point selected by the polynomial method could be predicted with the same level of error (RMSE=0.47 49μm/μm) as that of the threshold method (RMSE =0.49μm/μm) with the incorporation of average ring density. In the subset of rings used from which the anatomical data was derived, the dynamic measurements seemed to systematically underestimate the position of greatest lumen and cell wall thickness change in high density rings, and vice versa. The most likely source of these errors is the geometry of the density profiles, and the linear nature of the errors suggests they

could be reduced using a linear correction based on average ring density. The use of several methods simultaneously may provide researchers an inexpensive opportunity broaden the scope of xylem formation research.

Introduction

The annual rings of a tree contain valuable information regarding the quality of the wood contained within that tree and a record of the tree's response to the environment. The wood quality implications of density are well documented, and one of the most important contributors to density is the proportion of latewood produced. The calculation of the average density of an annual ring or a wood sample is intuitive, however, a variety of methodologies exist to classify portions of an annual ring into earlywood and latewood. One of the most frequently cited is Mork's definition (Mork 1928) in which latewood is generally described as those tracheids in which the thickness of the shared cell wall is greater than twice the diameter of the tracheid's lumen. The advent of commercially available X-ray densitometers has led to the frequent use of the threshold method in which latewood is assigned as those tracheids with a density above the threshold value (Polge 1978; Lasserre et al. 2009; Schneider et al. 2008; Clark et al. 2004; Antony et al. 2011). Density values in the range of 400kg/m^3 to 550 kg/m^3 are frequently used but the location of the transistion point defined using the threshold method can vary greatly with that defined by Mork's Index (Koubaa et al. 2002). Threshold measurements are generally simple to implement (excepting complications such as false rings or other aberrant growth patterns) but may not be the most effective measure of the physiological variations expressed in the density profile of an annual ring such as juvenile rings (Koubaa el al. 2002).

Alternative methodologies use the shape and characteristics of each annual ring density profile to determine the transition from earlywood to latewood. The intent of these techniques is to decouple the measurement of latewood percentage from the average density of the ring using a defined set of

rules to divide the annual rings into earlywood and latewood. The use of mean ring density (e.g. Dalla-Salda et al. 2011) or the midpoint density (e.g. Bower et al. 2005) as the demarcation between earlywood and latewood are simple examples of dynamic measures because they are not tied to any particular density or anatomical measurement. More complex dynamic latewood determination techniques focus on the degree of densification from tracheid to tracheid. An example used in prior research (Pernestal et al. 1995) was to calculate the slope of the density profile in the earlywood-latewood transition region and find the point at which the slope reached its maximum value, or the second derivative of the density profile slope equaled zero. The process can be automated by smoothing the individual data points and setting rules to ensure noise or density aberrations do not falsely trigger the algorithm (Pernestal et al. 1995; Koubaa et al. 2002, Antony et al. 2011). The definition of the earlywood-latewood transition would therefore shift from a fixed density threshold or anatomical measurement to a dynamic measure of density change in adjacent tracheids in the annual ring. Koubaa et al. introduced the idea of fitting a polynomial to the density profile, and calculate roots of the second derivative of the polynomial to identify the point at which the ring transitions from earlywood to latewood. The use of a well fit polynomial provides two advantages. First, the polynomial acts to smooth the raw data, and secondly, the identification of roots of the polynomial provide well defined points that can be selected as the transition from earlywood to latewood using standardized rules (Koubaa et al. 2002).

The application and comparison of several of these demarcation methodologies simultaneously may provide several advantages. Firstly, the use of a dynamic measure of earlywood-latewood transition may provide a means to compare the response of trees with varying average densities in a more consistent manner. By decoupling the transition from earlywood to latewood from a defined density, the dynamic measures seek to identify the point at which the difference in density from tracheid to tracheid is greatest. Similar methodologies have been used in place of traditional species-specific threshold definitions to develop more robust models of the transition from juvenile to mature wood

using segmented regression (Clark et al. 2006; Helinska-Raczkowska and Fabisiak 1999; Kouba et al. 2005; Wang et al. 2012). These dynamic methods are flexible enough to be applied across a wide range of individuals within and between species. Secondly, if the dynamic measures could accurately identify the region of the annual ring that expresses the greatest rate of anatomical change, it may be possible to correlate major shifts in moisture stress and xylem formation to a relatively inexpensive dynamic latewood measurement. Thirdly, by combining the individual methods, it may be possible to expedite the quality control process for large data sets in a systematic and partially automated manner that focuses researcher time on the most questionable or unusual rings.

Dynamic earlywood-latewood demarcation are difficult to interpret. It is not readily apparent which anatomical features of the annual ring are identified by the inflection and polynomial techniques, how closely the dynamic measures are related to average ring density, or how the resulting values may be interpreted and used. The objective of this study was to compare threshold, inflection, and polynomial latewood demarcation techniques in terms of their correlation to one another, correlation to average density, and the anatomy at the selected transition points.

Methods

In the summer of 2007, stand measurements and increment cores were collected from 297 small diameter Douglas-fir trees in mixed age stands in western Montana (Morrow et al. 2013) in an effort to develop models to predict the trees' stiffness. Increment cores from 45 trees of these were randomly selected for X-ray analysis. A summary of the tree and stand characteristics of the source trees for the increment cores studied here is given in Table 2.1. The increment cores were glued between wooden strips and ripped on a table saw with twin blades to produce a 1.5 mm strip from the center of the increment core. The radial strips were allowed to equilibrate to ambient laboratory conditions then scanned using a QTM-QTRX X-ray densitometer at 0.02 mm step intervals. The absorption coefficient used by the densitometer was established by finding the best-fit value for

predicting the density of 24 Douglas-fir samples of known density, which ranged in density from 440 kg/m3 to 700 kg/m3. Cracked or otherwise damaged rings were omitted from the final analysis, as were rings suspected to contain compression wood and the rings closest to the pith when the pith was not centered in the radial strip.

Table 2.1. Tree and stand characteristics of the Douglas-fir used in this study

Characteristic	Average	Range
Mean age in 2007 (yr)	77.4 (10.7)	57-105
Elevation (m)	1750 (217)	1420-2110
Basal area (m^2/ha)	13.8 (5.3)	4.6-29.7
DBH (cm)	23.1(5.6)	12.2-31.8
Total height (m)	15.9 (3.4)	7.0-24.1
Whole core SG	0.45 (0.02)	0.37-0.49

Latewood determination

Threshold method

The demarcation of the beginning, end, and earlywood-latewood transition of all rings was performed by the QTM-QTRX software using a threshold value of 500kg/m3. The beginning of a ring was defined as the point at which the density of the annual ring dropped below 500 kg/m^3 in the transition from one year's latewood to the next year's earlywood. The earlywood-latewood transition was defined as the point at which the density of the year's earlywood rose above 500 kg/m^3 and the end of the ring was located at the point at which the density fell back below 500 kg/m^3. Each X-ray density value was thus assigned a ring number and classified as either earlywood or latewood. A summary of each ring was produced that included: threshold ring length (TRLEN) threshold earlywood density (TEWDEN), threshold latewood density (TLWDEN), average ring density

(TAVGDEN), and threshold latewood percentage (TLWP). Rings with lengths less than 0.4mm were dropped from the data set because of limited resolution.

Inflection method

The raw densitometry data from each radial strip was initially assessed via a Microsoft Excel© Macro that identified the beginning and end of each annual ring by locating every other position at which the second derivative of the density plotted against position passed through a deadband value near zero and the 1st derivative of the density exceeded a predetermined value. Deadband values were set as percentages of the maximum and minimum first and second derivatives found for each ring to account for differences in ring length. Within each ring, while looping through the data, the script averaged the density of the latewood (INFLWDEN), noted the position and density (INFDEN) of the data point closest to the transition from latewood to earlywood (first and second derivative exceeded deadband values), averaged the density of the earlywood (INFEWDEN), and reported ring length (INFRLEN), percent latewood (INFLWP), and average ring density (INFAVGDEN). Ring lengths were checked against those found using the threshold method, and rings with disparate lengths were reanalyzed to ensure that the transition from ring to ring was assigned in accordance with the rules previously mentioned. Appendix A contains a more detailed description of the methodology and scripting.

Polynomial method

The raw densitometry data was entered into a Matlab© (Matlab 2013, MathWorks Inc. Natick, MA, 2013) script in which a 6th degree polynomial was fit to each ring individually using the start and stop position determined during the inflection method analysis. The position of the EW/LW transition was taken from the root of the second derivative of the polynomial that was: 1) closest to the bark, 2) between 10% and 80% of the total ring length, 3) occurred after (toward the pith) the maximum ring density, and 4) the 1st derivative of the polynomial at that point exhibited a negative

slope when read from bark to pith. The position and the density at the root of the polynomial that met the requirements were recorded. The position of the EW/LW transition was used to calculate polynomial earlywood density (PEWDEN), polynomial latewood density (PLWDEN), and polynomial latewood percent (PLWP). The average density of the rings using the polynomial method was the same as INFAVGDEN. Appendix B contains a more detailed description of the methodology and scripting.

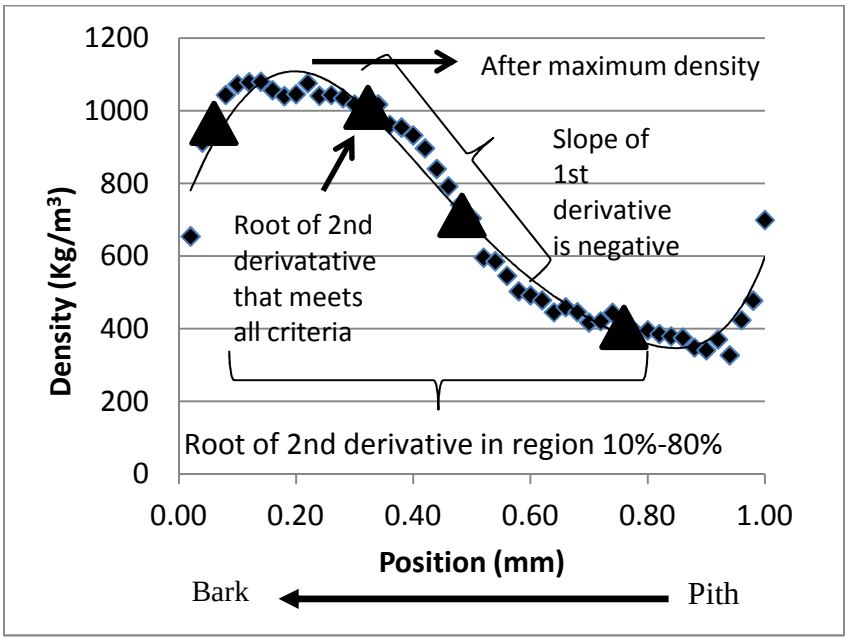

Figure 2.1 Selecting the appropriate root of the polynomial for latewood demarcation

Anatomical Measurement

Increment core strips from seven trees selected across the range of average densities were sliced for microscopy using a sliding microtome to produce transverse cross sections. Micrographs were made from five of the most recent rings from each strip using an Olympus BX51 (Olympus America, Center Valley, PA) microscope and cell measurements taken using Olympus software. For each ring, the radial dimensions of the cell walls and lumens were measured for five rows of tracheids. The cell wall and lumen data was assessed using curve fitting in Excel to define best fit estimates of average

wall thicknesses and lumen diameters. The curves were used to define the anatomy at the transition points selected by the three latewood methods. Appendix C contains a more detailed description of the methodology used to align and transfer the location of the latewood transition points from the densitometer data to the anatomical data

Results

Annual ring length assignments

In general, there was good agreement in the ring length assignments using the threshold and inflection method, with no indication of bias between methods. The distribution of differences appeared to be normally distributed with a mean of 0.0005 mm and a standard deviation of 0.031 mm. The distribution of deviations is shown in Figure 2.2. Within ring length quartile groups, the average difference in ring length between the two methods ranged from -0.0028mm for the first quartile to 0.0029 mm for the fourth quartile. Standard deviations ranged from 0.027mm to 0.033mm. Figure 2.3 shows the means of the ring length quartiles with error bars equivalent to one standard deviation. For this data set, 34% of the ring length assignments were exactly the same, 76% were within one step (±0.02mm), and 92% were within two steps (±0.04mm). Ring length disagreements of more than two steps seemed to occur most frequently in rings with less abrupt transitions from ring to ring and were usually paired with an adjacent ring with the equal and opposite deviation. In Figure 2.4, one such deviation is shown in which there is a 0.16mm difference in ring length because the density of the earlywood doesn't decline in the same manner as the surrounding rings. In this example, Ring A would register a relatively large negative deviation (TRLEN– INFRLEN) and Ring B would exhibit an approximately equal positive deviation.

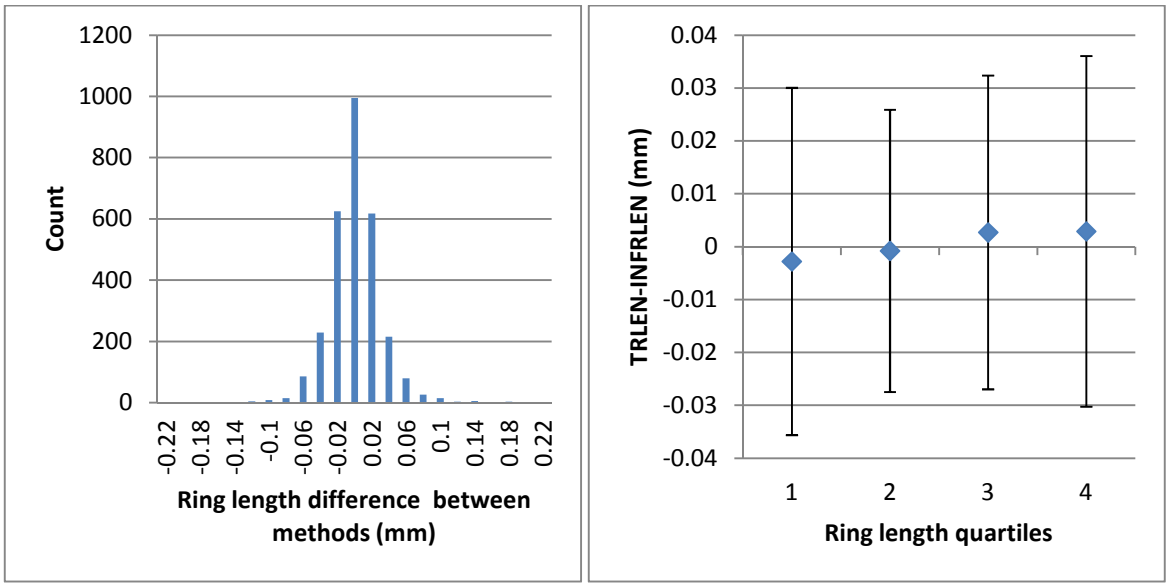

Figure 2.2 Distribution of deviations between threshold and inflection ring length assessments
Figure 2.3 Mean values of TRLEN – INFRLEN for ring length quartiles (error bars represent +/- 2SD)

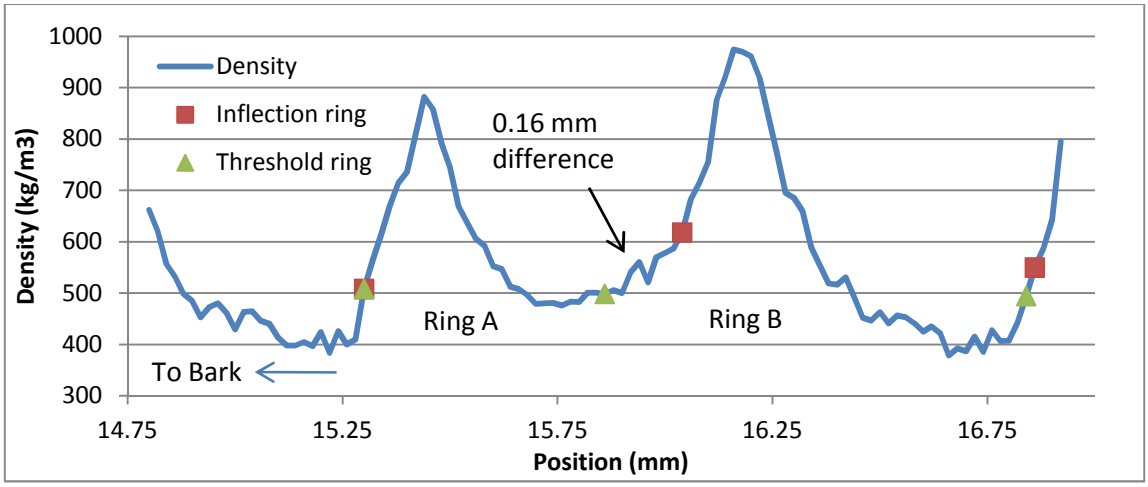

Figure 2.4. Deviation between inflection and threshold determination of ring length

Across the range of ring lengths encountered, there was a high level of correlation between ring length as shown in Figure 2.5. Because of the similarity in the regions assigned to each ring, the average density of the annual rings was likewise very similar (R^2=0.99) as shown in Figure 2.6.

Rings with unusual features, such as the ring with abnormally high earlywood density shown in Figure 2.4 are responsible for the outlying cases in Figure 2.6, especially in shorter rings. The threshold method did not seem to accommodate the abnormal earlywood of the middle ring, and reported a much shorter ring length than the inflection method.

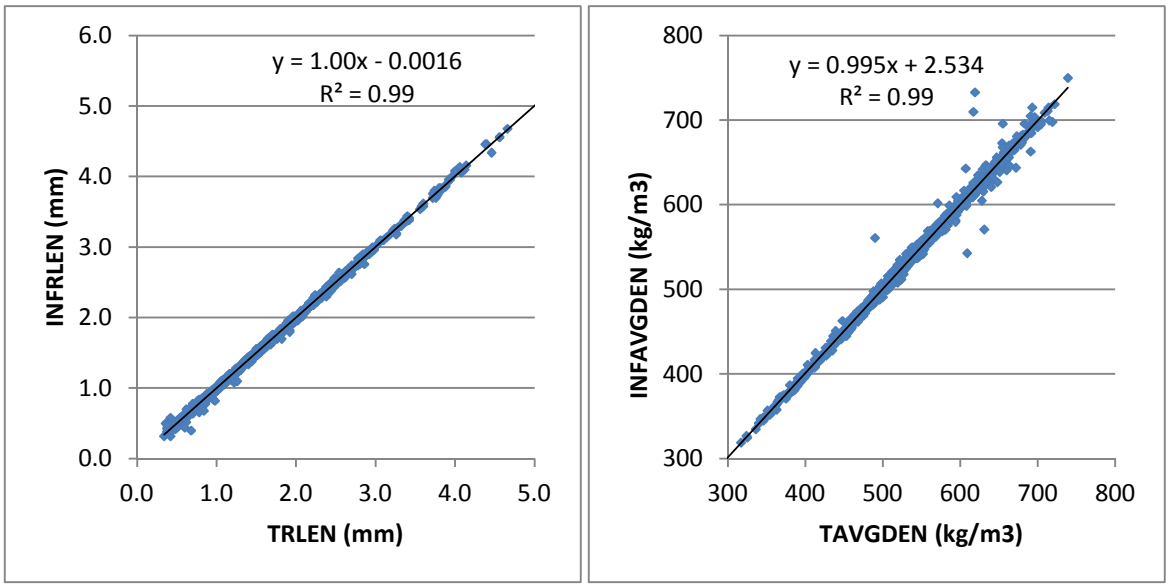

Figure 2.5. Similarities in ring length using the two demarcation methods
Figure 2.6. Similarities in INFAVGDEN and TAVGDEN using the two demarcation methods

Measures of latewood percentage

The three measures of latewood percentage did not show the same degree of agreement as the average density and ring length measurements. Figure 2.7 shows the correlation between TLWP and PLWP. On average the density identified at the inflection point for PINFDEN was 740 kg/m^3 , which was higher than INFDEN (657 kg/m^3), and far higher than the 500 kg/m^3 used for the threshold measure. PLWP was lower than TPLW for nearly all rings with average densities above 500 kg/m^3. Some of those rings that exhibited TAVGDEN below 500 kg/m^3 were found to have PLWP values higher than their respective TLWP values. Figure 2.8 shows the correlation of the difference between TLWP and PLWP on the average density of the ring. The PLWP method compensated for low average ring density by selecting lower density inflection points earlier in the

ring than the threshold method. In Figure 2.8, most of the annual rings follow a general trend of increasing difference in TLWP and PLWP with increasing density, but there is a group at the upper extreme that does not fit well with the rest. This group exhibits high earlywood densities and the threshold method measures little to no earlywood in these annual rings. In many of these rings, it was difficult to determine if they had abnormally high earlywood density, or were extreme examples of false rings. An example is shown in Figure 2.9 in which the a tree exhibits an abnormally high TLWP (100%) in two nearby annual rings as a result of unusually high earlywood densities, but the PLWP values are consistent with the surrounding rings.

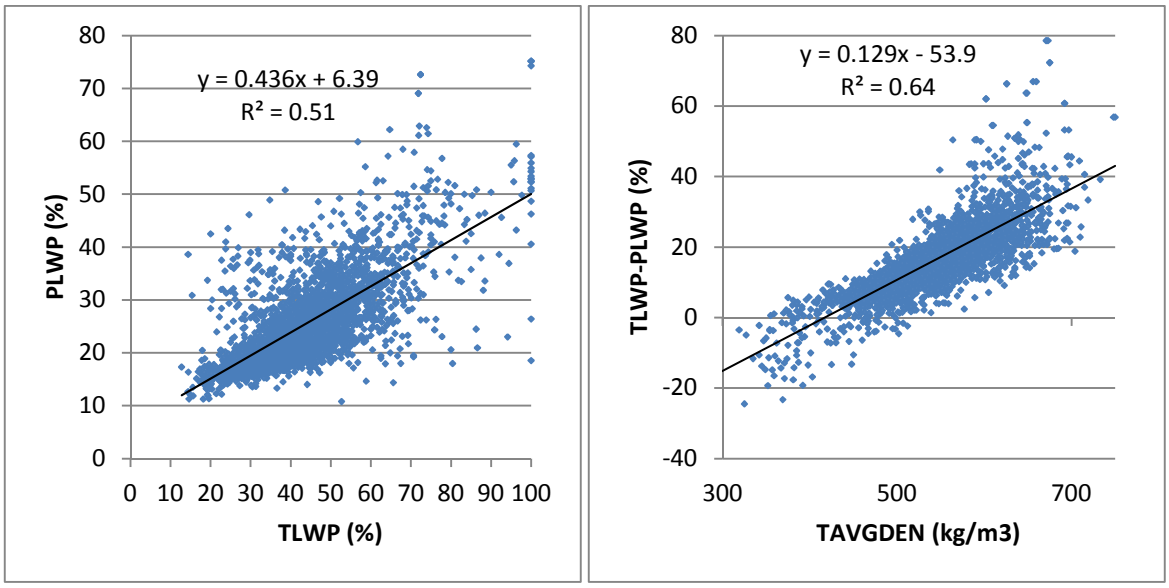

Figure 2.7. Comparison of PLWP and TLWP
Figure 2.8. Difference in TLWP and PLWP (TLWP-PLWP) regressed against TAVGDEN

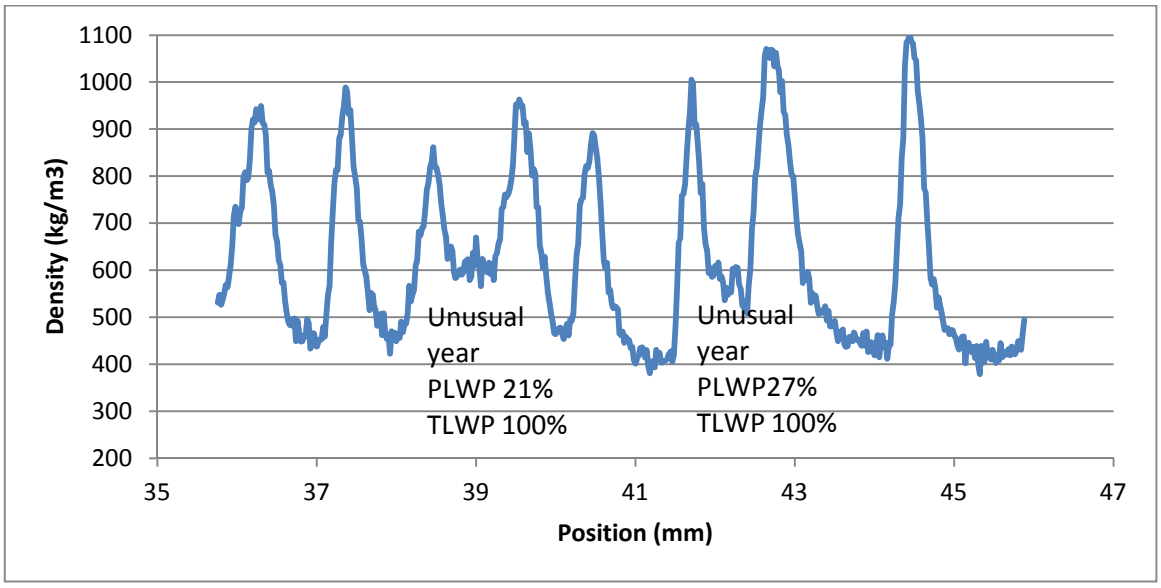

Figure 2.9. Unusual annual rings indicated by large deviation of TLWP and PLWP

INFLWP exhibited a very similar relationship with TLWP as PLWP, with a similar goodness of fit when regressed against TLWP as shown in Figure 2.10. As with PLWP, the difference between the threshold measurement of latewood and INFLWP shown in Figure 2.11 exhibited a positive correlation when plotted against average density indicating that the earlywood/latewood transition point identified by the inflection method was of a lower density in rings of lower average density and vice versa.

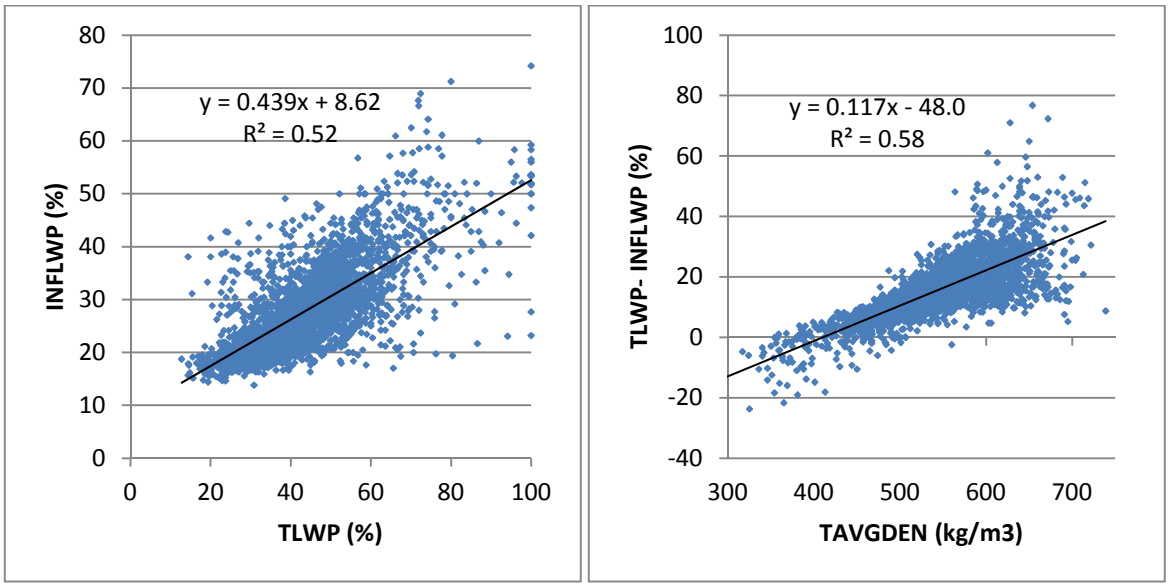

Figure 2.10. Comparison of INFLWP and TLWP
Figure 2.11. Difference between TLWP and INFLWP (TLWP – INFLWP) regressed against TAVGDEN

The inflection and polynomial methodologies produced identical or nearly identical results for many annual rings, however, there were some differences in the earlywood/latewood transition assignments. In Figure 2.12, INFLWP is plotted against PLWP and many of the annual rings demonstrate a one-to-one (or nearly so) relationship between the two measures. INFLWP was much lower than PLWP in a handful of annual rings, and upon further analysis, the inflection method in those cases identified the fluctuations similar to the beginning of a false ring in what would otherwise be considered latewood. When the transition from earlywood to latewood was rapid, or very linear, both methods returned similar transition points. When there was a “shoulder” during the transition from earlywood to latewood as seen in a dramatic example in Figure 2.13, the Polynomial method generally chose the upper part of the shoulder, and the Inflection method frequently chose the lower part of the shoulder if the slope of the upper shoulder was less than the cutoff set in the inflection methodology.

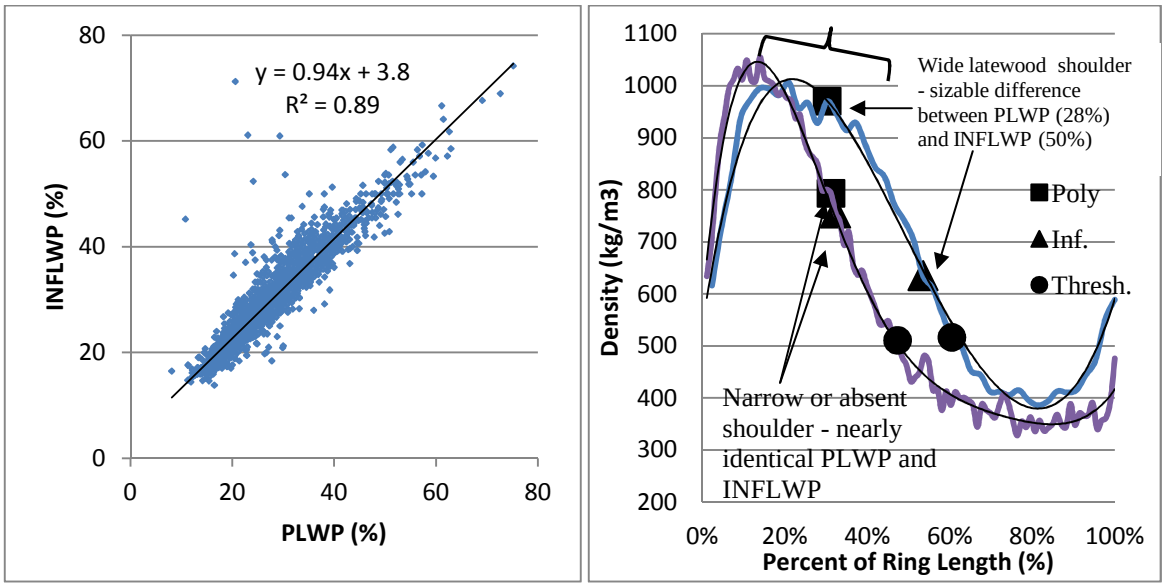

Figure 2.12. Fit of PLWP and INFLWP
Figure 2.13. Differences in PLWP and INFLWP affected by ring shape

TLWP was more closely correlated with average density than either PLWP or INFLWP. Figure 2.14(a) shows the fit of TLWP plotted against TAVGDEN, and shows the relatively high degree of fit (R^2=0.67) in annual rings measured in this study. Figure 2.14(b) shows PLWP regressed against INFAVGDEN, and shows a much poorer fit (R^2=0.16) between the polynomial measure of latewood percentage and the average density of the ring. As with the polynomial method, Figure 2.14(c) shows the poor fit (R^2=0.23) between INFLWP and average ring density. TLWP was by far the most correlated latewood measure with average density. INFDEN and PINFDEN provided better estimates of INFAVGDEN than INFLWP or PLWP with R^2=0.43 and R^2=0.31 for INFDEN and PINFDEN respectively.

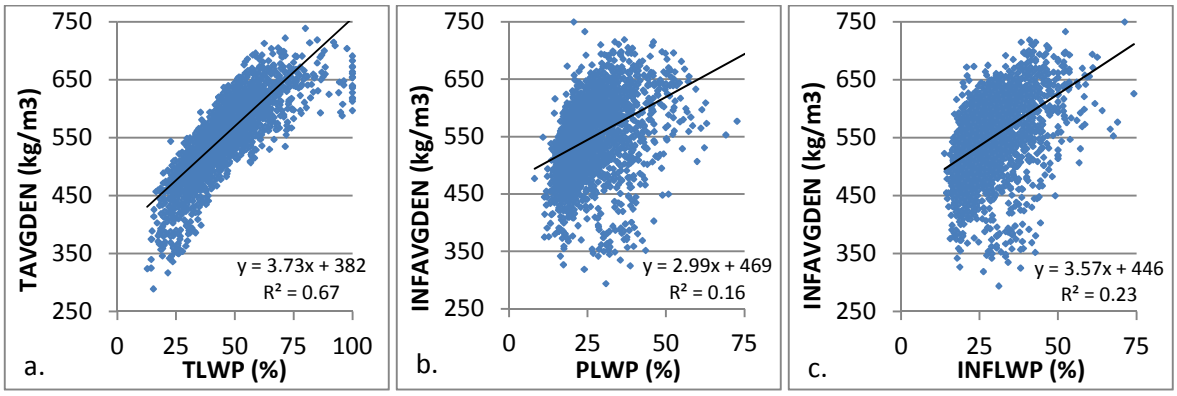

Figure 2.14. Correlations between latewood measures and average density. Correlation TLWP and TAVGDEN(a), correlation of PLWP and INFAVGDEN (b), correlation of INFLWP and INFAVGDEN(c).

Values of PINFDEN, the density at which the polynomial method indicated the transition had taken place, were more closely associated with differences in PLWDEN than PEWDEN. In Figure 2.15, PLWDEN and PEWDEN are regressed against PINFDEN. PLWDEN shows a very tight fit with PINFDEN, with an $R^2 = 0.91$ for the sample population. Over the range of PINFDEN measured in this data set, PEWDEN did not exhibit a great deal of variation compared to PLWDEN, and was shown to be more poorly fit with PINFDEN, with an $R^2 = 0.25$ for that regression. Differences in INFDEN were likewise more closely associated with changes in INFLWDEN than INFEWDEN, however the goodness of fit between INFDEN and INFLWDEN ($R^2 = 0.70$) was somewhat poorer than that of PINFDEN and PLWDEN as seen in Figure 2.16.

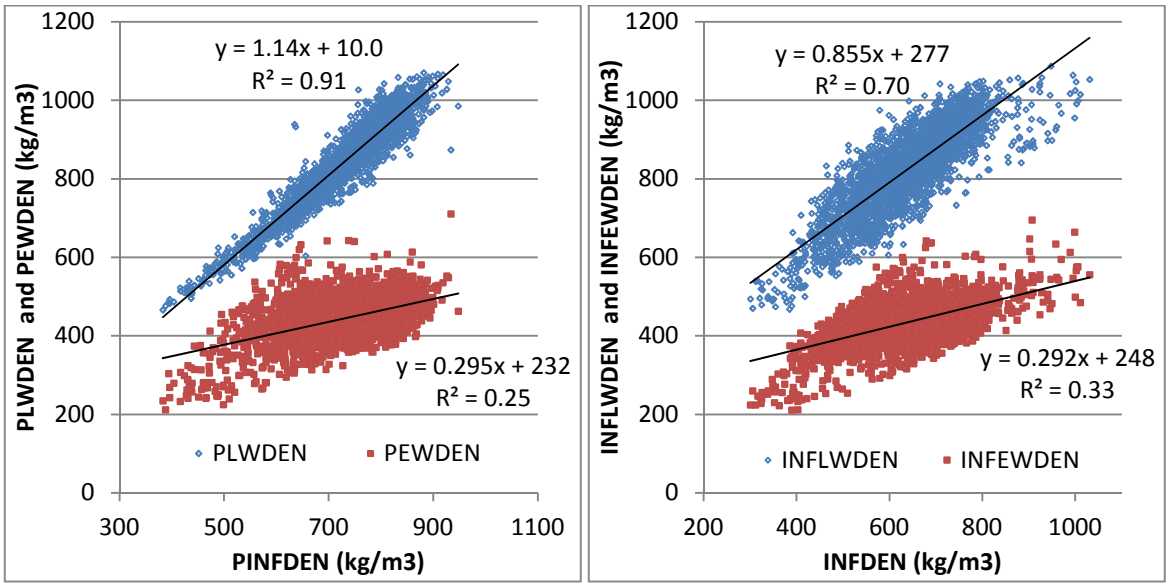

Figure 2.15. PLWDEN and PEWDEN regressed against PINFDEN
Figure 2.16. TLWDEN and TEWDEN regressed against PINFDEN

Anatomy

The increment cores of seven of the 45 trees were chosen for further microscopic analysis of radial cell wall widths and radial lumen diameters. The trees were chosen to span the range of average densities of the entire set of 45 trees. Measurements taken from seven selected trees indicated that the threshold method identified the transition from earlywood to latewood at a point slightly beyond Mork's definition (lumen diameter: single cell wall thickness = 4:1) while the inflection and polynomial methods identified points with much lower lumen diameter to cell wall ratios. Table 2.2 shows the lumen to cell wall ratios for the three methods and suggests that the ratios measured for the threshold latewood point were more consistent than those found for the inflection and polynomial methods. The threshold method identified regions with an average lumen to cell wall ratio of 3.9µm/µm with a standard deviation of .50µm/µm amongst all the rings measured, while the inflection and polynomial methods identified regions with ratios of 2.5µm/µm and 2.0 µm/µm with standard deviations of 1.3µm/µm and .87µm/µm respectively. A paired t-test indicated that the lumen to cell wall ratio of the points selected by all three methods were significantly different beyond a

95% significance level. For the seven trees analyzed, 94% of the points selected by the threshold method were within 5% of the total ring length from the position identified as meeting Mork's definition of latewood.

Table 2.2. Comparison of lumen diameter to cell wall thickness ratios using the three latewood measures

	Latewood determination method		
	Threshold lumen/wall (μm/μm)	Inflection lumen/wall (μm/μm)	Polynomial lumen/wall (μm/μm)
Mean	3.9	2.5	2.0
Standard Deviation	.50	1.3	.73
Minimum	3.1	1.2	.83
Maximum	5.3	7.4	3.6

Figure 2.17 shows the measurements of a typical annual ring encountered during the study. The lumen to cell wall ratio at the threshold latewood demarcation was 3.4:1 while the ratios at the inflection and polynomial inflection points were 2.1:1 and 1.9:1 respectively. While the lumen to cell wall ratio of the inflection and polynomial inflection points varied substantially from ring to ring, they consistently target the region of the most rapid change in cell wall thickness and lumen diameter, with the polynomial latewood point occurring slightly after the maximum slope was reached, and the inflection latewood point slightly before the maximum slope was reached. For the seven trees studied, the threshold method on average selected a point about 12% of total ring length before the maximum lumen slope, the inflection method on average selected a point about 3% before the maximum slope, and the polynomial method on average chose a point 2% after the maximum slope. The standard deviation of the distance from the point chosen by the threshold, inflection, and

polynomial method with relation to the position of the maximum slope were 8.1%, 7.9%, and 6.9% of total ring length. Evaluating the slope of the curve fit for cell wall thickness and lumen diameter, Figure 2.18 shows the location of the inflection and polynomial EW/LW transition points near the region with the highest rate of change in cell wall thickness and lumen diameter.

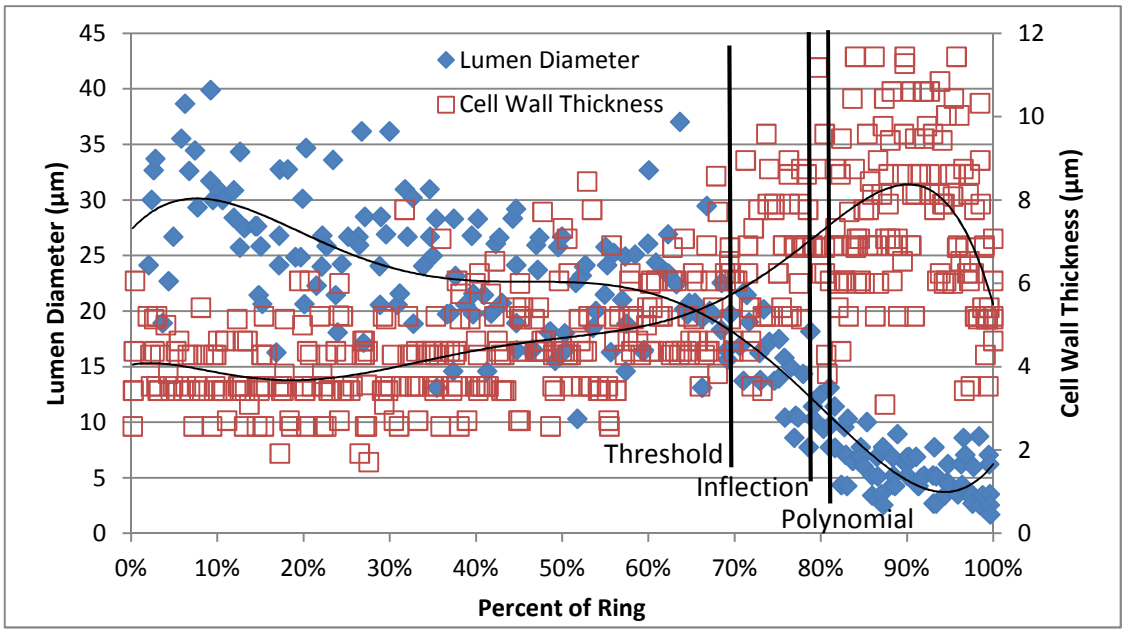

Figure 2.17. Lumen diameter and cell wall thickness across a typical annual ring, with the threshold, inflection, and polynomial latewood transition points identified.

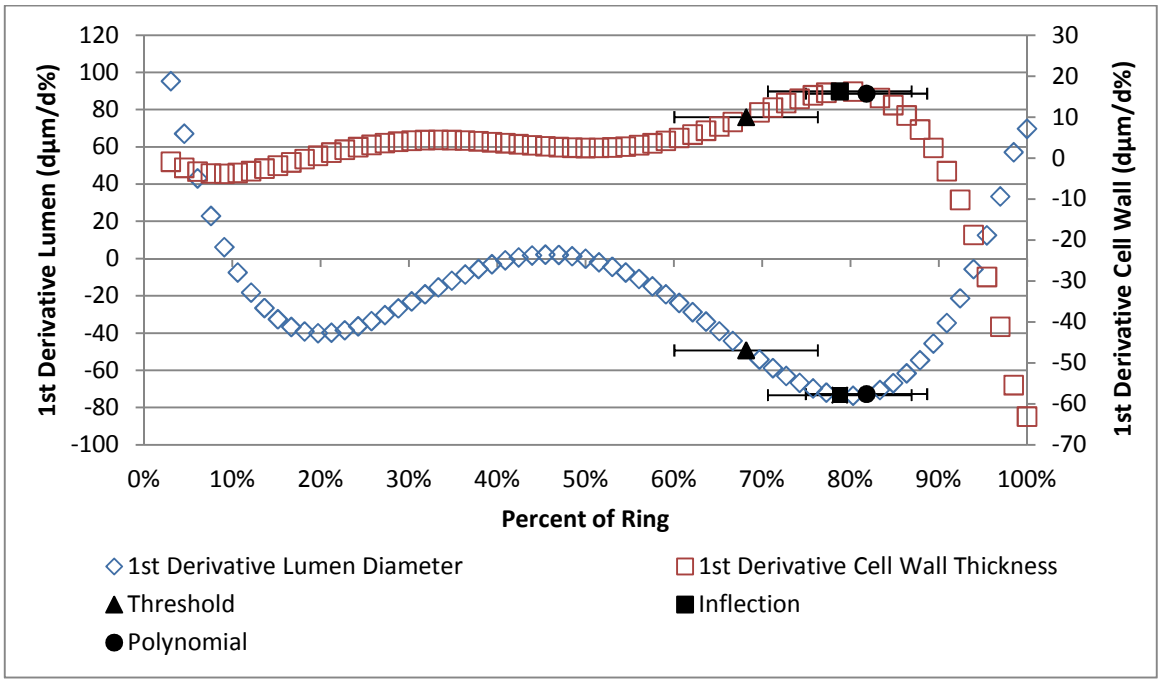

Figure 2.18. Rate of change in cell wall thickness and lumen diameter at locations identified as threshold, inflection, and polynomial earlywood-latewood transition points. Error bars represent one standard deviation.

As suggested in Figures 2.9 and 2.11, in lower density rings, the polynomial and inflection methods targeted regions with higher lumen to cell wall ratios (less dense) than in higher density rings. The threshold method exhibited very little bias for higher lumen to cell wall ratios in low density rings. Figure 2.19 shows the lumen to cell wall ratios for all the rings measured in the seven trees plotted against average ring density. The goodness of fit for the threshold measure was approximately 0.05, while the goodness of fit for the inflection and polynomial methods were 0.42 and 0.60 respectively. The fit of the inflection ring method was markedly less than the fit of the polynomial method for the rings studied, indicating more erratic performance. The Root Mean Squared Error (RMSE) for the regressions were 0.49µm/µm, 1.1 µm/µm, and 0.47 µm/µm for the threshold, inflection, and polynomial methods respectively.

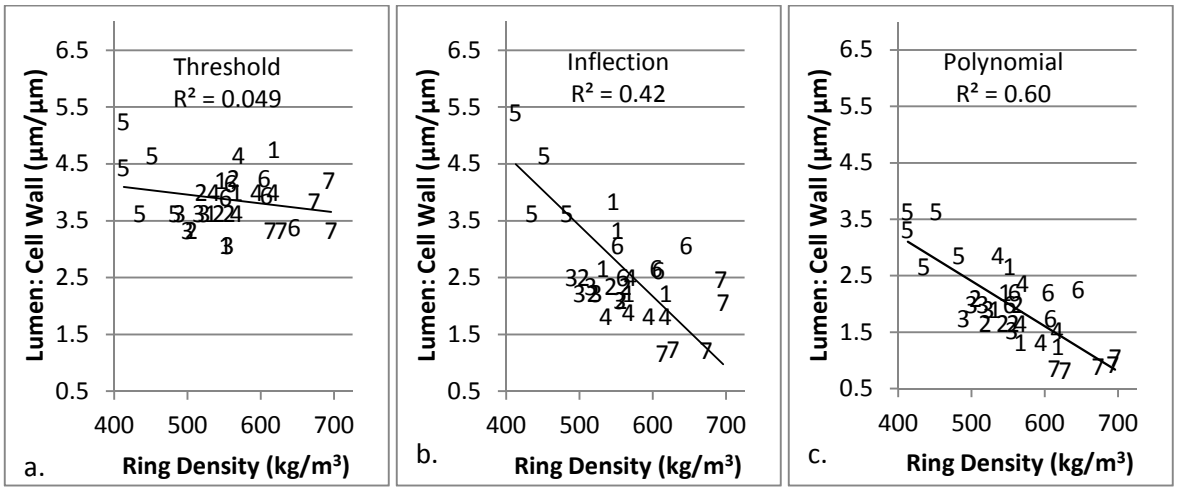

Figure 2.19. Graphs of fit for lumen diameter to cell wall ratio regressed against density for the positions identified by the three latewood demarcation methods: threshold (a), inflection (b), and polynomial (c). Symbols indicate tree number.

The intent of the dynamic measurements was to identify the point in the density profile during the transition from earlywood to latewood that exhibited the most change in density, and seemed to be associated with the simultaneous rapid decline in lumen diameter and increase in cell wall thickness, as shown in Figure 2.17. The threshold measurement was expected to identify a point close to Mork's definition of latewood, and not follow the point of maximum density change during the earlywood/latewood transition. The distance (in percent ring length) between the transition point identified by the latewood measures using the densiometric data and the location of maximum lumen and cell wall dimension change found in the anatomical data (DMAXSLP) was found to exhibit a correlation with the average ring density in the dynamic latewood measurements, and no correlation with average ring density for the threshold latewood measurement. These correlations are shown in Figure 2.20. The goodness of fit of DMAXSLP for the polynomial method regressed with TAVGDEN was the highest with an $R^2 = 0.38$, followed by the inflection method with an $R^2=0.23$, and finally the threshold method with an $R^2 \approx 0$. The dynamic methods appeared to select a transition point beyond the point of the most rapid change in lumen diameter and cell wall thickness

in dense rings (i.e. identify a point later in the ring or shorten the latewood period) and select a transition point before the point of most rapid change in lumen diameter and cell wall thickness in low density rings (i.e. identify a point earlier in the ring or lengthen the latewood period). The same phenomenon may also cause the deviations between TLWP and PLWP shown in Figure 2.9 to increase as the density of the annual ring increases.

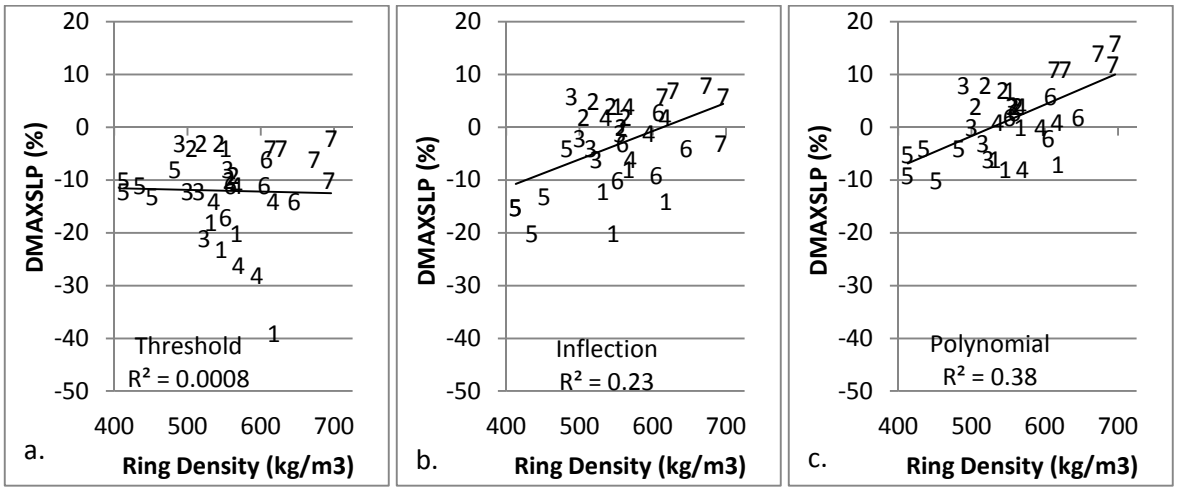

Figure 2.20. Percent of ring distance from point of maximum rate of change in lumen diameter versus average ring density for the three latewood demarcation methods: threshold (a), inflection (b), and polynomial (c). Positive distance indicates the transition point chosen occurred after maximum slope in lumen diameter. Symbols indicate tree number.

Discussion

Correlations between latewood measures and average density

Both the inflection and polynomial methods showed moderate agreement to the threshold latewood measurements in this study, but less than that reported by Antony et al. (2009) in a similar experiment (r = 0.99 for young loblolly pine). As seen in Figures 2.7 and 2.10 the goodness of fit generated by INFLWP and PLWP regressed against TLWP was slightly better than 0.50, but between half to two-thirds of the error variance between the threshold measure and the dynamic measures was correlated to the average density of the annual ring being studied as seen in Figures

2.8 and 2.11. This would seem to indicate that there is less random error between the static and dynamic measures than a simple correlation would suggest and that there is a more constant range of divergences for the static and dynamic measurements at a given annual ring density. Although not specifically mentioned in Antony et al, there appears to be a similar trend expressed in terms of the age/density relationship in their research: the first two rings from the pith (presumably denser than the next five or so rings) show T LWP being longer than the inflection measurement, and in the seven or so subsequent rings (presumably as the ring density decreases and then rebounds to mature levels) the threshold LWP was shorter than that of the inflection measurement. As the trees mature, the difference returns to near zero. In Koubaa et al. (2005), the plantation grown black spruce studied showed a similar relationship between the polynomial and threshold methods for the first five to seven rings from the pith with the threshold method returning longer latewood periods in the higher density early rings, and very little difference as the ring density moderated to presumably mature levels. Koubaa's figures indicate equivalence of the threshold and polynomial methods for rings with an average density of approximately 450 kg/m^3, virtually identical to the relationship found in the present research. The Douglas-fir studied for this paper did not exhibit an age based trend in the deviation between the threshold and dynamic measures. Because the dynamic measures seek the region with the most change in density, they tend to select points lower than 500 kg/m^3 in rings with average densities less than 450 kg/m^3 and points greater than 500kg/m^3 in rings with average densities greater than 450 kg/m^3, leading to the systematic positive and negative differences between the threshold and dynamic latewood measurements. Antony (2011) and Koubaa (2005) attribute this discrepancy to ring age; average ring density may provide an alternative or complementary explanation.

The dynamic inflection and polynomial methods showed a great deal of agreement in their latewood assignments for the rings studied here. The goodness of fit between the two shown in Figure 2.12 was approximately 0.89, with the regression indicating the inflection method increased nearly one-

to-one with the polynomial method. From the densitometry data, it seems as if these methods are essentially interchangeable. From a user's perspective, implementing a robust latewood measurement scheme for the polynomial method was far simpler than for the inflection method. To produce reliable results using MS Excel VBA with the inflection method required over 170 lines of code with multiple iterative loops and a great deal of trial and error to set dynamic parameters that could adequately handle the wide variety of ring lengths (0.4mm-4.5mm) and density profile shapes encountered in this study. The polynomial method implemented in Matlab required only 57 lines of code and required virtually no fine tuning to perform as expected.

There were 25 rings in this study which the threshold measure reported >95% latewood, and of those, 13 returned a value of 100% latewood when a threshold of 500kg/m^2 was used. If the threshold level were raised much higher, the lowest density rings examined here would register 0% latewood. These rings are rare, but beg the question as to how to address them. Changing the threshold value for the extreme rings is a possibility, but it would require reporting and analyzing those rings differently than the other rings. The dynamic measures for the "unusual" rings in Figure 2.9 had similar latewood percentages as the surrounding rings even though the average densities were quite different. For rings with elevated earlywood density, the dynamic measures performed more consistently. The dynamic methods, however, tended to select earlywood-latewood transition points on latewood shoulders in rings with gradual transitions and long latewood periods as shown in Figure 2.13. There were shortcomings with every method used.

One of the primary uses of latewood measurements in forest products research is to describe and predict average density. TLWP seemed to be the most highly correlated with average density, making it an obvious choice for inferences of properties associated with density. The two pieces of information inherent in the threshold measurement are the (1) proportion of the annual ring which has (2) a density greater than the threshold value. PINFDEN and INFDEN provided better fits with INFAVGDEN than PLWP or INFLWP, but still do not match the predictive power of TLWP. If the

density at which the inflection point takes place is combined with PLWP or INFLWP, an equivalent or better fit can be achieved with average density (not shown). Using the polynomial and inflection methods to predict average density requires an additional piece of information to produce an equivalent estimate of average density as TLWP.

Anatomy at the selected transition points

The anatomical measurements taken during this research indicated that the threshold method was the most consistent in terms of the ratio of radial lumen diameter to cell wall at the latewood transition points selected in the absence of any other information about the ring. The analysis indicated that Mork's definition of latewood was approximated, on average, with a threshold value of 500 kg/m^3 for the Douglas-fir samples measured in this study. Whether or not the standard deviation of 0.5μm/μm found for the radial lumen to cell wall thickness ratio is an adequate level of precision would depend on the needs of the individual researcher, but it would be far more consistent than the dynamic methods without additional density data. The lumen diameter to cell wall ratio at the threshold latewood transition point was virtually uncorrelated with the average density of the ring being measured. This consistency constitutes the greatest strength of the threshold method: it provided an anchor point in terms of the anatomy at the point selected.

The lumen to cell wall ratio at the positions selected by the dynamic measures showed significant correlation with the average density of the ring. These findings suggest that the average density of the ring, which would be collected during densiometric analysis, could be used to estimate tracheid anatomy at the selected positions with an estimated RMSE of 0.47 μm/μm using the polynomial method, generating a similar level of precision as that found for the threshold method. It seems probable however, that the relationship between average ring density and the lumen:cell wall ratio at the chosen latewood transition points would vary somewhat by species, especially between species that exhibit slow transitions from earlywood to latewood (eg. spruce) and rapid transition species

such as the Douglas-fir studied here. Baseline correlations of density and anatomy would still have to be developed for a species of interest, but there may be an opportunity to use a baseline model built with observed anatomical data to infer properties at the inflection point in rings for which no anatomical measurements were taken.

During xylogenesis, there seem to be periods in which the duration of the enlargement or thickening stages of forming xylem shift, and those changes in duration should result in changes in the density of the mature xylem cells (e.g. Cuny et al. 2012,Cuny et al. 2013, Dodd and Fox 1990). In Figures 2.17 and 2.18, the dynamic measures seem to be identifying the portion of the annual ring at which the lumen diameter and cell wall thickness are changing most rapidly, which would indicate a transition such as that shown in Cuny or Dodd and Fox. The duration profiles reported by Cuny et al. were developed using labor intensive microcoring and visual analysis techniques to determine changes in the number of cells in the various stages of development and estimate the time spent in each stage. In addition, localized irregularities in growth rates often make it necessary to sample large numbers of trees (Cuny et al. 2013). By benchmarking duration times in the enlargement and secondary wall thickening zones with various threshold measurements, researchers may be able to develop proxy models to correlate the time forming tracheids spent in individual zones of development with regions of the density profile which meet the threshold value. Dynamic latewood measurements could be used to identify the region of the annual ring that passed through the enlargement and secondary wall thickening stages while duration times were changing the most rapidly. Employing multiple measures of latewood may permit researchers to leverage fewer labor intensive microscopic analyses to increase the sample size and scope of their studies using relatively inexpensive densiometric analysis.

The inflection and polynomial methods are meant to identify the point of annual ring that exhibits the greatest rate of change in density, and by extension, enumerate the position of the ring with the greatest change in lumen diameter and cell wall thickness. The anatomical data, however, indicates

that while both the inflection and polynomial methods identified the region of greatest change in lumen diameter and cell wall thickness on average, they tended to systematically overshoot or undershoot the exact position of greatest change depending on the average density of the individual rings being measured. By reporting shorter than expected latewood lengths in high density rings, and longer than expected latewood periods in low density rings, the dynamic measures tended to homogenize latewood percentages. The reason for this phenomenon likely has to do with the interaction of the dynamic latewood transition selection criteria and the shape of density profiles in high and low density rings. The rings shown in Figure 2.13 may illustrate the point. In higher density rings, the transition from earlywood to latewood is typically less abrupt, and may contain several transition regions of different slopes. Both of the dynamic measures preferentially seek later inflection points, and are not required to select the inflection point with the greatest slope. In higher density rings, this may cause the dynamic measures to select inflection points later in the earlywood/latewood transition, thereby shortening the latewood period from the expected length. In lower density rings, there is frequently a very rapid and linear transition from earlywood to latewood, a short period of high density latewood production, and a relatively rapid transition to the next annual ring. This geometry may force the apparent inflection point earlier in the ring because the density profile appears to reach its maximum slope just after leaving the lower density latewood. Figures 2.20 b and c suggest that this error could be reduced by using a linear correction factor based on the average density of the ring, which would not affect rings of average density much, but would improve the accuracy of the dynamic measures for rings with more extreme average densities. These corrections may prove vital for researchers interested in correlating remotely collected measures of canopy moisture stress with xylem formation.

Quality control

Human error is a persistent issue in the collection and analysis of annual ring data in large data sets. The repetitive nature of the work can easily lead to errors that become increasingly difficult to

address as the analysis progresses. Even at very high accuracy rates, the sheer number of evaluations and decisions dictate that human error will be present. Comparing the results of multiple measures of latewood percentage provided an additional quality control check in the course of this research that identified errors not previously corrected. During the script building process, the comparisons proved invaluable in identifying code statements that required further refinement to accommodate the features of unusual rings and return more consistent latewood demarcation for all rings. Graphs of residuals such as Figure 2.8 and 2.11 were especially useful for identifying questionable latewood and ring length assignments because they provided a simple graphic to identify unusual rings. Combining methods to evaluate latewood assignments allowed the researcher to take advantage of the strengths of each method and produce the most accurate data set possible.

Conclusion

Three latewood demarcation methods: a static threshold, a dynamic inflection based, and dynamic polynomial based, were compared to determine the consistency between them, their correlations to average density, and the anatomy at the selected latewood transition points for the annual rings of 45 small-diameter Douglas-fir. At first glance, the dynamic measures seem to exhibit a moderate amount of agreement with the threshold method ($R^2 \approx 0.5$), but further analysis indicated that the differences between the static and dynamic measures were correlated to average density ($R^2 \approx 0.6$) indicating that comparisons between static and dynamic measures need to be made in the context of the average density of the ring because of the systematic deviations between the measures. The inflection and polynomial methods showed a high level of agreement ($R^2=0.89$), although in some instances, the shape of the density profile led to divergences, especially long latewood shoulders. As a standalone measurement, TLWP produced the greatest fit with average density ($R^2=0.67$) as compared to INFLWP ($R^2=0.23$), and PLWP ($R^2=0.16$). Anatomical measurements on a subset of the 45 trees indicated that the threshold value of 500 kg/m^2 identified a point, on average, very close

to Mork's definition where the radial lumen to cell wall ratio was 3.9 μm/μm with a standard deviation of 0.5 μm/μm. The lumen to cell wall ratio at the point identified by inflection and polynomial measures exhibited a linear relationship with average ring density , making it possible to estimate the lumen to cell wall ratio at that point with the same level of precision as the threshold measurement. The inflection and polynomial measurements also seemed to systematically over or underestimate the position of those annual rings with the most change in lumen diameter and cell wall width based on the average density of the annual ring. The geometry of the density profile may cause the systematic nature of these errors and future work should focus on incorporating rules or algorithms that are less affected by the geometry of the annual ring density profile. Each method has its strengths, and using several simultaneously may enable researchers to complement their current research and expand the scope and scale of future projects.

References

Antony F, Schimleck LR, Daniels RF, Clark III A. 2011. Effect of fertilization on growth and wood properties of thinned and unthinned midrotation loblolly pine (Pinus taeda L.) stands. Southern Journal of Applied Forestry 35(3): 142-147.

Bower AD, Adams WT, Birkes D, Nalle D. 2005. Response of annual growth ring components to soil moisture deficit in young, plantation-grown Douglas-fir in coastal British Columbia. Can. J. For. Res. 35(10): 2491-2499.

Brix H. 1972. Nitrogen fertilization and water effects on photosynthesis and earlywood-latewood production in Douglas-fir. Can. J. For. Res. 2(4):467-478.

Clark III A, Borders BE, Daniels RF. 2004. Impact of vegetation control and annual fertilization on properties of loblolly pine wood at age 12. Forest Products Journal 54(12): 90-96.

Clark III A, Daniels R, Jordan L. 2006. Juvenile/mature wood transittiotn in loblolly pine as defined by annual ring specific gravity, proportion of latewood, and microfibril angle. Wood and Fiber Science. 38(2):292-299.

Cuny HE, Rathberger CBK, Lebourgeois F, Fortin M, Fournier M. 2012. Life strategies in intra-annual dynamics of wood formation: example of three conifer species in a temperate forest in north-east France. Tree Physiology. 32: 612-625.

Cuny HE, Rathberger CBK, Kiesse TS, Hartmann FP, Barbeito I, Fournier M. 2013. Generalized additive models revea the intrinsic complexity of wood formation dynamics. Journal of Experimental Botany. 64(7): 1983-1994.

Dalla-Salda G, Martinez-Meier A, Cochard H, Rozenberg P. 2011. Genetic variation of xylem hydraulic properties shows that wood density is involved in adaptation to drought in Douglas-fir (Pseudotsuga menziesii (Mirb.)). Annals of Forest Science. 68(4): 747-757.

Denne MP. 1988. Definition of latewood according to Mork (1928). IAWA Bulletin 10(1): 59-62.

Dodd RS, Fox P. 1990. Kinetics of tracheid differentiation in Douglas-fir. Annals of Botany. 65(6):649-657.

Eilmann B, Zweifel R, Buchmann N, Pannatier EG, Rigling A. 2011. Drought alters timing, quantity, and quality of wood formation in Scots pine. Journal of Experimental Botany. 62(8): pp 2763-2771.

Gonzalez-Benecke CA, Martin TA, Clark A, Peter GF. 2010. Water Availability and genetic effects on wood properties of loblolly pine (Pinus taeda). Can. J. For. Res. 40(12): 2262-2277.

Helinska-Raczkowska L, Fabisiak E. 1999. Radial variation of earlywood vessel lumen diameter as an indicator of the juvenile growth period in ash (Fraxinus excelsior L.). Holz als Roh- und Werkstoff. 57(4):283-286.

Koubaa A, Zhang SYT, Makni S. 2002. Defining the transition from earlywood to latewood in black spruce based on intra-ring wood density profiles from X-ray densitometry. Ann. For. Sci. 59(5-6): 511-518.

Koubaa A, Isabel N, Zhang SY, Beauieu J, Bousquet J. 2005. Transition from juvenile to mature wood in black spruce (Picea mariana (Mill.) B.S.P.). Wood and Fiber Science. 37(3):445-455.

Laserre JP, Mason EG, Watt MS, Moor JR. 2009. Influence of initial planting spacing and genotype on microfibril angle, wood density, fibre properties and modulus of elasticity in Pinus radiate D. Don corewood. Forest Ecology and Management 258(9):1924-1931.

Mork E. 1928. Die Qualität des Fichtenholzes unter besonderer Rücksichtnahme auf Schleifuned Papeirholz. Der Papier-Fabrikant 26: 741-747.

Morrow CD, Gorman TM, Evans JW, Hatfield CA. 2013. Prediction of wood quality in small-diameter Douglas-fir using site and stand characteristics. Wood and Fiber Science. 45(1):49-61.

Pernestal K, Jonsson B, Larsson B. 1995. A simple model for density of annual rings. Wood Sci. and Tech. 29(6): 441-449.

Polge H. 1978. Fifteen years of wood radiation densitometry. Wood Sci. Technol. 12(3): 187-196.

Forest Products Laboratory. 2002. Wood Handbook: wood as an engineering material. Gen. Tech. Rep. FPL-GTR-113. Madison, WI: U.S. Department of Agriculture, Forest Service, Forest Products Laboratory. 463p.

Schneider R, Zhang SY, Swift DE, Begin J, Lussier JM. 2008. Predicting selected wood properties of jack pine following commercial thinning. Can. J. For. Res. 38(7): 2030-2043.

Wang M, Stewart J. 2012. Determining the transition from juvenile to mature wood microfibril angle in lodgepole pine: a comparison of six different two-segment models. Annals of Forest Science 69(8):927-937.

Zahner R, Lotan JE, Baughman WD. 1964. Earlywood-latewood features of red pine grown under simulated drought and irrigation. Forest Science 10(3): 361-370.

Chapter Three
The influence of soil bulk density and climate factors on wood quality in Douglas-fir trees

Abstract

Soil bulk density (SBD) appeared to be negatively correlated with a dynamic measure of stiffness in a study on suppressed small diameter Douglas-fir from the Bitterroot region of western Montana. When modeled in a repeated measures framework, X-ray densitometry from the increment cores of a subset of the sampled trees revealed that the trees grown in low SBD stands had significantly higher average density (P=.0088) and latewood period using three different measures of latewood (P= .025 to P=.039) across the model testing period. The difference in average ring density between the two groups showed a positive correlation (R^2=0.43) to July/August Cooling Degree Days (CDD), and during an extremely cool year, the SBD effect was even reversed. The concept of Least Limiting Water Range (LLWR) may provide a framework for explaining these findings such that trees growing in high SBD stands may experience limited access to late-season soil moisture due to the mechanical impediment to fine root egression in higher bulk density soils, making it difficult to remove soil moisture down to the wilting point. This improved understanding of the soil-climate-tree interaction may help forest managers prioritize stand improvement treatments to meet challenges stemming from changes in climate or market expectations of wood quality.

Introduction

The latewood proportion of an annual ring has been shown to be dependent on a variety of factors including environmental influences such as moisture availability and climate. Irrigation or readily available moisture generally delays the transition from earlywood to latewood (Zahner et al. 1964; Brix 1972) and dry conditions advance the date of transition (Kantavichai et al. 2010(b); Rozas et al. 2010). If conditions leading up to and following the transition are still conducive to latewood

formation, there is an opportunity to increase the latewood proportion of the annual ring (Kennedy 1961; Robertson et al. 1990; Gonzalez-Benecke et al. 2010; Eilman et al. 2011). An important consideration to draw from these studies, as noted by Larson et al. (2001) in a review of wood formation in southern pine, is that the timing of available moisture is a critical aspect in determining the effect of irrigation or climate on latewood percentage or ring. As Zahner and others have demonstrated, increasing the availability of moisture throughout the growing season with irrigation tended to delay the transition from earlywood to latewood, lead to increased amounts of earlywood and latewood, and resulted in latewood percentages similar to subjects exposed to season-long drought or control conditions (Zahner et al. 1964, Albaugh et al. 2004). Gonzalez-Benecke et al. (2010) applied irrigation to clonal loblolly pine plantations only in the summer and fall, and found a significant increase in the latewood percentage and specific gravity of rings grown under late-season irrigation. Increasing the year-round availability of soil moisture does not necessarily lead to increased latewood percentages or ring density, the timing is important.

Operational silvicultural practices such as thinning or fertilization can also influence latewood percentage. Thinning is meant to reduce competition for available soil moisture, nutrients, and light with the objective of improving growth, but when applied as a standalone treatment, studies suggest there is a modest or no effect (Brix and Mitchel, 1980; Cregg et al. 1988; Kantavichai et al. 2010(b)) on annual ring density or percent latewood. Several authors noted that the date of latewood initiation was delayed by the treatment but that the increased earlywood growth was matched with increased latewood growth, resulting in little significant change in latewood proportion of the annual rings (Brix and Mitchel 1980; Cregg et al. 1988). Fertilization treatments reduce nutrient constraints and are frequently applied to stimulate the photosynthetic capacity of the crown. Although the results are frequently complicated by site, stand, or species specific factors (Larson et al. 2001), there are frequently short-term reductions in ring density or latewood percentage reported (Jozsa and Brix

1989; Antony et al. 2009), although some effects may be seen for decades (Kantavichai et al. 2010 (a))

The influence of climatic conditions on latewood percentage and ring density may be thought to parallel those of irrigation for many species with site specific considerations. In a study of coastal Douglas-fir, Robertson et al. (1990) compared ring variables on xeric, submesic, and subhygric sites and found that differences between annual ring densities formed during dry (average 0.45 g/cm^3) or wet years (average 0.52 g/cm^3) were the highest in the xeric site. Their research and others have found that the sensitivity of ring variables to climatic variables is highest on marginal sites (Robertson et al. 1990; Savva et al. 2003). In addition, the percent latewood at the xeric site was most correlated with precipitation in June and early July, likely the period in which the transition from earlywood to latewood was occurring. Similarly, Kantavichai and others found that July precipitation or soil moisture deficit was a strong predictor of latewood percentage.

In addition to the timing of natural precipitation events, there exists the possibility that differences in soil texture may produce measurable differences in the proportion of latewood produced. The Least Limiting Water Range (LLWR) may provide a conceptual model to frame the influence of soil texture on tree growth, and specifically latewood period, for some stands. Many traditional estimates of moisture availability are based on proxy measurements of field capacity and the wilting point of the soil (USDA 2010) with assumption that all moisture between these two values is available for plant use. LLWR (Letey 1985; Da Silva et al. 1994; Schoenholtz et al. 2000) compliments these measures by incorporating limits imposed by lack of oxygen in the pore spaces at high moisture contents and impediment to root penetration at lower moisture contents. As the bulk density of the soil increases, these limits tend to narrow and reduce the amount of moisture available in a given volume of soil (Daddow and Warrington 1993; Da Silva et al. 1994). This phenomenon would provide a mechanism to limit late-season moisture availability, but only if there was active root growth during the late growing season or the high bulk density soils impeded access to soil moisture

late in the growing season. Many researchers have suggested that root growth ceases before the soil moisture content drops to the point where the bulk density of the soil would limit further root penetration (Joslin et al 2001; Lopez et al. 2001).

In addition to the well documented influence of wood density on the physical properties of forest products, the overall density of annual rings has also been shown to be an important predictor for surviving drought events. High average ring density and higher latewood percentage were associated with lower mortality in plantation grown Douglas-fir following a severe drought in 2003 that impacted much of Europe (Martinez-Meier et al. 2008; Dalla-Salda et al. 2009; Dalla-Salda et al. 2011). Possible explanations for latewood's role in the reduction in Douglas-fir mortality following an extreme drought event included the reduced incidence of embolism at extreme water potentials and increased water storage capability as compared to earlywood (Domec and Gartner 2002). These researchers suggest that at moderate levels of soil moisture deficit, the pits in the earlywood are able to block embolisms from spreading, while some of the most dense latewood pits do not. Water from a portion of the embolizing latewood tracheids is available as a short term reserve. With increasing negative pressure under severe drought conditions, some earlywood pits are unable to block air from leaking past the pit membranes resulting in a rapid decrease in conductance in the earlywood . Under those same conditions, latewood tracheids, still conductive by virtue of their pit geometry, are able to resist embolism and continue transporting water (Tyree and Sperry 1989; Domec and Gartner 2002). Experiments with the hydraulic conductivity of earlywood and latewood in Douglas-fir suggested that under favorable moisture conditions, latewood might only account for 5% of the total conductance of the stem, but under severe drought conditions, that proportion could reach 16% (Domec and Gartner 2002).

Morrow et al. (2013) found that small diameter Douglas-fir growing on low bulk density soils had consistently higher standing Dynamic Modulus of Elasticity (DMOE) values than their counterparts growing on high bulk density soils in suppressed stands in the Bitterroot National Forest outside

Darby, MT. We proposed that the framework of Least Limiting Water Range (LLWR) could explain the differences in DMOE by providing a mechanism for longer latewood periods. If slow growth were coupled with varying amounts of available soil moisture between soil types late in the growing season, then the development the annual rings should reflect those differences. The goal of this study was to determine if systematic differences in ring morphology exist in trees grown on high and low bulk density soils. Average ring density and three measures of latewood were used for comparison: a threshold measure, a smoothed slope inflection measure, and a polynomial measure. The threshold latewood method identifies the position at which the annual rings reached the threshold density, in other words, the position at which the ratio of lumen diameter to cell wall thickness reached a specific value. The dynamic inflection and polynomial methods measure the point at which the change in density reaches its peak, alternatively, the position at which the rate of narrowing lumen diameter and cell wall thickening reaches its peak.

Methods

Selection of subjects

Increment cores and tree measurements were collected from 247 small diameter (10.2-30.5cm diameter at breast height) Douglas-fir growing in the Trapper Bunkhouse region within the Darby Ranger District of the Bitterroot National Forest. Trees were sampled across four elevation zones ranging from 1280m to 2120m, and three stand density classes based on the percent of open canopy. Plots were located on north- to east-facing aspects in stands that were naturally regenerated. Increment cores were removed from the uphill side of three trees at every plot: 1) the one closest to 10cm DBH, 2) closest to 20cm DBH and 3) the one closest to 30cm DBH. After the fieldwork was completed, the soil bulk density on which the trees were growing on was determined using the USGS-NRCS SSURGO soil map for the region (USGS-NRCS 2006) with no spot checking of the soil bulk densities at the sites. The trees were classified into two groups based on the bulk density of

the soil on which they grew: the low Soil Bulk Density (SBD) group (soil density < 1.46 mg/m^3) and the high SBD group (soil density > 1.46 g/cm^3). A more detailed description of the field sampling is found in Morrow et al. (2013).

To avoid the effects of juvenile to mature wood transition, only rings with a cambial age greater than 25 years at breast height in 1976 (the start of the study period) were used. From the remaining 218 trees meeting the criteria, increment cores from 25 individuals from each soil bulk density group were chosen randomly to study the SBD effect. The 12 mm diameter increment cores were glued between pine blanks and ripped to 1.5mm thickness. The radial strips were scanned using a QMS QTRS-01X (Quintek Measurement Systems, Knoxville, TN) X-ray densitometer at 0.2mm intervals. The entire increment cores were scanned; however, only ring data from 1976 to 2005 was used in the analysis. Cracked or otherwise damaged rings were removed from the data set. The resulting set of rings was analyzed to determine if significant differences in the annual ring characteristics could be found in those trees growing on low bulk density soils and those growing on higher bulk density soils.

Average density and latewood measures

Three methods were used to measure the latewood percentage of the annual rings in this study and are outlined in more detail in Chapter Two. The first was a 500kg/m^3 threshold (TLWP) measurement generated by the QMS software. The second was an inflection measurement (INFLWP) generated using a purpose written script in Microsoft Excel VBA that identified the inflection point at which the second derivative of the density/position slope passed through zero during the transition from earlywood to latewood. The third measurement was a polynomial derived measurement (PLWP) similar to that proposed by Koubaa et al. (2002) generated using Matlab (Matlab 2013, MathWorks Inc. Natick, MA, 2013) script. The Matlab script fit a 6^{th} order polynomial and identified the points on the polynomial at which the roots of the second derivative of

the polynomial equaled zero. The latest root was chosen which occurred before the maximum density value, occurred between 20 and 90 percent of total ring length, and exhibited a positive slope when read from earlywood to latewood was chosen. The beginning and end positions of the rings for the threshold method were determined by the QMS software (QMS, Knoxville, Tennessee) at points in which the density passes through the threshold value during the transition from one year's ring to the next. The QMS software also measured the average density (AVGDEN) of the ring. The beginning and end points for the inflection and polynomial methods were determined by identifying the position during the transition from year to year in which the second derivative of the density position profile crossed through zero. An average density for the dynamic measures was also recorded, but because it was essentially identical to that generated by the QMS software, only the average density from the QMS software is reported here.

In Chapter Two, anatomical analysis of a subset of the study trees indicated that the inflection and polynomial methods tended systematically underestimate the amount of latewood in high density annual rings, and overestimate the amount of latewood in low density annual rings. The end result would be a reduction in the apparent difference in latewood percentage in the low and high density rings. To reduce the systematic component of the error present in the inflection and polynomial methods, a linear correction factor developed in Chapter Two was applied to these dynamic latewood measures using the following formulae:

Adjusted Inflection Latewood Percentage (ADJINFLWP)

$$ADJINFLWP = INFLWP + 0.054*AVGDEN - 32.95 \quad (1)$$

Adjusted Polynomial Latewood Percentage (ADJPLWP)

$$ADJPLWP = PLWP + 0.060 * AVGDEN - 31.44 \quad (2)$$

Statistical Analysis

Ring data from 1976 to 1985 was used to develop models for the ring properties using continuous ring characteristics and tree, stand, and site variables measured in 2007 at the time the samples were collected from the field. The potential tree and stand blocking variables as measured in 2007 were: percent green canopy height (PERGRN), basal area measured on plot center(BA), percent closed canopy at plot center(PERCOV), stand density index (SDI), inverse of the mean annual increment of the tree(MAI^{-1}), and elevation measured at plot center (ELEV). The ring characteristics used as blocking variables were: cambial age at breast height (BHAGE), average ring length for the modeling period (AVGRLN), and natural log of the annual ring length of the modeling period (LNAVGRLN). Soil Bulk Density (SBD) was derived from NRCS Soil Survey data as described in Morrow et al. (2013), and trees were divided into two groups (BDGROUP) based on the SBD on which they grew. The treatment variable BDGROUP, year (YEAR), and BDGROUP X YEAR were combined with covariates and interactions to identify significant variables for each ring property initially ignoring autocorrelation. After developing a reduced set of significant variables, random effects and autocorrelation models were established and the models further reduced until the models contained treatment, time, BDGROUP x time interaction, random effects, and two of the most significant and interpretable blocking variables.

Repeated measures Analysis of Variance (ANOVA) was used to model the ring series data collected from the cores using the MIXED procedure in SAS 9.2(SAS Institute, Inc., McGary, NC). Ring data from the ten year time period 1976-1985 was modeled using the two most significant and interpretable blocking variables, the main effects of SBD (BDGROUP), year (YEAR), and the interaction of SBD and year. The full linear mixed model would be the following**:**

$$y_{ijk} = \mu + \alpha y_{ij1} + \beta y_{ij2} + \lambda_i + \tau_k + (\lambda\tau)_{ik} + (S\lambda)_{j(i)} + e_{ijk} \qquad (3)$$

Where y_{ijk} = the ring characteristic from the kth year (1976, …, 2005) of the jth tree (1, …, 25) nested in the ith SBD (low or high). μ is the overall mean; α is the coefficient for the first blocking variable measured for tree y_{ij} ; β is the coefficient for the second blocking variable measured for tree y_{ij}; λ_i is the fixed effect of the ith SBD classification (low or high); τ_k is the fixed effect of the kth year; $\lambda\tau_{ik}$ is the fixed effect of the interaction between ith SBD and kth year; $S\lambda_{j(i)}$ is the random effect (random intercept) of the jth tree nested within the ith SBD classification, ~NID $(0, \sigma^2_{S\lambda})$; e_{ijk} is the random error term, ~NID $(0, \sigma^2)$.

Several covariance structures were tested to develop a best fit model for the correlated residual errors resulting from repeated sampling of the same individual trees through time. For each ring characteristic modeled, the structures tested were: unstructured, first order autoregressive, heterogeneous autoregressive, compound symmetric, heterogeneous compound symmetric, Toeplitz, and heterogeneous Toeplitz. The model that exhibited the lowest value for Schwartz's Bayesian Information Criterion (BIC) was selected as the final model used for that ring characteristic (Littell et al. 1996). Normality of the residuals and the assumption of constant variance of the errors were assessed visually. Once the models for each ring property were established for the calibration years of 1976-1985, the models were rerun using the test ring data from 1986-2005. The results from 1986-2005 were used to assess the significance of SBD on the ring characteristics measured. A primer on repeated measures analysis and more detail on the statistical analysis can be found in Appendix C.

Climate data was collected from the nearest NOAA weather station in Darby, MT, approximately 16 km from the study site and at an elevation of 1160 m (NOAA, 2013). Monthly precipitation and temperature data along with Cooling Degree Days (CDD) were used to investigate the influence of climate on the two SBD groups.

Results

Initially, the data for all rings larger than 0.2 mm were assessed for quality, but it became apparent during the model building process that the disagreements in ring length between the latewood methods and the location of the earlywood/latewood transition generated a great deal of variation in the ring characteristics of some of the smallest rings. Figure 3.1 shows TLWP regressed against ring length for all the rings above 0.2mm. The rings below 0.4mm were typified by extremely high or low earlywood density, rapid transitions from earlywood to latewood, and at times erratic density that caused all three methods of latewood demarcation to return erroneous results. To reduce the measurement uncertainty due to ring start/stop assignment, those rings less than 0.4mm were dropped. The rings shorter than 0.4mm that were dropped were assumed to be missing at random because the smallest rings had the greatest variation in all measures of latewood and average density. Of the initial 1000 rings collected for the test dataset, 43 were dropped because they were less than 0.2 mm or damaged, 85 were dropped because they were less than 0.4mm, the oldest tree in the high and low SBD group were dropped (5+ standard deviations from mean age, total of 40 rings), two trees were dropped because they only had 6 valid rings between them, and one tree from the low SBD group was dropped because it had unusually high latewood percentage and was suspected of containing compression wood. A total of 45 of the original 50 trees were used in the final analysis.

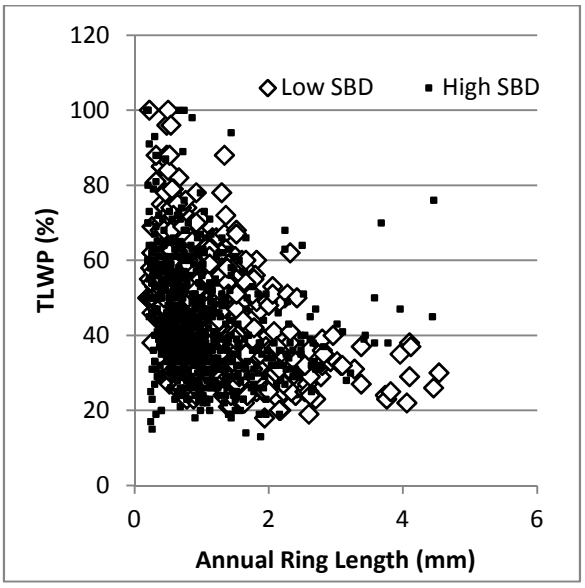

Figure 3.1. Plot of TLWP vs RINGLEN

Figure 3.1 also show the distribution of TLWP had a large right tail, as did all the other measures of latewood. After modeling the calibration data set, the residuals appeared to flare with increasing predicted TLWP (See Appendix C). The latewood measures were adjusted using a natural log transformation, and the resulting residuals exhibited constant variation across the range of predicted values with the prediction data set. The log transformed latewood measures were used for the final analysis.

A summary table of the trees included in this study is shown in Table 3.1. On average, the height and diameter were similar, likely owing to the similar age and stand density distributions. The average elevations were similar, but the distributions were somewhat different and are explained in the Discussion section.

Table 3.1. Low and high SBD sample populations, standard deviation in parentheses

Property	SBD group Low <1.46 g/cm^3	 High >1.46g/cm^3
Mean age in 1986 (yr)	55.9 (11.3)	56.0(9.6)
Elevation (m)	1774 (258)	1719 (170)
Oldest tree in 1986 (yr)	84	76
Youngest tree in 1986 (yr)	36	38
Basal area on plot(m^2)	14.6 (6.0)	12.9 (4.5)
DBH (cm)	22.7 (5.6)	23.5 (5.6)
Total height (m)	15.5 (3.4)	15.9 (3.4)
Average ring length 1986-2005 (mm)	0.94 (0.38)	1.00 (.49)
Number of trees in sample	22	23

Linear mixed model results

A description of the variable names are shown in Table 3.2 After determining the most significant and interpretable variables and covariance matrix that provided the best fit for the calibration data set from rings added between 1976 to 1985 (results shown in Table 3.3), the models were rerun with the ring data from 1986 to 2005, the results of which are shown in Table 3.4. The first order autoregressive covariance model was found to provide the best fit (using BIC) for all ring property models. All models indicated that YEAR was highly significant, likely indicating that variation in annual climate played an important role in the ring characteristics modeled.

Table 3.2. Descriptions of ring variables used in the analysis

Ring variable	Description
LNTLWP	Log transformed threshold latewood percentage
TAVGDEN	Average ring density using threshold method
LNPLWP	Log transformed polynomial latewood percentage
LNADJPLWP	Log transformed polynomial latewood after adjustment using equation 2
LNINFLWP	Log transformed inflection latewood percentage
ADJLNINFLWP	Log transformed inflection measurement after adjustment using equation 1

Table 3.3. Results of ring property models for calibration dataset

		Parameter Estimates		Type 3Test of Fixed Effects			
Property	Source	Coefficient	Std. Err.	Num d.f.	Den d.f.	F-value	P-value
LNTLWP	Intercept	3.42	.201	1	41.2	365	**<.0001**
	LNAVGRL	-0.184	0.0865	1	42.6	4.54	**.0389**
RMSE	BHAGE	0.00671	0.346	1	40.9	3.77	.0591
0.145	BDGRP	0.132	0.0869	1	41.5	2.21	.1443
Bias	YEAR			9	306	13.98	**<.0001**
-0.000787	BDGRP X						
	YEAR			9	288	3.19	**.0011**
TAVGDEN	Intercept	593	73.9	1	40.7	74.7	**<.0001**
	ELEV	-0.0869	0.0325	1	40.6	7.12	**.0109**
RMSE	BHAGE	2.00	0.714	1	40.7	7.82	**.0079**
27.8	BDGRP	44.4	17.8	1	41.1	1.95	.1704
Bias	YEAR			9	311	13.4	**<.0001**
-0.0693	BDGRP X						
	YEAR			9	293	4.20	**<.0001**
LNPLWP	Intercept	3.33	0.114	1	42.3	1280	**<.0001**
	LNAVGRL	-0.194	0.0789	1	43.1	6.02	**.0183**
RMSE	PERGRN	-0.226	0.157	1	42.8	2.08	.1567
0.155	BDGRP	0.0285	0.0845	1	41.3	1.87	.1787
Bias	YEAR			9	285	8.27	**<.0001**
-0.00150	BDGRP X						
	YEAR			9	285	2.77	**.0040**
ADJLNPLWP	Intercept	3.44	0.149	1	42.3	805	**<.0001**
	LNAVGRL	-0.203	0.104	1	43.1	4.95	**.0313**
RMSE	PERGRN	-0.346	0.205	1	42.8	2.84	.0992
0.195	BDGRP	0.107	0.109	1	41.3	2.04	.1607
Bias	YEAR			9	289	12.89	**<.0001**
-0.000770	BDGRP X						
	YEAR			9	289	3.60	**.0003**
LNINFLWP	Intercept	3.02	0.159	1	40.8	472	**<.0001**
	LNAVGRL	-0.186	0.0679	1	42.9	7.53	**.0088**
RMSE	BHAGE	0.00541	0.00269	1	40.5	4.05	.0508
0.166	BDGRP	0.0196	0.0783	1	41.2	2.10	.1653
Bias	YEAR			9	309	7.16	**<.0001**
-0.000800	BDGRP X						
	YEAR			9	291	2.10	**.0293**
ADJLNINFLWP	Intercept	2.55	0.252	1	40.7	140	**<.0001**
	LNAVGRL	-0.262	0.108	1	42.7	5.83	**.0201**
RMSE	BHAGE	0.0107	0.00430	1	40.4	6.16	**.0173**
0.242	BDGRP	0.124	0.253	1	41.1	2.64	.1116
Bias	YEAR			9	310	11.7	**<.0001**
-.000792	BDGRP X						
	YEAR			9	292	2.97	**.0022**

Table 3.4. Results of ring property models for Test period

		Parameter Estimates		Type 3Test of Fixed Effects			
Property	Source	Coefficient	Std. Err.	Num d.f.	Den d.f.	F-value	P-value
LNTLWP	Intercept	3.43	0.242	1	41.2	285	**<.0001**
	LNAVGRL	-0.139	0.102	1	41.3	1.87	.179
RMSE	BHAGE	0.00330	0.00318	1	41.2	1.08	.305
0.142	BDGRP	0.179	0.0814	1	41.1	5.39	**.0253**
Bias	YEAR			19	647	8.94	**<.0001**
-0.000768	BDGRP X						
	YEAR			19	652	0.81	0.695
TAVGDEN	Intercept	545	79	1	41.1	60.2	**<.0001**
	ELEV	-0.0683	0.0310	1	41.1	3.87	.0559
RMSE	BHAGE	1.28	0.679	1	41.2	3.56	.0661
28.4	BDGRP	44.4	17.6	1	41.1	7.56	**.0088**
Bias	YEAR			19	644	11.2	**<.0001**
-0.0500	BDGRP X						
	YEAR			19	651	1.26	0.202
LNPLWP	Intercept	3.26	0.127	1	40.8	952	<.0001
	LNAVGRL	-0.244	0.109	1	41	5.00	**.0308**
RMSE	PERGRN	-0.0502	0.167	1	40.8	0.09	.766
0.162	BDGRP	0.0513	0.0903	1	40.8	2.40	.129
Bias	YEAR			19	647	8.82	**<.0001**
-0.00169	BDGRP X						
	YEAR			19	647	1.27	0.196
ADJLNPLWP	Intercept	3.28	0.157	1	41	646	**<.0001**
	LNAVGRL	-0.283	0.135	1	41.2	4.40	**.0421**
RMSE	PERGRN	-0.108	0.207	1	41	0.27	.604
0.196	BDGRP	0.140	0.111	1	41	4.56	**.0387**
Bias	YEAR			19	647	9.85	**<.0001**
-0.00125	BDGRP X						
	YEAR			19	647	1.13	.319
LNINFLWP	Intercept	3.21	0.232	1	41	263	**<.0001**
	LNAVGRL	-0.241	0.0974	1	41.2	6.13	**.0175**
RMSE	BHAGE	0.00121	0.00304	1	41	0.16	.693
0.156	BDGRP	0.0777	0.0824	1	40.9	2.41	0.1281
Bias	YEAR			19	650	7.75	**<.0001**
-0.000824	BDGRP X						
	YEAR			19	651	1.2	.248
ADJLNINFLWP	Intercept	2.80	0.341	1	41.1	97.65	**<.0001**
	LNAVGRL	-0.324	0.143	1	41.3	5.12	**.0289**
RMSE	BHAGE	0.00397	0.00448	1	41.2	0.79	.3803
0.223	BDGRP	0.173	0.120	1	41	4.68	**.0365**
Bias	YEAR			19	647	8.12	**<.0001**
-.000845	BDGRP X						
	YEAR			19	650	1.02	.435

The significance of the blocking variables dropped somewhat for all ring models, though many retained significance at an alpha level of 95%, most notably, LNAVGRL. The parameter estimates for the blocking variables were also similar for the calibration and test periods, as were the measures of fit provided by RMSE and Bias calculated for the models. The most meaningful change from the calibration period models (1976-1985) to the test period models (1986-2005) was the shift in the significant treatment effects from the treatment by year interaction term in the calibration models to the treatment main effect term in the test models. All ring characteristic models had significant

BDGRP X YEAR interaction terms in the calibration models, and none of the test models had significant BDGRP X YEAR interactions. Instead, the models for the test period indicated that LNTLWP, TAVGDEN, ADJLNPLWP, and ADJLNINFLWP had significant main effects for BDGRP with parameter estimates that were not significantly different than the estimates from the calibration models. The nature of the differences in the previously mentioned ring characteristics between the low and high SBD groups changed from an intermittent significant difference to a sustained significant difference.

Threshold method and average density

From Table 3.4, BDGRP was found to be significant at the 95% confidence level for LNTLWP, with a marginal mean of TLWP of 47% and 40% for trees grown on low and high bulk density soils respectively, and a RMSEP of approximately 14% (or approximately 6% TLWP at the mean). Neither LNAVGRL nor PERGRN were significant at a 95% confidence level. Figure 3.2 shows LNTLWP transformed back to the original units for the test period. TLWP for the low SBD group was always higher during the test period, and the two SBD groups moved in concert with one another for the study period.

The model for TAVGDEN indicated that BDGRP was a significant at a 99% confidence level with marginal means of 571 kg/m3 and 532 kg/m^3 for the low and high bulk density groups respectively, for a difference of 40 kg/ m^3 (or 7.5%) between the groups on average across the study period. ELEV was somewhat significant with an estimated decrease of 0.02 kg/ m^3 per meter of elevation gain. Similarly, BHAGE was somewhat significant with an increase of about 1.3 kg/ m^3 per additional year of age. The model had a RMSEP of 28.4kg/ m^3 and the marginal means of TAVGDEN by year are shown in Figure 3.3

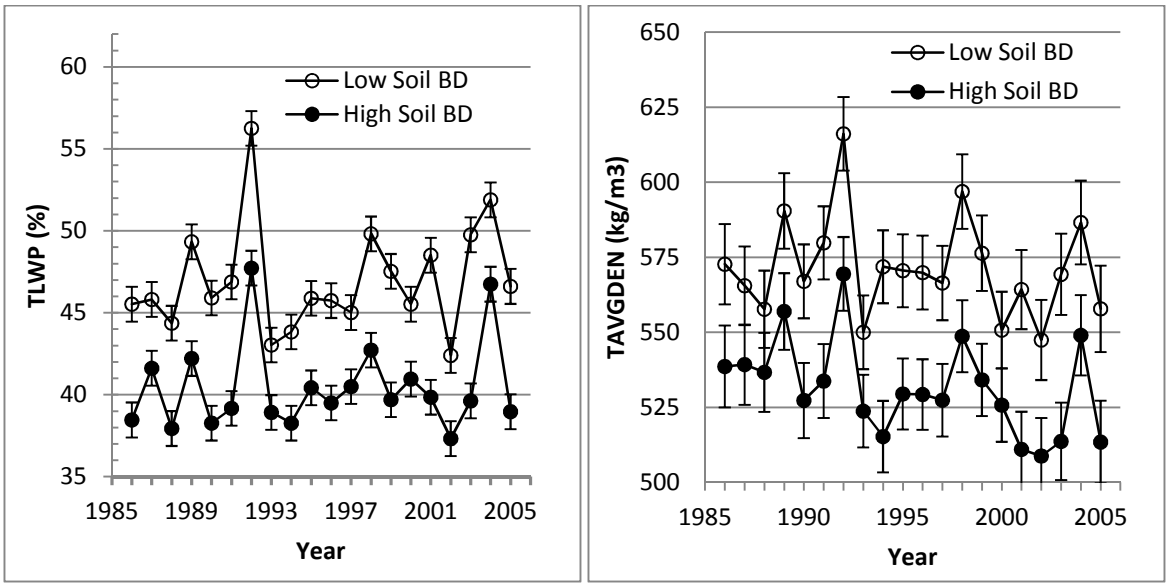

.

Figure 3.2. Marginal means of TLWP over the period 1986-2005 (Bars indicate one standard error)
Figure 3.3. Marginal means for TAVGDEN during the years 1986-2005 (Bars indicate one standard error)

Polynomial method

Table 3.4 shows that LNPLWP indicated that neither BDGRP nor BDGRP X YEAR were significant at a 95% level, with estimated average PLWP values of 28% and 25% for the low and high bulk density groups respectively and a RMSE of 4% PLWP at the mean. LNAVGRL was found to be significant with a 1% increase in average ring length resulting in a 0.24% decrease in PLWP. The marginal means of LNPLWP transformed back to the original units for the study period are shown in Figure 3.4.

The model for ADJLNPLWP indicated that BDGRP was significant at a 95% confidence level, with marginal means of 30% and 25% for the low and high SBD groups respectively with an RMSE of 5% at the mean. LNAVGRL was also found to be significant with a decrease of 0.28% PLWP for every 1% increase in ring length. Figure 3.5 shows the marginal means of LNADJPLWP transformed to the original units over the study period.

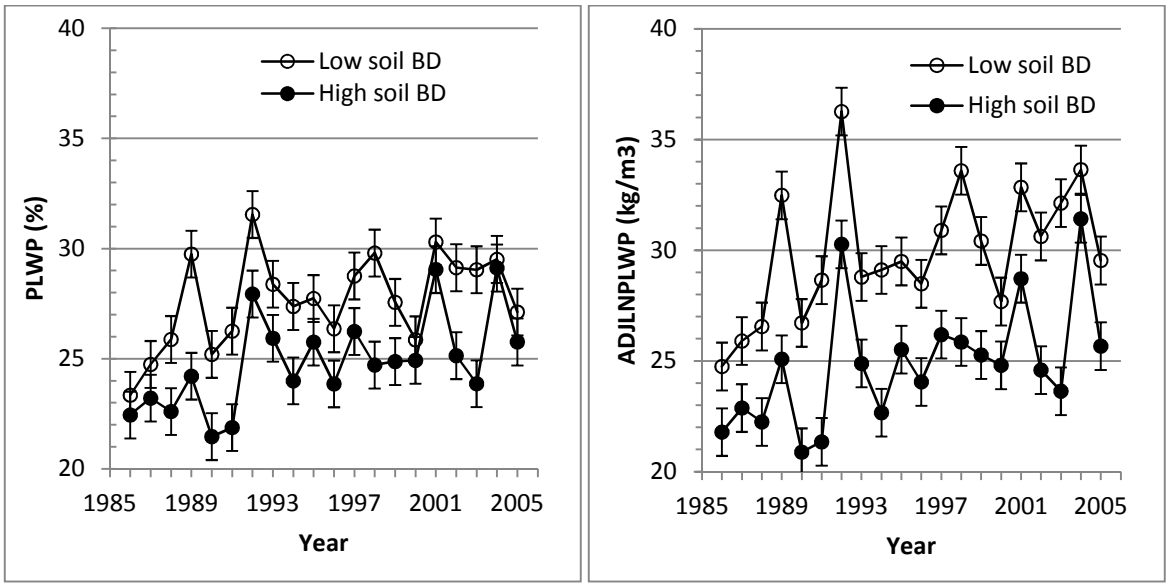

Figure 3.4. Marginal means of LNPLWP transformed to the original units for the study period (Bars indicate one standard error)
Figure 3.5. Marginal means of ADJLNPLWP transformed to the original units for the study period (Bars indicate one standard error)

Inflection method

From Table 3.4, neither BDGRP nor BDGRPxYEAR were found to be significant for LNINFLWP with estimated INFLWP levels of 30% and 27% for the low and high bulk density soils respectively. LNAVGRL was found to be significant at a 95% confidence level with a parameter estimate of 1% increase in ring length resulting in a 0.24% decrease in INFLWP. The marginal means of LNINFLWP transformed to its original units are shown in Figure 3.6.

The model for ADJLNINFLWP indicated that BDGRP was a significant factor (P=0.037), and that the BDGRPxYEAR interaction was not. The mean values of ADJLNINFLWP transformed back to the original units were 27% and 22% for the low and high SBD groups respectively. LNAVGRL was likewise significant at a 95% confidence level with a parameter estimate of 1% increase in ring length resulting in a 0.32% decrease in ADJINFLWP. The model had a RMSE of approximately 6%

ADJINFLWP at the mean. The marginal means of ADJLNINFLWP transformed to its original units are shown in Figure 3.7.

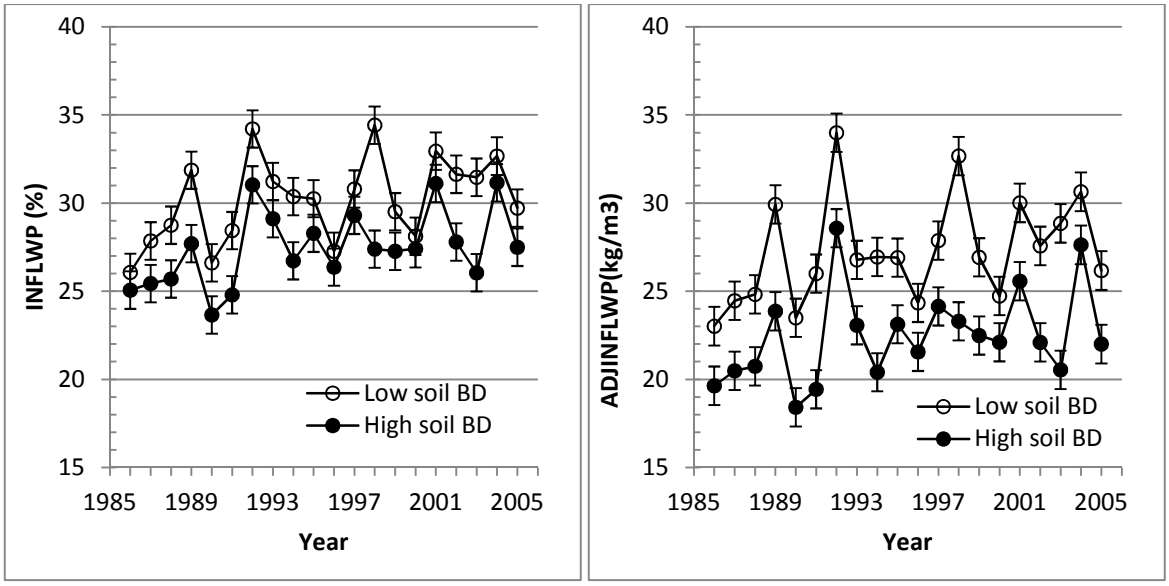

Figure 3.6. Marginal means of LNINFLWP transformed to the original units for the study period (Bars indicate one standard error)
Figure 3.7. Marginal means of ADJLNINFLWP transformed to the original units for the study period (Bars indicate one standard error)

Comparison of latewood measurement methods

The parameter estimates reported by the ANOVA for the effect of BDGRP and the significance of the BDGRP effect on LNTLWP, ADJLNPLWP, and ADJLNINFLWP were similar across both periods (Tables 3.3 and 3.4), and the measures generally reflected similar trends in the differences between SBD groups from year to year. Figure 3.8 shows the percent difference in latewood measures between the two SBD groups (trees on low bulk density soil had higher average latewood percentages for all years except 1980) for the entire study period. The adjusted polynomial and inflection methods occasionally reported more exaggerated differences between the two SBD groups than the threshold method (e.g. 2003, 1998, 1994, 1984), though for many years, there was no real difference between the latewood measures (e.g. 1976-1979, 1985-1988).

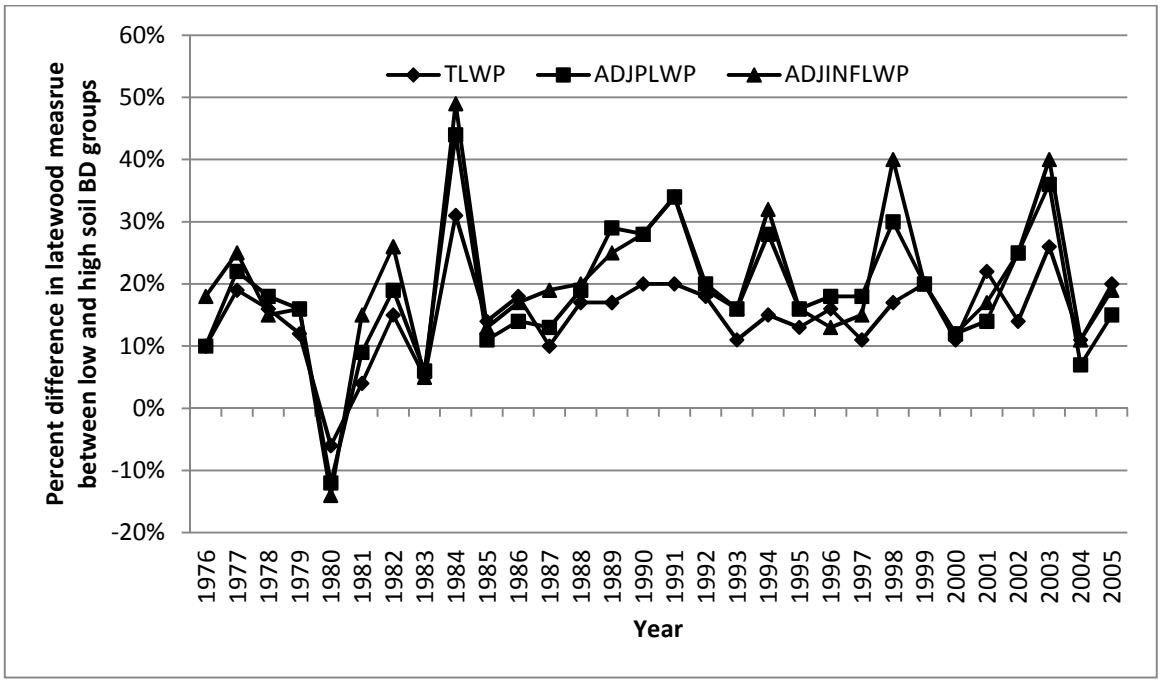

Figure 3.8. Percent difference in latewood percentage throughout the study period using the threshold, adjusted polynomial, and adjusted inflection methods.

The results of the models for the unadjusted polynomial and inflection latewood measures suggested there was much less difference between the two SBD groups. In Figure 3.9, the average percent difference between the two SBD groups are graphed for the entire study period. For all but a handful of years, the difference in SBD groups is less than that measured by the threshold method. This reduced level of difference is reflected in the ANOVA results for the test period in Table 3.4; BDGRP does not appear to be a significant factor when using the unadjusted dynamic latewood measures to compare the trees grown on low and high bulk density soils.

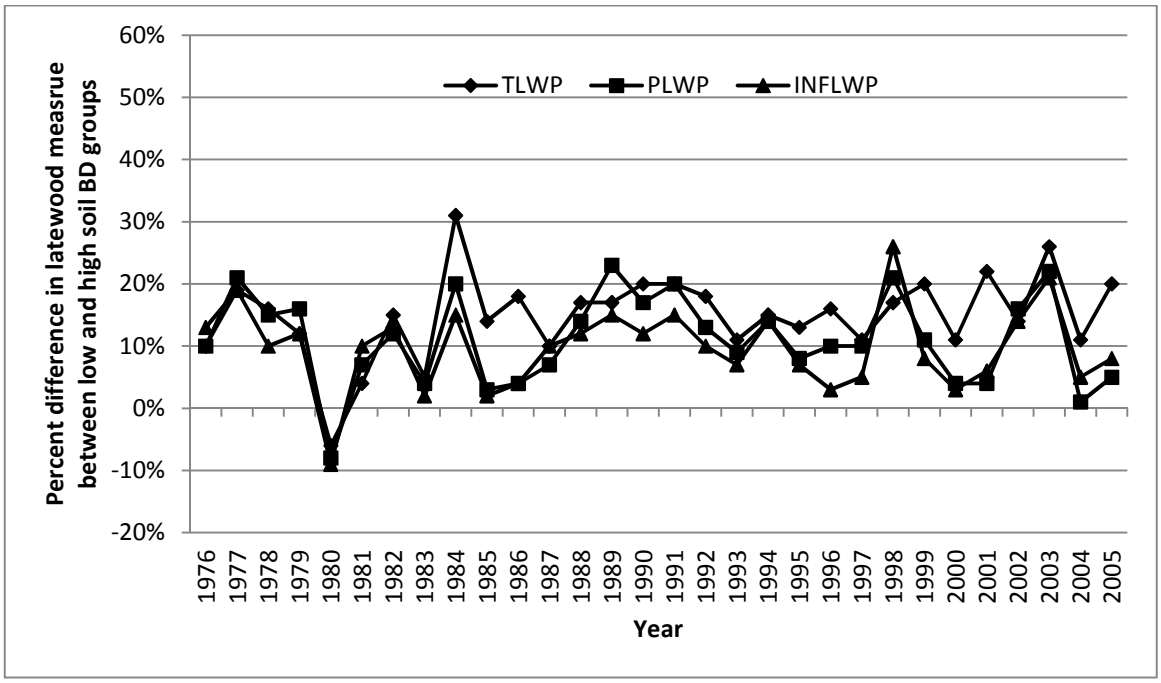

Figure 3.9. Percent difference in latewood percentage throughout the study period using the threshold, polynomial, and inflection methods

Climate effects

In an effort to understand the significance of YEAR and why the significant effect of BDGRP was found in the BDGRPxYEAR interaction for the calibration data set (1976-1985) and as a main effect in the test data set (1986-2005), climate data from the nearest weather station in Darby, MT (approximately 16 km from site and at elevation of 1160m) for all data periods were collected (NOAA, 2013). The most dramatic differences in climate between the periods were found in the extreme temperatures late in the growing season and May precipitation. Figure 3.10 shows the sum of Cooling Degree Days (18.3°C basis) for July and August from 1955 to 2005. During the calibration period, the trees experienced a narrower range and lower average levels of late season heat than during the test period. In addition, there was almost twice the range in May precipitation during the calibration period compared to the test period, as shown in Figure 3.11.

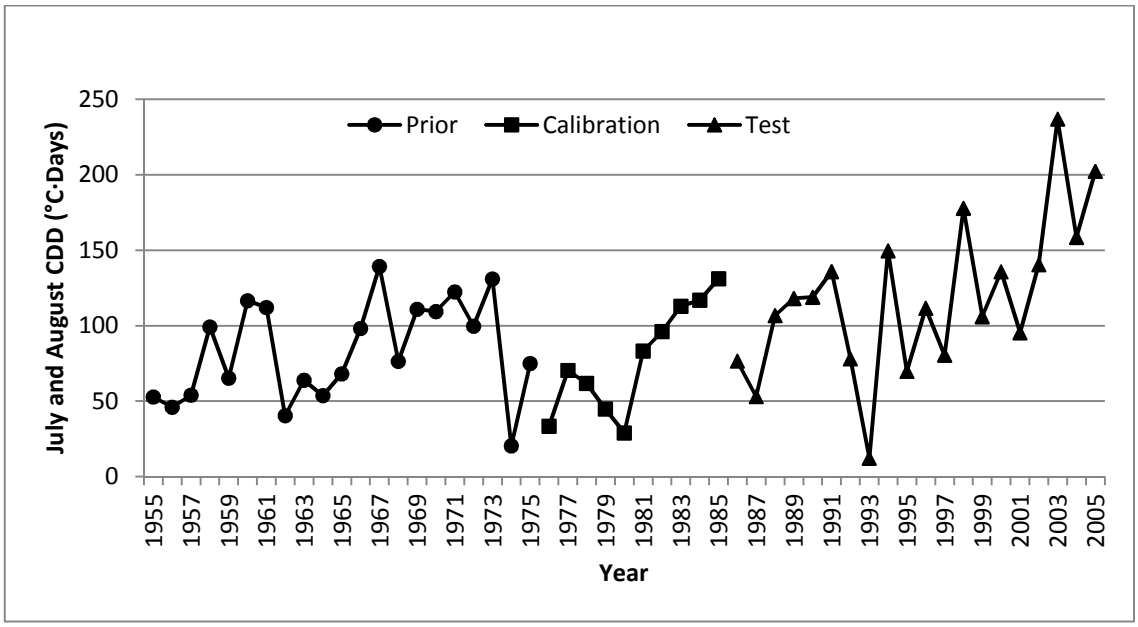

Figure 3.10 Sum of July and August CDD (65°F basis) from 1955 to 2005

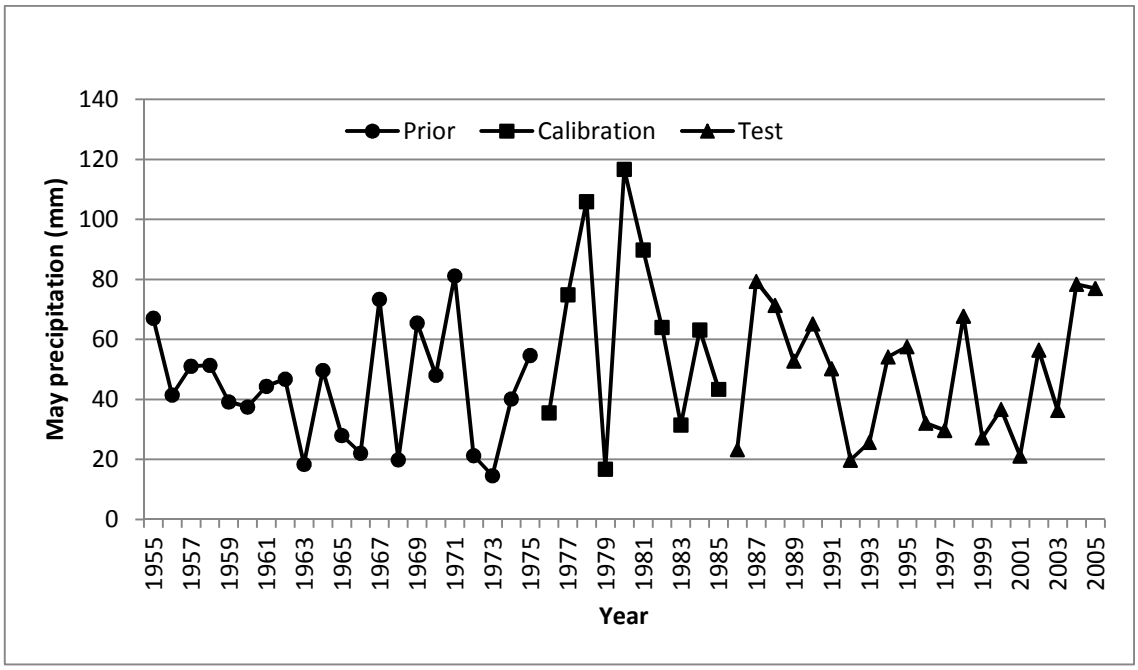

Figure 3.11 May Precipitation from 1955 to 2005

Table 3.4 shows the percent difference in average density for the calibration and test period between trees grown on low and high bulk density soils. During the calibration period, the average difference was 4%, but there was one year (1980) in which trees grown on high bulk density soils averaged 3% higher density than trees grown on low bulk density soils. Climate data for this year revealed that 1980 registered the highest May precipitation and the third coldest (in terms of CDD) July and August in the 50 year record.

Table 3.5. Percent difference in AVGDEN between low and high bulk density soil groups

Dataset	Mean	N	SD	Range	Minimum	Maximum
Calibration	4.0%	10	3.9%	14.5%	-3.0%	11.2%
Test	7.5%	20	2.0%	7.1%	3.9%	11.0%
Total	6.3%	30	3.2%	14.5%	-3.0%	11.2%

If the yearly percent differences in average density are binned by their Z-score, the resulting distribution by Z score is shown in Figure 3.12. Using the same Z-score grouping, monthly precipitation and CDD data are plotted in Figures 3.13 and 3.14. In Figures 3.13 and 3.14, the lines represent the average monthly precipitation and CDD for the years which produced AVGDEN differences of their respective Z scores, with the average (circles) for the 30 years with error bars representing one standard error from the 30 year average. The year producing the least difference were years with higher than average May (and June for the year 1980) rainfall seen in Figure 3.11 and considerably lower than average temperatures as seen in Figure 3.10. Conversely, those years producing the highest difference between the SBD groups exhibited slightly lower than average rainfall during May and June, but experienced higher than average CDDs during July and August. As shown in Figure 3.15, plotting May precipitation (a) and July/August CDD (b) against the percent difference in AVGDEN between the two SBD groups, the trend with precipitation is very weak and seems to be heavily dependent on the extremely high precipitation year 1980, but the trend for July/August CDD appears to be a much better fit with an $R^2 = 0.43$.

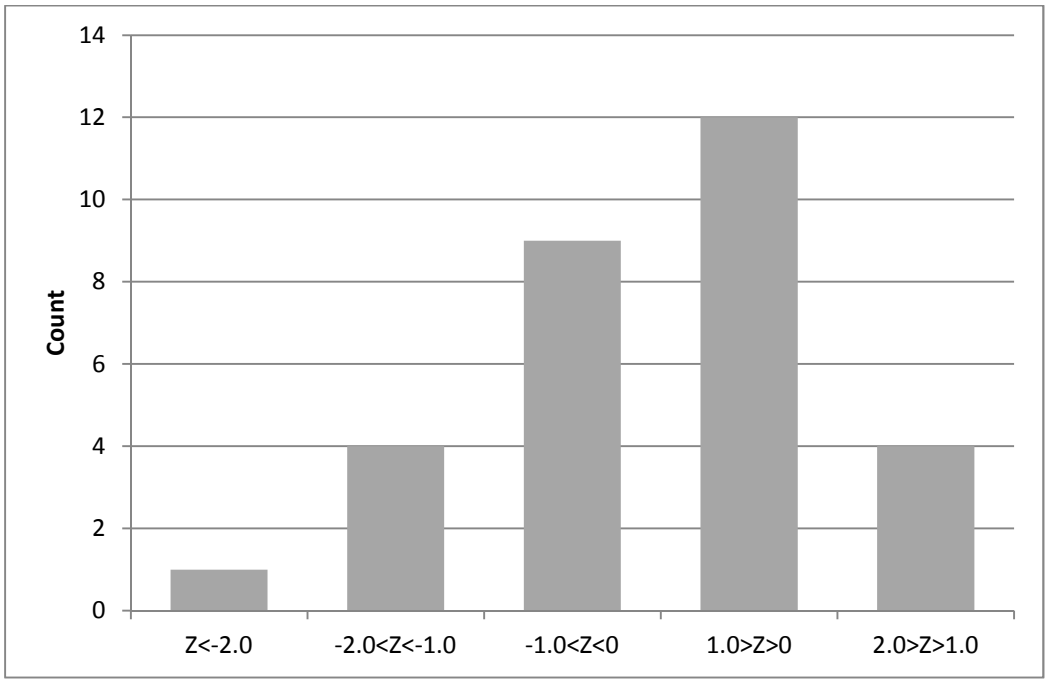

Figure 3.12. Distribution of Z scores for the percent difference of AVGDEN between SBD groups

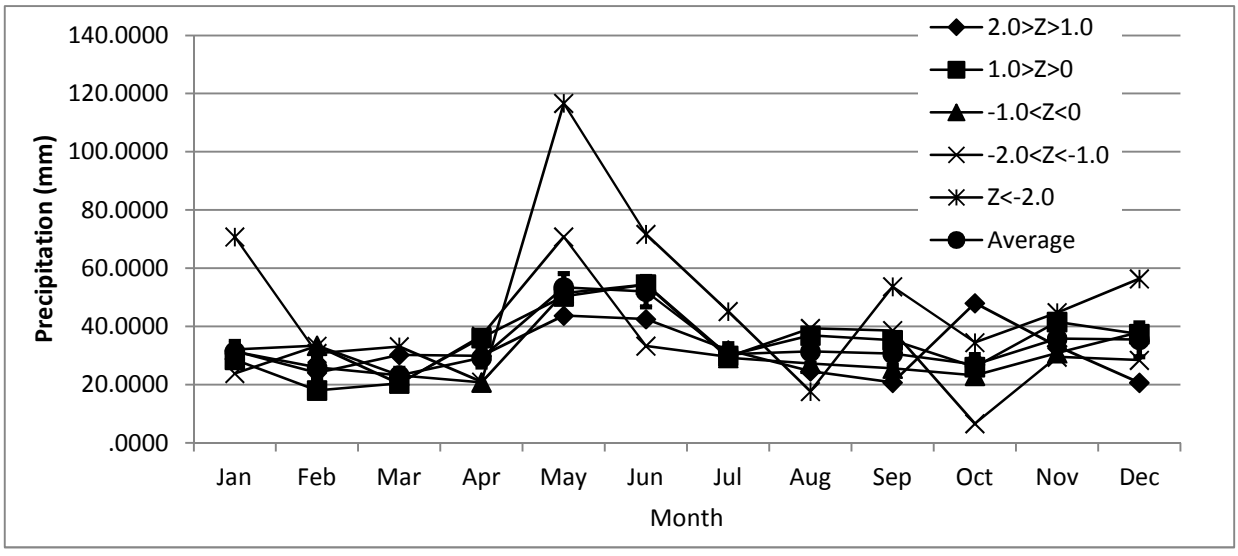

Figure 3.13. Mean monthly precipitation for entire study period by Z-score of AVGDEN difference between low and high bulk density soils (error bars represent one standard error)

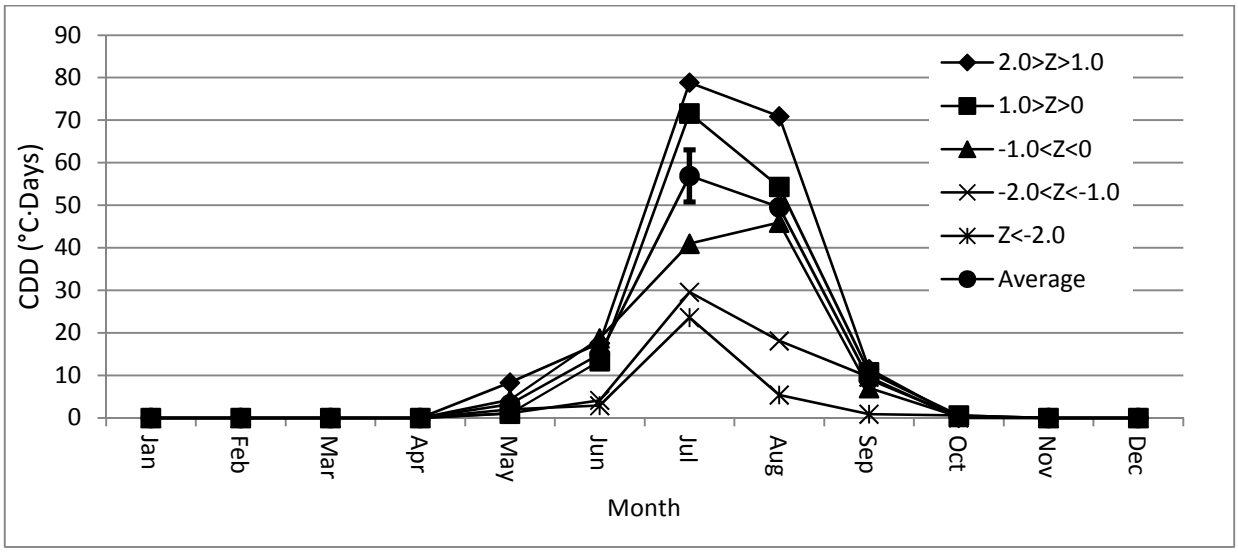

Figure 3.14. Mean monthly CDD for entire study period by Z-score of AVGDEN difference between low and high bulk density soils (error bars represent one standard error)

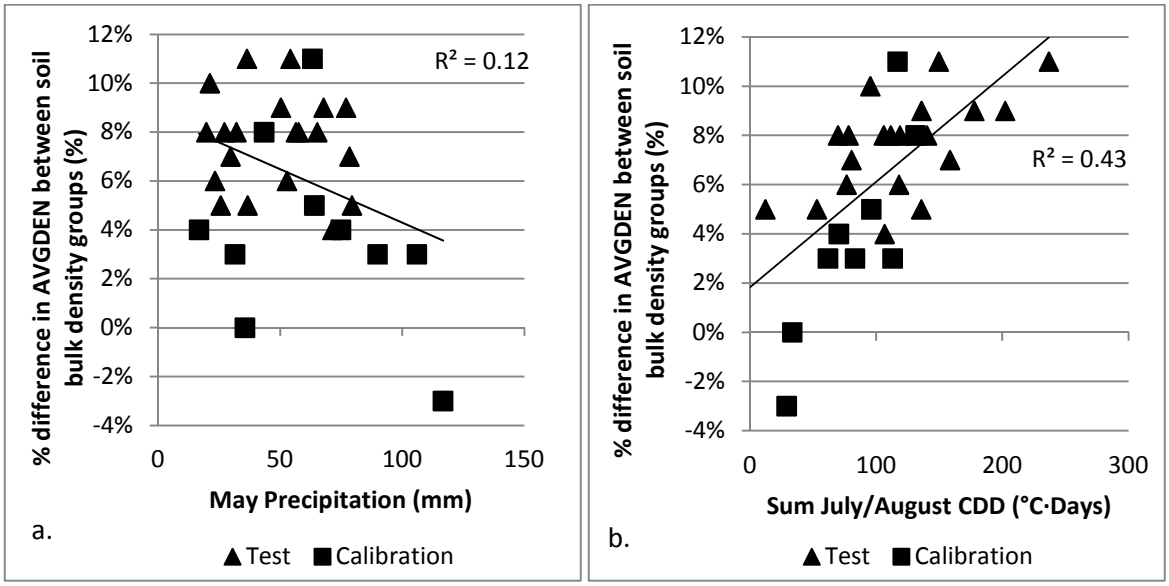

Figure 3.15. Fit of May precipitation and percent difference in AVGDEN between the two SBD groups (a). Fit of July/August CDD and percent difference in AVGDEN between the two SBD groups (d). Regression lines represent the best-fit for both periods combined

Discussion

The working hypothesis at the outset of this research was that trees grown on low bulk density soils had increased availability of soil moisture in the late growing season over trees grown on higher bulk density soils. It was theorized that this persistent late season differential in available soil moisture would manifest itself as longer latewood percentages and increased average densities in those trees grown on low bulk density soils. The models built to test the significance of SBD supported that hypothesis on several levels.

Comparison of latewood measures

For the test data set (rings added between 1986-2005), the models indicated that trees grown on low bulk density soils had higher latewood percentage, but the difference was not significant for all measures. The ANOVA models (Table 3.4) suggest that during the test period, the difference between the two groups ranged between a significant 18% difference for the threshold method to a non-significant 5% difference for the unadjusted PLWP. The polynomial and inflection methods produced mixed results dependant on whether or not the adjusted values were used. The polynomial and inflection methods were intended to identify the point at which the thickening cell walls and narrowing lumen create the highest rate of change in density from tracheid to tracheid along a radial profile. The adjustment factors used for this Chapter (equations 1 and 2) were instituted to try and reduce the systematic errors found in Chapter Two, to improve the dynamic measures' ability to identify the point-of-most-change in cell wall thickness and lumen diameter. In the unadjusted values found in the anatomical section of Chapter Two, the dynamic measures seemed to systematically overestimate the amount of latewood in low density rings and underestimate the amount of latewood in higher density rings, leading to reduced apparent differences. The models in Table 3.4 for the unadjusted polynomial and inflection latewood methods indicated that the effect of BDGRP was not significant, with parameter estimates of 5% and 8% for the effect of BDGRP on the models for the

polynomial and inflection methods respectively. These would translate to differences of 3% PLWP and 3% INFLWP on average through the study period.

After adjustment, however, the model for dynamic measures of latewood percentage returned similar results as the model for TLWP. The model for adjusted PLWP indicated a difference of 14% (or 5% higher PLWP for low SBD) between low and high SBD groups, and the model for adjusted INFLWP estimated a 17% difference (or 5% higher INFLWP for low SBD trees). The models for the threshold and adjusted dynamic measures all suggested the same thing; there was a significant difference in between SBD groups of between 5% and 7% actual latewood percentages on average over the course of the test period. The fact that the results were so similar may be related to the rapid transition from earlywood to latewood typical in Douglas-fir annual rings (Bowyer et al. , 2003), and the findings in Chapter Two that large deviations between the threshold and dynamic measures are generally only seen in rings exhibiting extreme values of average density.

Average density and climate interaction with SBD

The model for AVGDEN suggested that the effect of BDGRP was highly significant (beyond 99% confidence level) during the test period and that the difference in AVGDEN over the test period was approximately 40kg/m^3 at laboratory conditions. Transforming the densities for each SBD group at lab conditions to an estimated green specific gravity, the average for the low SBD group was about 0.49, while the average for the high SBD group was about 0.45 (USDA 2001).

In addition to the significance of the effect of BDGRP during the test period, the contrasting behavior of the models from the calibration period (1976-1985) to the test period (1986-2005) further supports a site affect associated with SBD. Using AVGDEN as an example, the calibration model indicated a highly significant ($P<0.0001$) BDGRP X YEAR interaction. When the model was employed on the test period data, the interaction term was not found to be significant, but the main

effect of BDGRP was. Variation in climate variables seems to explain the significance of both the interaction and the main effect.

During the calibration period, two cold years: 1976 and 1980, presented conditions that resulted in no difference (1976), and the only year in the 30 studied in which the high SBD group had higher AVGDEN than the low SBD group (1980). When growing conditions were exceedingly mild and sufficient soil moisture was present, there was no difference between the two SBD groups, and even a reversal of the SBD effect. Removing these two years from the calibration dataset results in a non-significant BDGRPxYEAR interaction, as well as a non-significant main effect for BDGRP during the calibration period. Mild conditions during 1976-1985, excepting 1976 and 1980, contributed to a higher, but not significantly higher, average density for trees growing on low bulk density soils.

During the test period, there was a relatively sustained difference in AVGDEN between the two SBD groups, a consistently higher average density in low SBD trees, and is reflected in the significance of the main effect of BDGRP, not the interaction with year. In Figure 3.10 and 3.11, it can be seen that the severity of the July/August period was frequently more extreme in the test period than the calibration period, and there were no cold/wet years like 1976 or 1980. Figure 3.15b suggests a good fit between July/August CDD and the percent differences of AVGDEN between SBD groups across both the calibration and the test periods. More frequent hot July/August in the test period seemed to lead to a significant BDGRP main effect for AVGDEN.

The only other broad-scale site variable collected that seems likely to cause this sort of difference with AVGDEN would be elevation. If the two SBD groups examined here were not drawn from equivalent elevations, there could be an opportunity for elevationally induced climate variation to appear as an effect of SBD, leading to larger latewood percentages and higher average density due to uneven sampling, not SBD. To explore if differences in elevation distributions between SBD groups could explain the differences, Figure 3.16a shows the distribution of elevations for the two SBD

groups that were included in the study. The trees sampled from each group cover approximately the same range, but the low bulk density trees seem to have more individuals from the lowest and highest elevation levels, while the high SBD group has more individuals in the middle elevation levels. However, the residuals for AVGDEN from both SBD groups in Figure 3.16b appear to be similarly distributed across their shared elevation range, indicating that even though the distribution of elevations was not identical, there was no systematic difference in the random errors across the elevation range between the two groups. Although the elevational composition of the two SBD groups were not identical, they appeared to be adequately similar for comparison purposes.

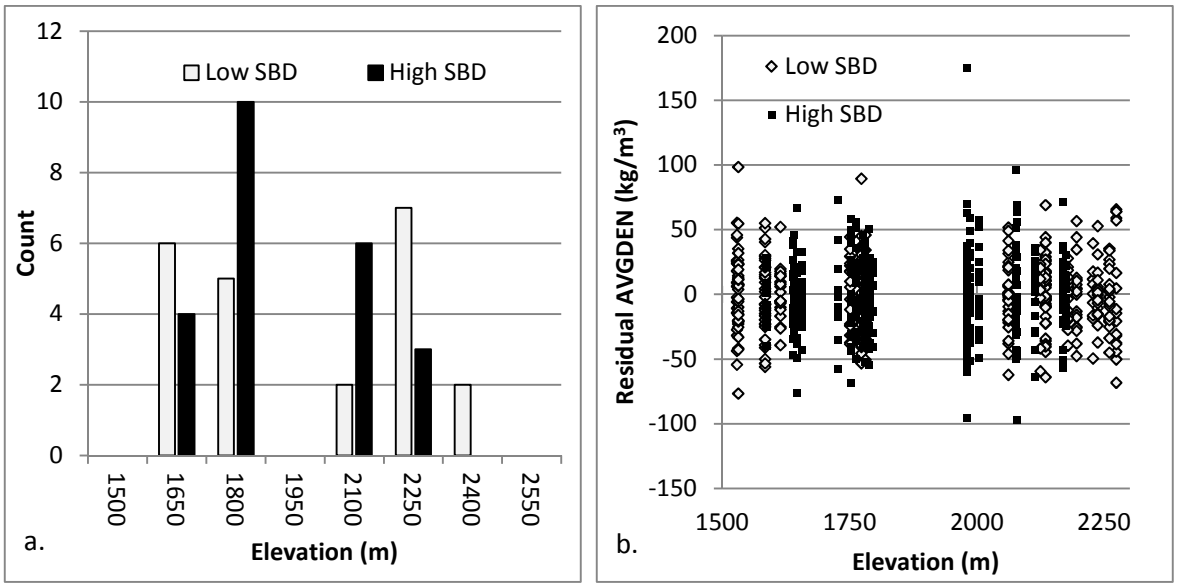

Figure 3.16. Comparison of elevations between SBD sample groups. Histogram of elevation distribution for the two sample groups (a), residuals of AVGDEN fit against elevation for the two treatment groups (b).

When additional interactions between BDGRP, ELEV, and YEAR are added using the same covariance framework as the base models found in Tables 3.2 and 3.3, the model indicates that all the 2 way and the 3-way interaction are significant, but all the interactions significantly raise the BIC value, indicating a less parsimonious or more overfit model compared to the base model. The behavior accounted for by the interactions is illustrated in Figure 3.17. Figure 3.17a shows

AVGDEN for all trees in 1980, the coldest and wettest in the study period, across the elevation gradient sampled. As mentioned previously, 1980 was the only year in which the marginal mean of AVGDEN was higher for the high SBD group than the low SBD group, and both sample groups seem to exhibit a similar negative correlation with elevation. Of all the years for which measurements were taken, 1980 should have been the least limited by soil moisture. Conversely, Figure 3.17b shows the AVGDEN of all trees across the elevation gradient for the year 2003, the hottest year in the study period. The AVGDEN of the low SBD group exhibits an almost identical regression to ELEV as in 1980, but the high SBD group, especially those below 2000m, dropped by approximately 100kg/m^3 when taken as a group. In addition to being the hottest year in the study period, 2003 was the third year of an extended drought as measured by the Palmer Drought Severity Index published for the region (NOAA, 2013(a)). 2003 should have been one of the years most limited by low soil moisture. The magnitude of this gap seems to drive the differences in AVGDEN between the groups seen in Figure 3.15b, and the introduction of ELEVXYEAR, BDGRPXELEV, and BDGRPXELEVXYEAR interactions all refine the patterns in Figure 3.17 to the detriment of the BIC values of their respective models. During the moderate climatic conditions of most of the calibration period, the difference between SBD groups was modest, during the hotter and drier test period; the difference between SBD groups exemplified in Figure 3.17b was sustained through much of the period.

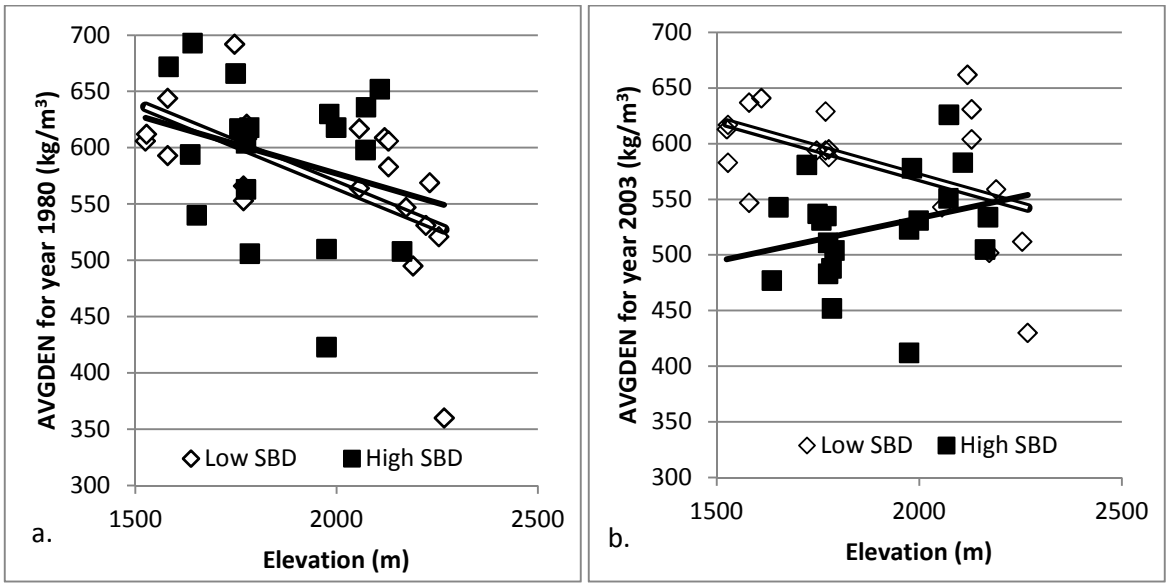

Figure 3.17. Average density by elevation for the low and high SBD groups in 1980 (a), and 2003(b).

The LLWR concept provides a possible explanation for these findings. As discussed in Morrow et al, the LLWR model suggests that trees growing on lower bulk density soils should, on average, have more water available after decreasing soil water potential triggers the thickening of tracheids and before the soil dries to the point where additional root penetration is not possible or the wilting point. The work of Larson and others suggests that the timing of available moisture is a critical factor in the creation of additional latewood, and the LLWR concept provides an explanatory mechanism by which trees on low bulk density soils, receiving similar amounts of total precipitation and experiencing similar climatic conditions have extended access to soil moisture specifically during the latewood formation period over trees grown on high bulk density soils.

Increasing SBD has been demonstrated to reduce seedling growth in Douglas-fir and other species (e.g. Cochran and Brock 1985; Heninger et al. 2002; Bulmer and Simpson 2010). Although these studies focus on the effect of soil compaction (raising SBD via compression) on height and volume growth, the same soil porosity and hardness characteristics could affect latewood percentage and average density. Bulmer and Simpson's research suggests that soil mechanical resistance

experienced as the soil dried was a greater restraint on the growth of lodgepole pine and Douglas-fir seedlings within the range of field capacity and the wilting point than aeration limits in wet soil. This restriction increases as SBD increases, and prevents trees growing on higher bulk density soils from being able to extract soil moisture all the way down to the wilting point, but has much less affect the trees' ability to extract soil moisture before the transition to latewood tracheid production. This soil-tree-water interaction could explain many of the findings in this research. In Figure 3.17a, 1980 seems likely to be the year in which growth was limited most by growing season, and not moisture. With relatively moderate evaporative and transpirational demands, all trees were given greater ability to add as much latewood as possible late in the growing season. Decreasing average density with increasing elevation for both SBD groups may have also been induced by shortened growing season length, and both groups show the same elevation/AVGDEN relationship. During 2003, as shown in Figure 3.17b, those trees growing on high bulk density soils at lower elevations exhibited a reduced AVGDEN, but those at higher elevation had almost identical AVGDEN values as during 1980. The climate moderating effect of elevation may have allowed the high elevation/ high SBD group to continue growing latewood beyond the ability of low elevation/high SBD trees. The low elevation/high SBD trees may have reached the soil mechanical limit at which further exploitation of the soil moisture was limited, stunting the latewood period. Trees grown on low bulk density soils show a similar relationships between AVGDEN and elevation for both extreme years, indicating a similar earlywood/latewood ratio, and possibly a greater limitation by growing season than soil moisture across all elevations during 2003.

Roots of forest trees frequently do not continue to grow at the low moisture levels that would cause impediment to growth (Joslin et al. 2001, Lopez et al. 2001) suggested by the LLWR model. We hypothesized that this impediment to growth would limit late season availability to moisture, but without measurements of soil moisture and root growth, we cannot conclude that there is an impediment to root growth. Another plausible explanation could be ash caps present in the forest

soils studied. The soil series descriptions for several of the low bulk density soils listed ash as a parent material. The improved water holding capacity of soils that include ash caps (McDaniel and Wilson 2007) may provide an alternative mechanism for late season moisture availability for trees growing on low bulk density soils. The slow growth of the trees studied may indicate they have modest moisture requirements. The slow utilization of soil moisture may prolong the latewood period in trees growing on low bulk density soils as compared to high bulk density soils.

Several important caveats should be considered in extrapolating the findings here with other stands. The effects that seem to be associated with SBD are likely amplified by the crowded nature of the stands and marginal growing conditions for Douglas-fir found on much of the Trapper-Bunkhouse region of the Darby Ranger District in which this study took place. High stocking levels have led to slow growth in these suppressed stands, and space limitations likely prevent trees from expanding their root systems to the fullest extent possible. If there was no competition between trees (i.e. a new plantation or a thinned stand) or other vegetation, even those trees on high bulk density soils would have access to untapped soil moisture late in the season, and we would expect to see the differences between SBD groups to diminish accordingly. Likewise, lower precipitation and warmer climatic conditions, especially at lower elevations in this study, may further accentuate the affect of SBD. Forests with more hospitable conditions for Douglas-fir (or higher elevations in this study) may not exhibit as much of a difference between SBD groups. Secondly, the stands chosen were all naturally regenerated, leading to the possibility that the expression of genetic factors in the face of climatic variations may contribute to differences found in average density and latewood percentage between subpopulations. Thirdly, the estimates of SBD were derived from soil surveys conducted by the Natural Resources Conservation Service (as outlined in Morrow et al. 2013) for the region, and were not spot checked, leading to the possibility that unaccounted-for localized microsite effects may affect the results presented here.

Further research is needed to determine the extent to which these findings are applicable. Monitoring the soil moisture status, root growth, and xylem formation simultaneously in these suppressed stand may provide a better understanding of the mechanisms at work. Crowded stands in marginal Douglas-fir habitat would be the most likely to respond to the SBD affect, and an expanded network of sampling may provide some boundary conditions (e.g. age, stand density, elevation, aspect, etc) inside which we would expect to find similar differences between SBD groups, providing forest managers and researchers with an improved understanding of the scope of the SBD effect. Perhaps more importantly, the assumptions presented here are that the effect of SBD exhibits a linear relationship with climatic variables, especially July/August CDD. Climatic conditions studied in this research did not seem to reach a threshold at which the relationship was broken, despite experiencing some of the hottest and coolest summers since the Dust Bowl years of the 1930's (NOAA 2013(b)). Expanded sampling programs into more extreme Douglas-fir habitat, or, if climate change predictions come to fruition, monitoring the same stands, may better define the climatological limits of the SBD effect.

The influence of SBD on average density and latewood period, and the interaction with climate could create many interesting opportunities for managers of these forests depending on their management objectives. Managers interested in preparing current forests to meet the near-term challenges associated with projections of increasing temperatures changing weather patterns as a result of climate change (IPCC 2007) may want to consider the research of Dalla-Salda and Martinez-Meier and others who suggest that Douglas-fir with increased average density may be better able to survive drought (Martinez-Meier et al, 2008; Dalla-Salda et al. 2009; Dalla-Salda et al. 2011) and prioritize high SBD areas, especially at lower elevations for remedial treatments to reduce moisture stress or possibly the introduction of more drought tolerant species. Forest managers interested in marketing high quality forest products may consider incorporating SBD in stand delineation decisions to deliver more uniform and higher quality raw material as increasing average

temperatures contribute to increasing CDD in July and August, and increasing divergence between SBD groups. The estimated green specific gravities for the two groups over the test period were 0.49 (low SBD) and 0.45 (high SBD), which is more than the difference between the marketing categories DF-L and DF-L South, for which different allowable engineering values are used (WWPA 2001), and would place the average specific gravity for the low SBD trees in the middle range of the southern yellow pines for the test period (USDA 2001). As discussed in Morrow et al. (2013), the incorporation of SBD into sale layout operations may help attract buyers interested in high quality forest products to these remote forests.

Conclusions

The results of this study indicate that the interaction of soil bulk density and climate may induce significant differences in latewood percentage and average density in mature suppressed Douglas-fir stands in the Inland Northwest. Through the use of Repeated Measures Analysis of Variance over a 30 year period, dichotomous grouping into high and low SBD groups explained a significant amount of variation using threshold ($P=0.025$) and adjusted polynomial and inflection measures ($P= 0.039$, $P=0.036$ respectively) of latewood, as well average density ($P=0.0088$). The degree of difference in average density of trees between SBD groups showed a strong correlation to climatic conditions, especially to July/August Cooling Degree Days ($R^2=0.43$) across the entire 30 year study period. By virtue of the relatively long scope of the study period, instances of the negation and even reversal of the effect were found during extremely cool years. The concept of Least Limiting Water Range (LLWR), and especially the resistance to root penetration in high bulk density soils at low soil moisture contents, may provide an explanation for the direction and magnitude of the differences found between SBD groups. These results further emphasize the importance of soil-climate interactions in the study of tree-ring and wood quality characteristics, and may help forest managers make more efficient and effective decisions regarding the health and productivity of dynamic forest environments.

References

Adams, HD, Kold TE. 2004. Drought responses of conifers in ecotone forests of northern Arizona: tree ring growth and leaf C13. Oecologia (140):217-225.

Albaugh TJ, Allen HL, Dougherty PM, Johnsen KH. 2004. Long term growth response of loblolly pine to optimal nutrient and water resource availability. Forest Ecology and Management. 192(2004): 3-19.

Antony F, Jordan L, Daniels RF, Schimleck LR, Clark A, 2009. Hall DB. Effect of midrotation fertilization on growth and specific gravity of loblolly pine. Can. J. For. Res. 39(5): 928-935.

Antony F, Schimleck LR, Daniels RF, Clark III A. 2011. Effect of fertilization on growth and wood properties of thinned and unthinned midrotation loblolly pine (Pinus taeda L.) stands. Southern Journal of Applied Forestry 39(5): 142-147.

Bowyer JL, Shmulsky R, Haygreen JG. 2003. Forest Products and Wood Science: An Introduction. Iowa State Univeristy Press. Ames, Iowa. 554pp.

Brix H. 1972. Nitrogen fertilization and water effects on photosynthesis and earlywood-latewood production in Douglas-fir. Can. J. For. Res. 2(4):467-478.

Bulmer CE, Simpson DG. 2010. Soil compaction reduced growth of lodgepole pine and Douglas-fir seedlings in raised beds after two growing seasons. Soil Science Society of America Journal 74(6):2162-2174.

Clark III A, Borders BE, Daniels RF. 2004. Impact of vegetation control and annual fertilization on properties of loblolly pine wood at age 12. Forest Products Journal 54(12): 90-96.

Cochran PH, Brock T. 1985. Soil compaction and initial height growth of planted ponderosa pine. Res Note PNW-434. USDA Forest Service, Pacific Northwest Forest and Range Exp. Stn., Portland, OR.

Cook ER, Seager R, Cane M, Stahle DW. 2007. North American drought: Reconstructions, causes, and consequences. Earth-Science Review 81: 93-134.

Daddow RL, Warrington GE. 1983. Growth limiting soil bulk densities as influenced by soil texture. WSDG-TN-00005. Fort Collins, CO: U.S. Department of Agriculture, Forest Service, Watershed Systems Development Group.17p. Available online at: http://www.wecs9.com/Reference/GLBD1983.pdf accessed December 19, 2012.

Dalla-Salda G, Martinez-Meier A, Cochard H, Rozenberg P. 2009. Variation of wood density and hydraulic properties of Douglas-fir (Psuedotsuga menziesii (Mirb.) Franco) clones related to a heat and drought wave in France. Forest Ecology and Management 257(1): 182-189.

Dalla-Salda G, Martinez-Meier A, Cochard H, Rozenburg P. 2011. Genetic variation of xylem hydraulic properties shows the wood density is involved in adaptation to drought in Douglas-fir (Pseudotsuga menziesii (Mirb.)). Annals of Forest Science 68(4): 747-757.

Da Silva AP, Kay BD, Perfect E. 1994. Characterization of least limiting water range of soils. Soil Science Society of America Journal 58(6): 1775-1781.

Denne M.P. 1988. Definition of latewood according to Mork (1928). IAWA Bulletin 10(1): 59-62.

Domec J-C, Gartner BL. 2002. How do water transport and water storage differ in coniferous earlywood and latewood. Journal of Experimental Botany 53(379): 2369-2379.

Eilmann B, Zweifel R, Buchmann N, Pannatier EG, Rigling A. 2011. Drought alters timing, quantity, and quality of wood formation in Scots pine. Journal of Experimental Botany. 62(8): 2763-2771

Fitzmaurice GM, Laird NM, Ware JH. 2011.Applied Longitudinal Analysis-2nd ed. John Wiley & Sons Inc., Hoboken, New Jersey. 1211p.

Heninger R, Scott W, Dobkowski A, Miller R, Anderson H, Duke S. 2002. Soil disturbance on 10-year growth response of coast Douglas-fir on nontillled and tilled skid trails in the Oregon Cascades. Can. J. For. Res 32(2): 233-246.

IPCC. 2007. Climate Change 2007: Synthesis Report. Contribution of Working Groups I, II and III to the Fourth Assessment Report of the Intergovernmental Panel on Climate Change. Core Writing Team, Pachauri, RK and Reisinger A (eds). IPCC, Geneva, Switzerland, 104 p.

Gonzalez-Benecke CA, Martin TA, Clark A, Peter GF. 2010. Water Availability and genetic effects on wood properties of loblolly pine (*Pinus taeda*). Can. J. For. Res. 40(12): 2262-2277.

Joslin JD, Wolfe MH, Hanson PJ. 2001. Factors controlling the timing of root elongation intensity in a mature upland oak stand. Plant and Soil 228: 201-221.

Jozsa LA, Brix H. 1989. The effects of thinning on wood quality of a 24-year-old Douglas-fir stand. Can. J. For. Res. 19(9): 1137-1145.

Kantavichai R, Briggs D, Turnblom E. 2010 (a). Modeling effects of soil, climate, and silviculture on growth ring specific gravity of Douglas-fir on a drought-prone site in Western Washington. Forest Ecology and Management 259(6): 1085-1092.

Kantavichai R, Briggs DG, Turnblom EC. 2010 (b).Effect of thinning, fertilization with biosolids, and weather on interannual ring specific gravity and carbon accumulation of a 55-year-old Douglas-fir stand in western Washington. Can. J. For. Res. 40(1):72-85.

Koubaa A, Zhang SYT, Makni S. 2002. Defining the transition from earlywood to latewood in black spruce based on intra-ring wood density profiles from X-ray densitometry. Ann. For. Sci. 59(5-6): 511-518.

Larson PR, Kretschmann DE, Clark A, Isebrands JG. 2001. Formation and properties of juvenile wood in southern pine: A synopsis. Gen Tech. Rep. FPL-GTR-129. Madison, WI: U.S. Department of Agriculture, Forest Service, Forest Products Laboratory. 42p.

Laserre JP, Mason EG, Watt MS, Moor JR. 2009. Influence of initial planting spacing and genotype on microfibril angle, wood density, fibre properties and modulus of elasticity in Pinus radiate D. Don. corewood. Forest Ecology and Management 258(9):1924-1931.

Littell RC, Milliken GA, Stroup WW, Wolfinger RD.1996. SAS System for Mixed Models. SAS Institute Inc.: New York.

Letey J. 1985. Relationship between soil physical properties and crop production. Advances in Soil Science 1: 267-294.

Lopez B, Sabate S, Gracia CA. 2001. Annual and seasonal changes in fine root biomass of a *Quercus ilex* L. forest. Plant and Soil 276: 125-134.

McDaniel PA, Wilson MA. 2007. Physical and chemical characteristics of ash-influenced soils of Inland Northwest forests. Forest Service Proceedings RMRS-P-44. p 31-45.

Morrow CD, Gorman TM, Evans JW, Kretschmann DE, Hatfield CA. 2013. Prediction of wood quality in small-diameter Douglas-fir using site and stand characteristics. Wood and Fiber Science 45(1):49-61.

National Oceanic and Atmospheric Administration. 2013(a). Custom Monthly Summaries of GHCN-Daily CSV- Darby, MT US. http://gis.ncdc.noaa.gov, Accessed April 1, 2013.

National Oceanic and Atmospheric Administration. 2013(b). Palmer Drought and Crop Moisture Data. ftp://ftp.cpc.ncep.noaa.gov/htdocs/temp2, Accessed April 2, 2013.

Oehlert GW. 2000. A first course in design and analysis of experiments. W.H. Freeman and Company. New York, New York. Pp.659.

Pernestal K, Jonsson B, Larsson B. 1995. A simple model for density of annual rings. Wood Science and Technology 29(6): 441-449.

Polge H. 1978. Fifteen years of wood radiation densitometry. Wood Sci. Technol. 12(3): 187-196.

Palmer WC. 1965. Meteorological drought. US Weather Bureau, Research Paper No. 45, 58 pp. http://www.ncdc.noaa.gov/temp-and-precip/drought/docs/palmer.pdf, Accessed April 25, 2013

Robertson EO, Jozsa LA, Spittlehouse DL. 1990. Estimating Douglas-fir wood production from soil and climate data. Can. J. For. Res. 20(3): 357-364.

Savva, Y., F. Schweingruber, E. Vaganov, L. Milyutin. 2003. Influence of climate changes on tree-ring characteristics of scots pine provenances in southern Siberia (forest steppe). IAWA Journal 24(4):371-383.

Schneider R, Zhang SY, Swift DE, Begin J, Lussier JM. 2008. Predicting selected wood properties of jack pine following commercial thinning. Can. J. For. Res. 38(7): 2030-2043.

Schoenholtz, S. H., H. Van Miegroet, J.A. Burger. 2000. A review of chemical and physical properties as indicators of forest soil quality: challenges and opportunities. Forest Ecology and Management (138):335-356.

Tyree MT, Sperry JS. 1989. Vulnerability of xylem to cavitation and embolism. Annu. Rev. Plant. Phys. Mol. Biol 40(1): 19-38.

U.S. Department of Agriculture. 2002. Wood Handbook: wood as an engineering material. Forest Product Laboratory. Madison, WI.

U.S. Department of Agriculture, Natural Resources Conservation Service. 2010. National Soil Survey Handbook, title 430-VI. Part 618 Available online at: http://soils.usda.gov/technical/handbook, Accessed 12/18/2012.

USGS, NRCS. 2006. Soil survey database for Bitterroot National Forest area, Montana, 2006.Vector digital data. Retrieved July 15, 2007, from http://soildatamart.nrcs.usda.gov

WWPA. 2001. Western lumber product use manual. Western Wood Products Association. Portland, OR. 24p.

Zahner R, Lotan JE, Baughman WD. 1964. Earlywood-latewood features of red pine grown under simulated drought and irrigation. Forest Science. 10(3): 361-370.

Chapter Four
Predicting mechanical properties in Douglas-fir using latewood demarcation methods

Abstract

Fundamental wood properties such as density and latewood percentage have been shown to be important predictors of wood quality, and are frequently reported as variables of interest in forest-related research. The ability of two density and three latewood measures derived from small clear samples to predict the Modulus of Elasticity (MOE) and Modulus of Rupture (MOR) in the small samples and their matched lumber was assessed using 75 Select Structural 2x4s. The weight/volume and X-ray derived average small clear sample density measurements proved to be the best predictors with adjusted R^2 as high as 0.79 for MOR to 0.42 for MOE in the small clear samples The threshold latewood demarcation method exhibited a better fit with MOE (adj. R^2=0.32) and MOR (adj. R^2=0.54) than the inflection and polynomial latewood demarcation methods. The goodness-of-fit of all measures dropped considerably when predicting 2x4 MOR, but retained a majority of their predictive ability for MOE in the high-grade 2x4s studied here. This study suggests that density measurements and threshold latewood demarcation methods are better predictors of mechanical properties than the inflection and polynomial latewood demarcation methods.

Introduction

Density has been found to be an important predictor of strength and stiffness in lumber (Newlin and Wilson 1917; Markwardt and Wilson 1935; Doyle 1968; Lachenbruch et al 2010). Because the cell wall material of any species of tree has a specific gravity of

approximately, 1.5 (USDA, 2002), the density or specific gravity of a wood sample reflects the amount of cell wall material present and provides a useful and relatively simple-to-measure assessment of many mechanical and physical properties.

The proportion of high density latewood in an annual ring is an important contributor to the density of an annual ring in many species and is the result of xylogenic processes in the stem of living trees. During xylem formation, newly divided tracheids undergo enlargement and densification before reaching maturity (Wilson et al. 1966; Cuny et al. 2013). In the early part of the growing season, developing tracheids in Douglas-fir experience rapid radial expansion and a short secondary cell wall deposition period that result in the relatively low density wood found in earlywood (Dodd and Fox 1990). As the growing season progresses, the rate and duration of radial expansion decrease, and the duration of cell wall deposition increases creating narrow tracheids with thick cell walls that form the latewood in an annual ring. The tracheid formation process is malleable, and many natural and human influenced factors can affect the latewood proportion and density of wood (Jozsa and Brix 1989; Antony et al. 2009; Gonzalez-Benecke et al. 2010; Kantavichai et al. 2010).

There are many methods available for measuring latewood percentage, and the choice of method likely depends on the goal of the study. Because there is no universally accepted definition of earlywood or latewood, many approaches have been developed to identify the earlywood/latewood transition point. One of the oldest and most frequently cited is Mork's (1928) definition. As reported by Denne (1988), Mork's definition of the latewood transition is the point in the annual ring at which the shared cell wall between tracheids is greater than twice the radial lumen diameter. Identifying the latewood transition point using Mork's

definition requires microscopic examination and is relatively time consuming. With the commercial availability of X-ray densitometers, a threshold density method has been developed which defines the latewood as the portions of the rings that exceed a predetermined threshold density (Polge 1978). The threshold densities are often set at a level that approximate Mork's definition of latewood and are easy to perform.

One of the shortcomings reported for threshold measurements of latewood is an inability to accommodate intra-ring variability (Koubaa et al. 2005; Antony and Schimleck 2012). The presence of false rings and the differences in ring characteristics between juvenile and mature wood lead to inconsistency in the earlywood and latewood traits measured between rings of the same tree. This variation in measurement adds to uncertainty and complicates studies that measure the effect of treatments on these ring characteristics. Dynamic latewood demarcation methods were introduced in an attempt to improve the consistency of earlywood and latewood traits between rings (e.g. Pernestal et al. 1995; Koubaa et al. 2005).

Dynamic latewood methods measure the shape and geometry of the density profile in individual annual rings and select a latewood transition point that best fits a series of criteria or rules. Antony et al. (2012) for example applied a segmented smooth spline method to the density profile of individual rings to identify the point at which the second derivative of the slope of the density/position curve passed through zero to identify the earlywood-latewood transition. They compared this inflection method with Mork's definition of latewood and a threshold demarcation method and suggest that the inflection method identified latewood more consistently between juvenile and mature rings in loblolly pine. Koubaa et al. (2005) proffered a polynomial method whereby the density profile of an individual ring was fit with

a 6^{th} order polynomial, and the root of the second derivative that met certain criteria was chosen as the earlywood latewood transition. Their results suggested that the polynomial method provided a more consistent latewood proportion measured between juvenile and mature wood. Both studies offered evidence that these dynamic measures may provide more consistent estimations of latewood percentage in studies analyzing intra-ring density variations, and may provide a more accurate representation of physiological processes at work during ring formation.

Research concerning the correlations of density and threshold percent latewood to mechanical properties has been well documented. However, correlations of the inflection and polynomial latewood measures to physical and mechanical properties are limited. In Chapter Three, we found that Douglas-fir growing on low bulk density soils had significantly higher average density and latewood percent using a threshold, inflection, and a polynomial method. Several studies were available to predict the increases in wood quality using density and threshold latewood percentage, but very little research was found to translate the increases in inflection and polynomial latewood percentage to predicted improvements in wood quality. The main objective of this study was to compare the ability of measurements of density and latewood percentage to predict clear wood mechanical properties in Douglas-fir from the inland Northwest. A secondary objective of the paper was to develop best case estimates of the ability of the density and latewood percentage methods to predict the mechanical properties of high quality visually graded lumber.

Methods

560 – 10ft Number 1 and Better 2x4s from two mills in the Inland Northwest were regraded by a Western Wood Products Association representative. A 25mm x 25mm x 500mm small clear sample for bending was cut from the ends of the 2x4s, and all small clear samples and 2x4s were conditioned to 12% MC. After the specimens equilibrated, they used for bending tests as per ASTM 4761 and ASTM 143 respectively to find the Modulus of Elasticity (MOE) and Modulus of Rupture (MOR) of the samples. The load was applied to the radial face of the small clear specimens to reduce variation resulting from the presence of wide earlywood or latewood bands at the compression and tension faces. Moisture content samples were used to measure the specific gravity at 12% MC immediately after testing (SG_{2x4} and SG_{sc} for the 2x4s and small clears respectively) according to ASTM D2395-93 Method A. Of the initial 560 boards, 336 met Select Structural grade requirements, and 144 of these were removed because they contained pith or very small annual ring radii. From the remaining set of 192 Select Structural 2x4s, 75 were randomly chosen, 75 were randomly chosen to assess the correlations between the average ring characteristics of the small clear samples and MOE and MOR for the small clear specimens and 2x4s.

After the small clear specimens were tested, a 1.5mm cross section was cut from each, allowed to equilibrate to laboratory conditions, and was scanned using a QTM-QTRX X-ray densitometer. The densitometer was calibrated using 24 Douglas-fir samples of verified average density ranging from 400 kg/m^3 to 700 kg/m^3. The threshold latewood percentage generated using a 500 kg/m^3 threshold level (TLWP) and average density (AVGDEN) for each ring was calculated by the QTM software. The raw data from the X-ray scans was entered into the Inflection Ring Calculator described in Chapter One, and the inflection

latewood percentage (INFLWP) was determined for each complete ring in the small clear specimen cross sections. The procedure developed to calculate INFLWP broke the collection of annual rings from the raw data into individual annual rings, and then selected the point at which the 2nd derivative passed through zero and the 1st derivative of the density/position curve exceeded a predetermined value while moving from the latewood to the earlywood. As described in Chapter One, the polynomial latewood percentage (PLWP) was determined using a Matlab script which fit a 6th degree polynomial to each annual ring and identified the position of the latest root of the 2nd derivative of the polynomial that occurred before the maximum density found in the ring and occurred between 20% and 90% of the total ring length.

Ring-width weighted averages of TLWP ($TLWP_w$), AVGDEN (DEN_w), ILWP ($ILWP_w$), and PLWP ($PLWP_w$) were calculated for all the small samples. The correlations and simple regressions were produced using SPSS 17.0 (SPSS Statistics for Windows, Version 17.0. Chicago:SPSS Inc.). Constant variance and normal residual assumptions were checked visually.

Results

The mean, standard deviation, coefficient of variation, minimum and maximum values of the properties measured are presented in Table 4.1. As with previous experiments described in Chapter Two, $TLWP_w$ was on average larger than $ILWP_w$, and $PLWP_w$ was the shortest. The specimens tested covered a broad range of specific gravity, MOE, and MOR.

Table 4.1. Summary of specimens tested

Property	Mean	SD	CV	Min	Max	Description
MOE_{sc} (GPa)	11.8	1.9	0.16	7.8	16.3	Static MOE of small clear samples
MOR_{sc} (MPa)	92.1	12.2	0.13	69.6	120.6	Static MOR of small clear samples
SG_{sc}	0.475	0.055	0.12	0.380	0.621	SG of small clear samples at 12% MC
$TLWP_w$ (%)	38.1	8.7	0.23	21.8	61.5	Ring width weighted average threshold latewood percentage
DEN_w (kg/m^3)	542	57	0.11	429	678	Ring width weighted average ring density at laboratory EMC
$ILWP_w$ (%)	29.3	7.0	0.24	18.8	50.5	Ring width weighted average inflection latewood percentage
$PLWP_w$ (%)	25.0	5.8	0.23	16.6	42.1	Ring width weighted average polynomial latewood percentage
MOE_{2x4} (GPa)	12.2	2.0	0.17	8.2	17.2	Static MOE of 2x4s
MOR_{2x4} (MPa)	62.7	17.3	0.28	22.4	94.2	Static MOR of 2x4s
SG_{2x4}	.476	.055	0.12	.378	.659	SG of 2x4s at 12% MC

Simple correlations between properties are shown in Table 4.2. All correlations were significant to at least $p < 0.01$. For the small clear samples, MOE_{sc} was most correlated with the measures of density: SG_{sc} and DEN_w ($r = 0.69$ and $r = 0.66$). Of the latewood percentage measurements, MOE_{sc} was most correlated with $TLWP_w$ ($r = 0.57$) and least correlated with $ILWP_w$ ($r = 0.45$). MOR_{sc} was most correlated with SG_{sc} ($r = 0.89$) and DEN_w ($r = 0.79$), but $TLWP_w$ exhibited nearly the same correlation to MOR_{sc} as DEN_w likely owing to the high correlations between SG_{sc}, DEN_w, and $TLWP_w$.

Table 4.2. Simple correlations between average ring and mechanical properties for the small clear and 2x4 samples

Property	MOE_{SC}	MOR_{sc}	SG_{sc}	$TLWP_w$	DEN_w	$ILWP_w$	$PLWP_w$	MOE_{2x4}	MOR_{2x4}	SG_{2x4}
MOE_{SC}	-	.85	.69	.57	.66	.45	.52	.72	.41	.59
MOR_{sc}	.85	-	.89	.74	.79	.64	.68	.73	.56	.76
SG_{sc}	.69	.89	-	.88	.89	.80	.82	.64	.52	.85
$TLWP_w$	.57	.74	.88	-	.90	.86	.86	.54	.42	.76
DEN_w	.66	.79	.89	.90	-	.83	.84	.60	.49	.79
$ILWP_w$	.45	.64	.80	.86	.83	-	.96	.52	.49	.74
$PLWP_w$	.52	.68	.82	.86	.84	.96	-	.57	.45	.75
MOE_{2x4}	.72	.73	.64	.54	.60	.52	.57	-	.73	.67
MOR_{2x4}	.41	.56	.52	.42	.49	.49	.45	.73	-	.62
SG_{2x4}	.59	.76	.85	.76	.79	.74	.75	.67	.62	-

Note: All correlations are significant at $p < 0.01$.

Simple regressions between mechanical and ring properties were run to check the differences between slope parameters. The regressions in Table 4.3 suggest, like the Pearson's correlations, that for the small clear specimens, SG_{sc} exhibited the best fit, followed by DEN_w, $TLWP_w$, $PLWP_w$, and finally $ILWP_w$. With respect to MOE_{sc}, the parameter estimates for SG_{sc} and DEN_w, after accounting for the differences in units, were not significantly different, with estimates that would be within one standard error of each other. The same held true for the measures of latewood: the greatest difference was between $ILWP_w$ and $PLWP_w$, and the comparison of these parameters would result in a t-score of approximately 1.7. For MOR_{sc}, the density and ring properties followed the same ranking in terms of goodness of fit. After accounting for differences in units between SG_{sc} and DEN_w, the slope parameters exhibited a significant difference with a t-score for the comparison of approximately 2.6. Although the slopes are different, they only produce meaningfully different estimates for the samples near the maximum of the density range tested. The coefficients for $TLWP_w$ and $PLWP_w$ were significantly different for MORsc but the regression equations would only predict slight differences in boards with the narrowest latewood period.

A comparison of the results between small clear samples and the 2x4s demonstrated that there were no significant changes in the slope parameters, but there was the expected reduction in the goodness of fit for most of the ring properties. The regressions for $ILWP_w$ and $PLWP_{w,}$ however, suggested an increase in the adjusted R^2 from MOE_{sc} to MOE_{2x4}. From the RMSEs of the regressions, inferences about MOE_{2x4} using density and ring properties had similar levels of residual error as inferences about MOE_{sc}, with increases in RMSE between 3% and 14%. For MOR, RMSE increased by 62% to 165% from predictions

for small clears to the 2x4s. The regressions suggest that the latewood measures performed similarly when making predictions about 2x4 properties.

Table 4.3. Results of simple regressions between average ring properties and mechanical properties

Property	Intercept (SE)	Coefficient (SE)	Adj. R^2	RMSE
MOE_{sc} (GPa)				
SG_{sc}	0.581 (1.38)	23.6 (2.89)	0.47	1.36
$TLWP_{sc}$	7.13 (0.808)	0.122 (0.0207)	0.32	1.54
DEN_w	0.229 (1.57)	0.0213 (0.00287)	0.42	1.42
$ILWP_w$	8.29 (0.841)	0.120 (0.0279)	0.19	1.68
$PLWP_w$	7.59 (0.823)	0.169 (0.0321)	0.26	1.60
MOR_{sc} (MPa)				
SG_{sc}	-2.25 (5.71)	199 (11.9)	0.79	5.62
$TLWP_{sc}$	52.5 (4.32)	1.04 (0.111)	0.54	8.26
DEN_w	1.09 (8.33)	0.168 (0.0153)	0.62	7.54
$ILWP_w$	59.5 (4.73)	1.12 (0.157)	0.40	9.45
$PLWP_w$	56.3 (4.62)	1.44 (0.180)	0.46	8.99
MOE_{2x4} (GPa)				
SG_{sc}	.990 (1.58)	23.5 (3.30)	0.40	1.55
$TLWP_{sc}$	7.44 (0.892)	0.124 (0.0228)	0.28	1.70
DEN_w	0.863 (1.79)	0.0209 (0.00329)	0.35	1.62
$ILWP_w$	7.81 (0.865)	0.149 (0.0288)	0.26	1.73
$PLWP_w$	7.28 (0.858)	0.196 (0.0334)	0.31	1.67
MOR_{2x4} (MPa)				
SG_{sc}	-15.8 (15.2)	165 (31.8)	0.26	14.9
$TLWP_{sc}$	30.7 (8.31)	0.837 (0.213)	0.16	15.9
DEN_w	-16.8 (16.9)	0.147(0.0310)	0.22	15.3
$ILWP_w$	27.2 (7.64)	1.21 (0.254)	0.24	15.3
$PLWP_w$	29.0 (8.03)	1.35 (0.313)	0.19	15.6

In Chapter Two, plots comparing TLWP with ILWP and PLWP showed that ILWP and PLWP behaved differently across the density range of annual rings. The same behavior was observed in this study, with the deviation between the threshold measures and the inflection and polynomial increasing as average density increased. Figure 4.1 shows the relationship

between TLWP and PLWP for the rings analyzed in this study. Figure 4.1 suggests that as the average density of the ring increased, the disparity between TLWP and PLWP increased, and that difference decreases to near zero for the least dense rings in the data set.

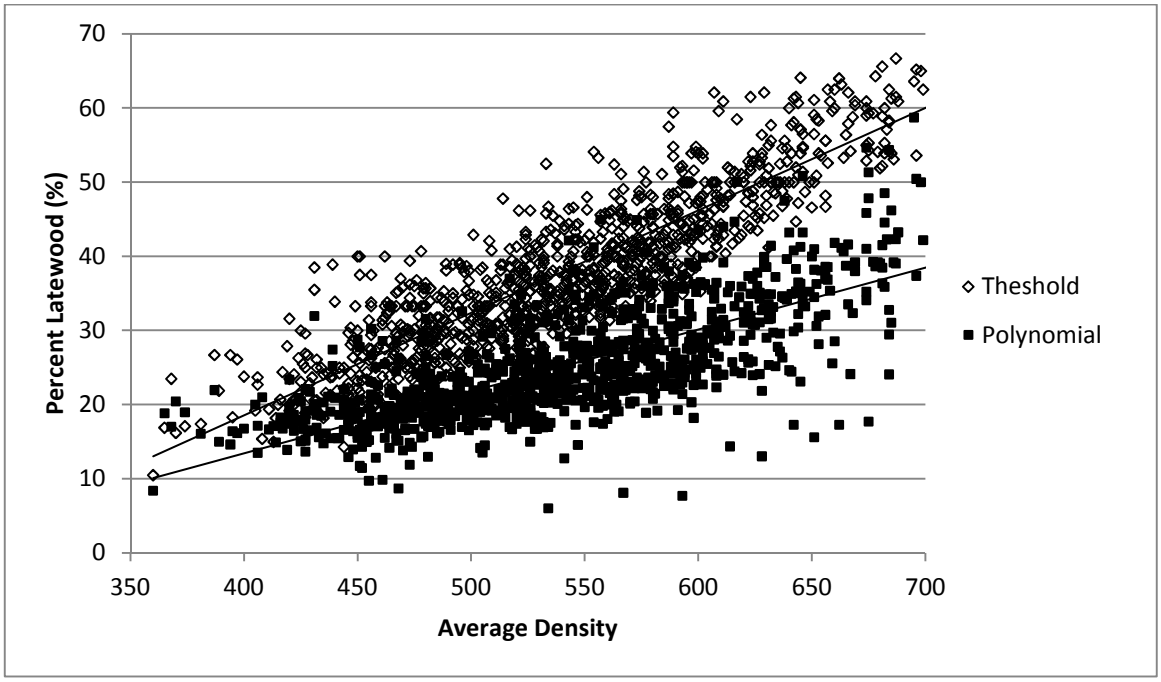

Figure 4.1. Fit of average ring density to TLWP and PLWP

To illustrate the cause of the deviations between TLWP and PLWP, Figure 4.2a shows an annual ring that exhibited a modest difference between TLWP (29%) and PLWP (33%), and Figure 4.2b shows and annual ring with a very large difference between TLWP (63%) and PLWP (33%). Lower density rings tended to make a relatively brief and abrupt transition from earlywood to latewood, while higher density rings made a more gradual transition. In low density rings, the rapidly densifying tracheids reach a maximum density and immediately made the transition to the next annual ring. This geometry forces the last infection point of the second derivative relatively early in the transition from earlywood to latewood, often before the threshold latewood transition in the lowest density rings. In

higher density rings the polynomial method frequently identified shoulders such as that depicted in Figure 4.2b as the latewood transition point when the shoulders provided a region of linear density increase. These patterns seem to be the cause of much of the discrepancies in latewood percentage seen in Figure 4.1.

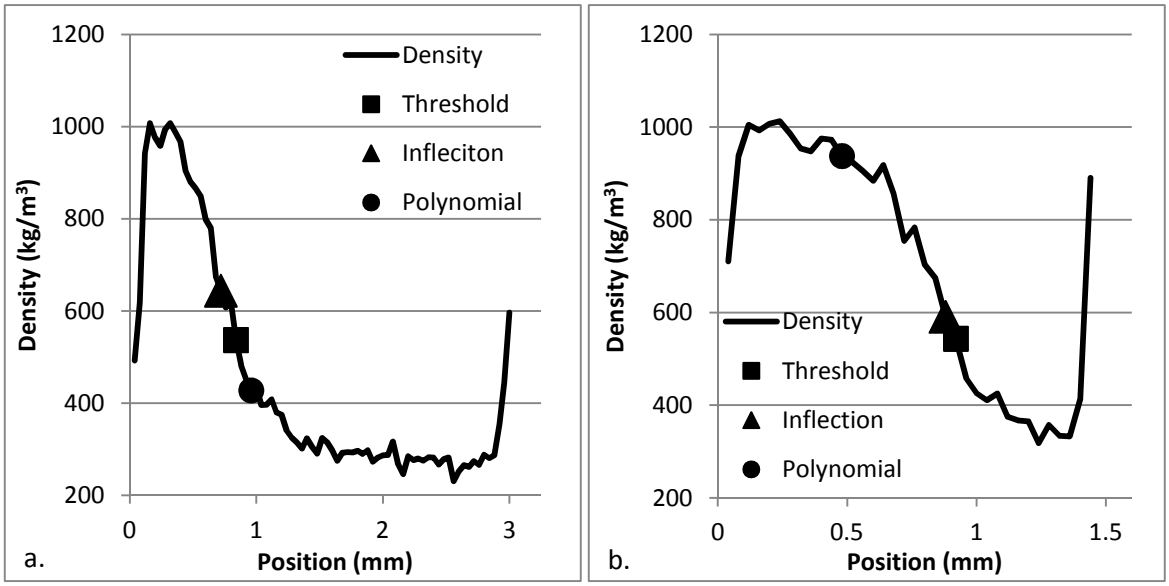

Figure 4.2. Comparison of latewood transition point chosen by the threshold, inflection, and polynomial methods. Low density ring with PLWP<TLWP (a). High density ring with PLWP>>TLWP(b).

Discussion

Prediction of small clear sample mechanical properties

Pearsons correlations and simple regressions suggested that measures of density were better predictors of MOE_{sc} and MOR_{sc} than the measures of latewood percentage. The predictive ability of density has been a common finding in many studies investigating the relationships between ring properties and mechanical properties (e.g. Newlin and Wilson 1917; Markwardt and Wilson 1935; Choi 1986; Lachenbruch et al. 2010; El-Kassaby et al. 2011). The correlation between the measures of density (SG_{sc} and DEN_{sc}) in Table 4.2 for the small

clear specimens and MOE_{sc} and MOR_{sc} were within the range of those found in other studies of Douglas-fir. Lachenbruch et al. (2008) found correlations between small clear sample density and MOE and MOR of 0.67 and 0.63 respectively and parameter estimates that were within, although correlations as low as r = 0.44 (Knowles et al. 2004) and as high as 0.716 and 0.829 (El-Kassaby et al. 2011) have been reported. A source of this variability between studies likely stems from the proximity of the density measurement to the specimen being sampled, with the densities in the studies reporting the weakest correlations derived from tree disks or increment cores and the densities for studies with stronger correlations derived from the specimens themselves. The density samples used to predict MOE_{sc} and MOE_{sc} came directly from the small clear samples.

Common to many of the previous studies is the fact that not all density measurements perform equally. Lachenbruch and others found a reduction in the correlation between density and MOE when moving from a weight/volume measure of density to an X-ray based measurement of density. Similar results were found in the present study, and the reduction in the descriptive power of the density measurements is seen in the decreasing correlations and goodness-of-fit and increasing RMSE in Tables 4.2 and 4.3 when comparing SG_{sc} with DEN_w for small clear sample mechanical properties. The densitometer was calibrated using full sample width scans of 24 Douglas-fir samples of known density from 440 kg/m^3 to 700 kg/m^3, and the calibration resulted in R^2= 0.97 and RMSE of 14 kg/m^3 between actual density and the average whole sample density determine by X-ray. A likely source of disagreement between SG_{sc} and DEN_w stems from the fact that only intact annual rings were analyzed using the X-ray densitometer for the samples used in this study to produce the DEN_w measurement. Thus, omitting the edge rings from the DEN_w measurement may have

produced density measurements that were not able to fully describe the density of the small clear specimens.

The measures of fit between $TLWP_w$ and MOE_{sc} and MOR_{sc} in Table 4.3 were similar to other studies. Using a threshold measurement similar to $TLWP_w$, Mamdy et al. (1999) found a goodness of fit of r^2=0.26 between latewood proportion to board MOE in Douglas-fir. Choi (1986) found an r^2=0.54 between latewood percentage and MOE, and an r^2=0.44 when latewood percentage was regressed against MOR in Douglas-fir. $TLWP_w$ was the most correlated latewood measurement with MOE_{sc} and MOR_{sc}, followed by $PLWP_w$ and finally $ILWP_w$. The order and magnitude of these measures' correlation to MOE_{sc} and MOR_{sc} seem to follow closely with their correlations to measures of average density. Logically, $TLWP_w$ should have been, and was, the most correlated with density because it implicitly gives information about the amount of an annual ring with a density above the predetermined threshold. As seen in Figures 4.2a and 4.2b, the inflection and polynomial methods can vary in the density at which they determine the transistion from earlywood to latewood has occurred. If all the annual rings were more homogenous, then all three methods would likely exhibit similar correlations with density as $TLWP_w$. Across varied annual ring geometries however, $PLWP_w$ and $ILWP_w$ were less stable, and provided poorer predictions of mechanical properties.

$ILWP_w$ and $PLWP_w$ were both poorer predictors of MOE and MOR than $TLWP_w$ but they were still able to account for 19% to 26% of the variation in MOE_{sc} and 40% to 46% of the variation in MOR_{sc} when regressed singly. When the measures of latewood are paired in a multiple regression with SG_{sc} or DEN_w to predict MOE_{sc} (not shown), $ILWP_w$ is significant

($p = 0.045$ and $p = 0.033$ paired with DEN_w and SG_{sc} respectively) but only explains an additional 2% of the error variance above density measures alone. For the same pairings to predict MOR_{sc} $ILWP_w$ is significant when paired with SG_{sc} ($p= 0.016$), but only accounts for an additional 1% of error variance over SG_{sc} alone. The measures of latewood did not provide meaningful predictive ability beyond that of measures of density.

In the small clear samples studied, both the measures of density and latewood explained more variation in MOR_{sc} than in MOE_{sc}. Similar studies have found mixed results with several reporting better fit for MOE than MOR (Choi 1986; for X-ray density Lacenbruch et al. 2010) and others reporting poorer fit with MOE than MOR (for volume based density Lacenbruch 2010; El-Kassaby et al. 2011). SG_{sc} was likely the most accurate measure of small clear sample density, and also exhibited the highest correlation and best fit with MOR_{sc}, and the correlations between MOR_{sc} and DEN_w and the latewood measures closely match their relative correlations with SG_{sc}. If MOR is limited by the worst defect in the sample, then the density measurements for the small clear samples may have provided provide more information about the worst defect in the relatively uniform small clear samples.

Prediction of 2x4 mechanical properties

MOE_{2x4} was best predicted by SG_{sc}, followed by DEN_w, $PLWP_w$, $TLWP_w$, and finally $ILWP_w$. The density measures were still the best predictors, but SG_{sc}, DEN_w, and $TLWP_w$ experienced and 4%-7% drop in the amount of explained variance compared to MOE_{sc}. This drop contrasts sharply with the 5% and 7% increase in explained variance reported for $PLWP_w$ and $ILWP_w$ respectively. Checking the model results for fit and residuals (not

shown), there didn't appear to be a dramatic change compared to the regressions with MOE_{sc}, and the rise in goodness of fit seems to be an artifact of the data and doesn't suggest an improved ability to predict 2x4 stiffness over small clear sample stiffness. The density and latewood measures retained most of their ability to predict MOE in the 2x4 samples.

MOR_{2x4} exhibited the best fit with SG_{sc} followed by $ILWP_w$, DEN_w, $PLWP_w$, and finally $TLWP_w$. There was also a large decrease in explained variance and increase in the RMSE for the density and latewood properties in the prediction of MOR_{2x4} compared to MOR_{sc}. The fact that $ILWP_w$ seemed to provide a better fit than DEN_w could be attributed to a same artifact in the data that suggested a better fit with MOE_{2x4} than MOE_{sc} for $ILWP_w$ and $PLWP_w$. The correlations between MOR_{2x4} and the study variables are similar to those found for Douglas-fir (Lachenbruch et al. 2010) and southern yellow pine (Doyle 1968; Biblis 2004) This reduction likely reflects the more complex nature of defects found in the 2x4 specimens and the dependence of MOR on localized strength reducing characteristics (Doyle 1968; USDA 1999).

Comparison of density and latewood measurements

SG_{sc} was the best predictor of MOE and MOR for both the small clear and 2x4 samples, and the X-ray derived DEN_w value also gave good predictions. These findings are similar to those published by other researchers. An important point to consider is that the correlation between MOE_{sc} and MOE_{2x4} was 0.72 and the correlation between density measures and MOE_{2x4} were quite close to that value ($r=0.64$ and $r=0.60$ for SG_{sc} and DEN_w). This would suggest that SG_{sc} explained approximately 80% as much of the error in MOE_{2x4} as MOE_{sc} did. Similarly, SG_{sc} explained approximately 85% as much of the error in MOR_{2x4} as MOR_{sc}

did. DEN_w did seem to be a slightly poorer predictor the mechanical properties, but in studies that report changes in annual ring average density such as Chapter 2, the findings here could be used to gauge the significance of those findings in terms of the expected mechanical properties of small clear samples, and to a limited extent, 2x4s derived from those trees.

The measures of latewood generally did not predict MOE and MOR as well as did the density measurements. For the small clear samples, $TLWP_w$ provided the best fit for mechanical properties, but for the 2x4s, the results were less clear. It is difficult to develop a valid explanation as to why $PLWP_w$ and $ILWP_w$ would be better predictors of MOE_{2x4} than $MOE_{sc.}$ On average, $PLWP_w$ and $ILWP_w$ identify latewood transition points later in the annual ring than $TLWP_w$, but even this pattern is confounded in low average density rings such as that shown in Figure 4.2. Although other researchers have found merits in the consistency in latewood transition assignments using the polynomial and inflection methods (Koubaa et al. 2005; Antony and Schimleck 2012), they were generally worse predictors of mechanical properties in the samples studied here.

Factors not included in the study and future work

Microfibril angle (MFA) was not measured in the course of this study, but the influence of MFA may be inferred from other similar studies. MOE has been shown to vary with MFA; with decreasing angle of the fibrils within the cell wall associated with greater Young's Modulus in the longitudinal axis of softwood tracheids (Cave and Hutt 1968) and increasing resistance to longitudinal tension or compression in bending members. In Douglas-fir, correlations between r=-0.42 to -0.58 have been reported (Lachenbruch et al. 2010; Vikram

et al. 2011), but as noted by Vikram and others, there seemed to be weaker correlations between MFA and MOE for Douglas-fir than for other species such as eucalyptus (r=0.67; Hein and Lima 2012; r=-0.93; Yang and Evans 2003) or radiata pine (r=-0.82; Raymond et al. 2007; r=-0.76; Cown et al. 1999). In addition, the more mature (17 to 49 yr old) Douglas-fir Lacenbruch et al. studied exhibited less variation in MFA than in juvenile wood used in other studies. Lucenburch et al found that the addition of MFA in a regression of MOE with density increased the adjusted R^2 from 0.45 for density alone to 0.51 with the addition of MFA. The inclusion of MFA in a regression with density to predict MOR resulted in no change in the adjusted R^2 over density alone. Because the samples selected for this study were chosen to limit the amount of juvenile wood, we would expect to have similar modest effects of MFA.

Knots, slope of grain, and other defects all influence the mechanical properties of lumber, but represent a second tier of growth characteristics beyond the fundamental wood properties such as density and latewood percentage that many studies such as Chapter Three and others focus on (e.g. Brix 1972; Jozsa and Brix 1989; Kantavichai et al. 2010). The primary goal of the study was to compare the ability of the inflection and polynomial latewood methods with conventional threshold and density to predict the mechanical properties of clear lumber. These estimates were intended to be used to assess the practical effects of proposed models in the Northwest that compare site differences, silvicultural treatments, climate change, or other influential factors in terms of basic ring characteristics such as density and percent latewood. The extension of the study to predict the mechanical properties of select structural grade lumber was meant to provide a best case estimate of differences in the predictive ability of the density and latewood methods, not to provide an

exhaustive quantification of predictive performance across multiple grades. The inclusion of lower grades of lumber will almost certainly reduce the fit between small clear density and latewood and mechanical properties.

The ability of density and threshold measurements to predict mechanical properties has been well studied, but the ability of the inflection and polynomial latewood demarcation methods has not been as well documented. Although the present study found poorer predictions using ILWP and PLWP in high quality Douglas-fir lumber, there may be species and lumber grade categories for which they perform better. Koubaa et al. (2005) developed the polynomial method to assess black spruce, a species with a less abrupt transition from earlywood to latewood than the Douglas-fir studied here (USDA 2002). The polynomial and inflection methods may behave more consistently in slow-transition species, and thus should be a focus of future research. In addition, a wider range of lumber grades should be assessed. The study of lower grades of lumber would provide a more complete understanding of the capabilities of the polynomial and inflection methods to predict mechanical properties in more complex defect combinations than those found here.

Conclusions

In this study, we tested the ability of a weight/volume density measurement (SG_{sc}), a X-ray density measurement (DEN_w), a threshold latewood demarcation method ($TLWP_w$), an inflection latewood demarcation method ($ILWP_w$), and a polynomial demarcation method ($PLWP_w$) to predict MOE and MOR in Douglas-fir small clear specimens 2x4 lumber. The results showed that the SGsc was universally the best predictor of MOE (R^2=0.47, R^2=0.40) and MOR (R^2=0.79, R^2=0.26) for both small clears and 2x4s respectively. DEN_w provided

slightly less predictive ability of MOE (R^2=0.42, R^2=0.35) and MOR (R^2=0.62, R^2=0.22) for small clears and 2x4's respectively. Of the latewood demarcation methods, $TLWP_w$ was the best predictor for most of the properties exhibiting fits of R^2=0.32 and R^2= 0.28 with MOE and R^2=0.54 and R^2=0.16 with MOR for the small clears and 2x4s respectively. Density was the best predictor in this study, and $PLWP_w$ and $ILWP_w$ were more poorly correlated with density and erratic in their latewood selection points than $TLWP_w$. The results suggest that studies attempting to extrapolate mechanical properties from annual ring characteristics should use a density or a threshold latewood measurement.

References

Antony F, Jordan L, Daniels RF, Schimleck LR, Clark A, 2009. Hall DB. Effect of midrotation fertilization on growth and specific gravity of loblolly pine. Can. J. For. Res. 39(5): 928-935.

Antony F, Schimleck LR. 2012. A comparison of earlywood-latewood demarcation methods- a case study in loblolly pine. IAWA Journal 33(2): 187-195.

Biblis E, Meldahl R, Pitt D, Carino HF. 2004. Predicting flexural properties of dimension lumber from 40-year-old loblolly pine plantation stands. Forest Product Journal 54(12): 109-112.

Brix H. 1972. Nitrogen fertilization and water effects on photosynthesis and earlywood-latewood production in Douglas-fir. Can. J. For. Res. 2(7):467-478.

Cave ID, Hutt L. 1968. The anisotropic elasticity of the plant cell wall. Wood Science and Technology 2(4): 268-278.

Choi ASC. 1986. Correlation between mechanical strength of wood and annual ring characteristics of Douglas-fir juvenile and mature wood. Master of Science Thesis. Oregon State University, OR. 1986, 84p.

Cown DJ, Herbert J, Ball R. 1999. Modelling Pinus radiata lumber. Part 1: Mechanical characteristics of small clears. New Zealand Journal of Forestry Science 29(2): 203-213.

Cuny HE, Rathberger CBK, Lebourgeois F, Fortin M, Fournier M. 2012. Life strategies in intra-annual dynamics of wood formation: example of three conifer species in a temperate forest in north-east France. Tree Physiology 32: 612-625.

Denne MP. 1988. Definition of latewood according to Mork (1928). IAWA Bulletin 10(1): 59-62.

Dodd RS, Fox P. 1990. Kinetics of tracheid differentiation in Douglas-fir. Annals of Botany 65(6): 649-657.

Doyle DV. 1968. Properties of No. 2 dense kiln-dried southern pine dimension lumber. USDA FPL-RP-96. Madison, WI.

El-Kassaby YA, Mansfield M, Isik F, Stoehr M. 2011. In situ wood quality assessment in Douglas-fir. Tree Genetics and Genomes 7(3): 553-561.

Gonzalez-Benecke CA, Martin TA, Clark A, Peter GF. 2010. Water Availability and genetic effects on wood properties of loblolly pint (Pinus taeda). Can. J. For. Res. 40(12): 2262-2277.

Hein PRG, Lima JT. 2012. Relationships between microfibril angle, modulus of elasticity and compressive strength in Eucalyptus wood. Maderas. Ciencia y tecnologia. 14(3):267-274.

Jozsa LA, Brix H. 1989. The effects of thinning on wood quality of a 24-year-old Douglas-fir stand. Can. J. For. Res. 19(9): 1137-1145.

Kantavichai R, Briggs D, Turnblom E. 2010. Modeling effects of soil, climate, and silviculture on growth ring specific gravity of Douglas-fir on a drought-prone site in Western Washington. Forest Ecology and Management 259(6): 1085-1092.

Koubaa A, Zhang SYT, Makni S. 2002. Defining the transition from earlywood to latewood in black spruce based on intra-ring wood density profiles from X-ray densitometry. Ann. For. Sci. 59(5): 511-518.

Lachenbruch B, Johnson GR, Downes GM, Evans R. 2010. Relationships of density, microfibril angle, and sound velocity with stiffness and strength in mature wood of Douglas-fir. Can. J. For. Res 40(2010):55-64.

Mamdy C, Rozenburg P, Franc A, Launay J, Schermann N, Bastien JC. 1999. Genetic control of stiffness of standing Douglas-fir from the standing stem to the standardized wood sample, relationships between modulus of elasticity and wood density parameters. Ann. For. Sci. 56(2):133-143.

Markwardt LJ, Wilson TRC. 1935. Strength and related properties of woods grown in the United States. USDA FPL Tech Bul No. 479. Madison WI. http://naldc.nal.usda.gov/download/CAT86200473/PDF.

Morrow CD, Gorman TM, Evans JW, Hatfield CA. 2013. Prediction of wood quality in small-diameter Douglas-fir using site and stand characteristics. Wood and Fiber Science. 45(1):49-61.

Mork E. 1928. Die Qualität des Fichtenholzes unter besonderer Rücksichtnahme auf Schleifuned Papeirholz. Der Papier-Fabrikant 48: 741-747.

Newlin JA, Wilson TRC. 1917. Mechanical properties of woods grown in the United States. USDA FPL. Bulletin No 556. Madison WI. Accessed https://archive.org/details/mechanicalproper556newl.

Peck E. 1933. Specific gravity and related properties of softwood lumber. USDA FPL Tech Bul. No. 343. Madison, WI. http://ir.library.oregonstate.edu/xmlui/handle/1957/833.

Polge H. 1978. Fifteen years of wood radiation densitometry. Wood Sci. Technol. 12(3): 187-196.

Raymond CA, Joe B, Evans R, Dickson RL. 2007. Relationship between timber grade, static and dynamic modulus of elasticity and SilviScan properties for Pinus radiata in New South Wales. New Zealand Journal of Forestry Science. 37(2): 186-196.

U.S. Department of Agriculture. 2002. Wood Handbook: wood as an engineering material. Forest Product Laboratory. Madison, WI.

Vikram V, Cherry ML, Briggs D, Cress DW, Evans R, Howe GT. 2011. Stiffness of Douglas-fir lumber: effects of wood properties and genetics. Can. J. For. Res. 41(6): 1160-1173.

Wilson BF, Wodzicki TJ, Zahner R. 1966. Differentiation of cambial derivatives: proposed terminology. Forest Science 12(4): 438-440.

Yang JL, Evans R. 2003. Prediction of MOE of eucalypt wood from microfibril angle and density. Eur. J. Wood Prod. 61(6):449-452.

Chapter Five
Conclusions

The findings reported in this paper offer an improved understanding of the inflection and polynomial latewood demarcation methods from the significance of the point selected as the Earlywood (EW) Latewood (LW) transition to the ability of Inflection Latewood Percentage (ILWP) and Polynomial Latewood Percentage (PLWP) to predict the mechanical of small clear specimens and high grade lumber.

In Chapter Two, we found that Threshold Latewood Percentage (TLWP) was moderately correlated with ILWP and PLWP, but that ILWP and PLWP were poorly correlated with Average Density (AVGDEN). The threshold method, when using a 500 kg/m^3 threshold was able to identify a point on average that was very close to Morks definition of latewood, and the anatomy at the point selected for the EW-LW transition was not affected by AVGDEN of the ring. We found that ILWP and PLWP seemed to target the point in the annual ring at which the rate of lumen diameter decrease and cell wall thickness increase are at their peak. Thus, the anatomy at the EW-LW transition point determined by the inflection and polynomial methods is variable, and we found it may be subject to bias based on annual ring geometry and AVGDEN. For a researcher interested in studying xyolgenic response, the threshold measurement represents a certain combination of duration and rates of radial expansion and duration of cell wall thickening in developing tracheids to produce a tracheid of a threshold density. The inflection and polynomial transition points represent the tracheids that were forming as the same expansion and thickening stages were changing the most rapidly. This research may provide a means to expand wood formation research by providing improved tools to replace or augment traditional microscopy with relatively easier X-ray densitometry analysis.

With the ability to interpret the EW-LW transitions developed in Chapter Two, the results in Chapter Three suggest the significant effect of Soil Bulk Density (SBD) on TLWP and the adjusted inflection

and polynomial methods have different interpretations. Tress in the low SBD groups reached the tracheid expansion and densification combination that produced tracheids with a density of 500 kg/m^3 earlier in their relative growing season (significant difference in TLWP) and also reached the point at which forming tracheids' radii were shrinking and cell walls thickening at the greatest rate earlier (significant difference in adjusted ILWP and PLWP). This suggests that the transition from earlywood to latewood was similarly abrupt for both groups on average, but the trees growing on low bulk density soils had longer periods of the late season latewood accrual. In addition, in the two coldest summers on record, the effect was negated, and even reversed. This phenomenon would be consistent with the Least Limiting Water Range described in Chapter Three. The three latewood methods seemed to describe the same differences between groups, and no method stood out with in terms of the parameter estimates or model components.

Finally, we studied the ability of AVGDEN, TLWP, PLWP, and ILWP to predict MOE and MOR in small clear samples and the matching high grade 2x4s. We found that AVGDEN and TLWP were better predictors for small clear properties, but PLWP and ILWP had some predictive ability. All measures were better predictors of MOR in the small clears and MOE in the 2x4s. The results could be used to make inferences about the wood quality implications of studies measuring tree responses. The results of the three studies presented form a basis with which to interpret ILWP and PLWP in the context of both tree response to the environment and the mechanical properties of the wood in Douglas-fir.

Future work regarding these methods should focus on improving the consistency of the inflection and polynomial methods. Because ring geometry seems to affect the latewood transition location decision, an approach needs to be developed that can simultaneously provide smoothing but is not as influenced by the shape of the density/position curve before and after the region of most change in density. In addition, similar studies should be conducted with different species to determine if the

other patterns of growth such as slow transition from EW to LW cause the same problems seen with Douglas-fir studied here.

Appendix A
Inflection method

Introduction

The inflection ring calculator reads densitometry data imported manually, and reports ring characteristics based on the script at the end of the Appendix. This code was written to automate the process of identifying the start and stop of the ring and the transition from earlywood to latewood based on the inflection of the second derivative of the position/density slope. At the same time, it calculates the earlywood and latewood densities, the average density, ring length, and the latewood proportion using the inflection point method. The idea for the calculator came from Koubaa et al (2002) and Pernesal et al (1995) but the methodology and coding represent the author's own work.

Inflection Ring Calculator Instructions

The coding for determining the inflection position was developed using Microsoft Visual Basic (VB) 6.5 in conjunction with Microsoft Excel 2007. A user will open the inflection ring calculator Excel file, and paste the raw densitometry data in the first 4 columns. The first column must be position, the second must be density. The third and fourth columns were reserved for automatic output from the QTM-QTRX raw data and contain the QTM's determination (based on threshold method) of ring number and earlywood or latewood. The fifth column calculates the slope of the density and position data for the three data points centered on the row in question and the sixth column calculates the 2^{nd} derivative at the row in question using the same five data point range. The user will clear any old data from I2:U?, then run the InflectionRingCalc macro. Results will be reported in columns I through U on Sheet "1_1". A graph below the output will show the density profile with the ring divisions and inflection points graphed for quality control purposes. The second sheet of the excel file contains instructions.

Inflection Ring Calculator Script

```
Sub InflectionRingCalc()    'Script to identify the start and stop of ring using inflection and EW/LW
‘transition using inflection method, will also report EW and LW densities


'Declare variables
Dim StartPosition As Single ' position at start of ring
Dim StopPosition As Single 'position at end of ring
Dim CurrentPosition As Integer ' counter that keeps track of current position in loops
Dim RingLength As Single ' variable calculated and reported for ring length
Dim RingCount As Integer ' ring number
Dim CurrentDensity As Single ' the density at RowPositionInRaw
Dim RowPositionInRaw As Integer ' current row on active worksheet
Dim WhileCount As Single ' loop counter
Dim WholeRingDensity As Single ' ring density variable
Dim Current2ndDer As Single ' Second derivative at RowPositionInRaw
Dim Current1stDer As Double ' first derivative at RowPositionInRaw
Dim InflectionDensity As Single ' Density at point determined to be EW/LW inflection
Dim InflectionPosition As Single ' position at point determined to be EW/LW inflection
Dim LWDensity As Single ' Latewood density variable
Dim EWDensity As Single ' Earlywood density variable
Dim StartDensity As Single ' Density at StartPosition
Dim StopDensity As Single ' Density at StopPosition
Dim RingDensityIntegration As Single ' Used for summing densities at all points
Dim EWCount As Single ' Number of positions in Earlywood
Dim LWCount As Single ' Number of positions in Latewood
Dim AverageDensity As Single 'Average density variable
Dim PositionForRingLength As Integer ' Used to track position in file during initial ring length
estimate
Dim NumberOfPointsForRingLength As Integer ' Number of data points in ring length estimate
Dim NumberOfCellsForSlopeMeasurement As Integer ' Variable to determine how many points
should ‘be included in smoothing
Dim RowPositionSlopeWrite As Integer ' Variable to track position in active worksheet while
writing ‘new first and second derivatives


Dim MaxFirst As Single ' Maximum first derivative in ring, helps identify inflection point
Dim MinFirst As Single ' Minimum first derivative in ring, helps identify inflection point
Dim Maxsecond As Single ' Maximum second derivative in ring, helps identify inflection point
Dim MinSecond As Single ' Minimum second derivative in ring, helps identify inflection point


Dim FirstRange As Range ' Range variable used to calculate first and second derivatives
Dim SecondRange As Range ' Range variable used to calculate first and second derivatives
Dim ThirdRange As Range ' Range variable used to calculate first and second derivatives
Dim FourthRange As Range ' Range variable used to calculate first and second derivatives

Range("G2:U10000").ClearContents 'delete old results
```

```
RowPositionInRaw = 43 ' First row to start looking for valid densitometry data

PositionForRingLength = RowPositionInRaw  'Point row position values to the same row

RingCount = 1 'These are initial values for the first ring
RingLength = 1
MinSecond = -1000
Maxsecond = 5000
MinFirst = -1000
MaxFirst = 2000

'read the first and second derivative at the current row position
Current2ndDer = Worksheets("1_1").Cells(RowPositionInRaw, 6).Value
Current1stDer = Worksheets("1_1").Cells(RowPositionInRaw, 5).Value
CurrentDensity = Worksheets("1_1").Cells(RowPositionInRaw, 2).Value

' skip scanning of air, step through data until you find wood
While CurrentDensity < 500

        Do

          RowPositionInRaw = RowPositionInRaw + 1 ' index to next data position
          StopPosition = Worksheets("1_1").Cells(RowPositionInRaw, 1).Value
          CurrentDensity = Worksheets("1_1").Cells(RowPositionInRaw, 2).Value
          Current2ndDer = Worksheets("1_1").Cells(RowPositionInRaw, 6).Value
          Current1stDer = Worksheets("1_1").Cells(RowPositionInRaw, 5).Value
          PositionForRingLength = RowPositionInRaw

      Loop Until (Current2ndDer < 0 And CurrentDensity > 500) ' loop until we are in wood

Wend

'as long as there is still valid data to be read
While Worksheets("1_1").Cells(RowPositionInRaw, 6).Value <> ""

   PositionForRingLength = RowPositionInRaw
   Application.ScreenUpdating = False ' turn off screen update to speed up program
   WholeRingDensity = 0 ' Reset the ring density
   RingDensityIntegration = 0 ' Reset this secondary ring density helper variable
   StopPosition = Worksheets("1_1").Cells(RowPositionInRaw, 1).Value
   CurrentDensity = Worksheets("1_1").Cells(RowPositionInRaw, 2).Value
   NumberOfPointsForRingLength = 0

      While Current2ndDer < 1000 ' find the length of the latewood to scale slope measurements

        Do


          NumberOfPointsForRingLength = NumberOfPointsForRingLength + 1
          PositionForRingLength = PositionForRingLength + 1
```

```
            'read the new 1st and 2nd derivative values to see if we are still in latewood
            Current2ndDer = Worksheets("1_1").Cells(PositionForRingLength, 6).Value
            Current1stDer = Worksheets("1_1").Cells(PositionForRingLength, 5).Value

        'Loop to Do statement until these conditions are met ie, pass ew/lw inflection
        Loop Until ((Current2ndDer > Maxsecond / 20) And (Current1stDer < (MinFirst / 2)))

    Wend

    While Current2ndDer > 0 ' find the length of the earlywood to scale slope measurements

        Do

            NumberOfPointsForRingLength = NumberOfPointsForRingLength + 1
            PositionForRingLength = PositionForRingLength + 1

            'see if the next row is the same ring or not
            Current2ndDer = Worksheets("1_1").Cells(PositionForRingLength, 6).Value
            Current1stDer = Worksheets("1_1").Cells(PositionForRingLength, 5).Value

        'Loop to the Do statment until the following conditions are met ie leave the ring
        Loop Until (Current2ndDer < MinSecond / 10 And Current1stDer > MaxFirst / 4) '

    Wend

    'determine how many points to take the slope of for the inflection latewood determination use
    10% ‘of the ring length
    NumberOfCellsForSlopeMeasurement = Int((NumberOfPointsForRingLength \ 10) \ 2)

    'If the ring is short, use at least 3 positions to smooth
    If NumberOfCellsForSlopeMeasurement < 3 Then NumberOfCellsForSlopeMeasurement = 3

    'Reset row position to write new 1st and 2nd derivatives
    RowPositionSlopeWrite = RowPositionInRaw

    'record the new and improved 1stder measurements in the 7th column
    While RowPositionSlopeWrite < PositionForRingLength

        Do

            'debugging tools
            Worksheets("1_1").Cells(RowPositionSlopeWrite, 7).Value = RowPositionSlopeWrite
            Worksheets("1_1").Cells(RowPositionSlopeWrite, 9).Value = _
NumberOfCellsForSlopeMeasurement

            'set the ranges so we can calculate the first derivative
            Set FirstRange = Worksheets("1_1").Range(Cells((RowPositionSlopeWrite - _
NumberOfCellsForSlopeMeasurement), 2), Cells((RowPositionSlopeWrite + _
NumberOfCellsForSlopeMeasurement), 2))

            Set SecondRange = Worksheets("1_1").Range(Cells((RowPositionSlopeWrite - _
NumberOfCellsForSlopeMeasurement), 1), Cells((RowPositionSlopeWrite + _
NumberOfCellsForSlopeMeasurement), 1))
```

```
            'calculate first derivative
            Current1stDer = WorksheetFunction.Slope(FirstRange, SecondRange)

            'write the first derivative on the sheet
            Worksheets("1_1").Cells(RowPositionSlopeWrite, 7).Value = Current1stDer

            RowPositionSlopeWrite = 1 + RowPositionSlopeWrite

          'keep writing ‘first derivatives in column 7 for twice the estimated ring length
           Loop Until RowPositionSlopeWrite = PositionForRingLength + RingLength * 50

        Wend

        RowPositionSlopeWrite = RowPositionInRaw

        'record the new and improved 2ndder measurements in the 8th column
        While RowPositionSlopeWrite < PositionForRingLength

           Do

            'Set ranges to point to the 1st derivative and position to calculate 2nd derivative

           Set SecondRange = Worksheets("1_1").Range(Cells((RowPositionSlopeWrite -  _
NumberOfCellsForSlopeMeasurement), 1), Cells((RowPositionSlopeWrite + _
NumberOfCellsForSlopeMeasurement), 1))

           Set ThirdRange = Worksheets("1_1").Range(Cells((RowPositionSlopeWrite - _
NumberOfCellsForSlopeMeasurement), 7), Cells((RowPositionSlopeWrite + _
NumberOfCellsForSlopeMeasurement), 7))

            'calculate 2nd derivative
            Current2ndDer = WorksheetFunction.Slope(ThirdRange, SecondRange)

            'write 2nd derivative on worksheet
            Worksheets("1_1").Cells(RowPositionSlopeWrite, 8).Value = Current2ndDer

            RowPositionSlopeWrite = 1 + RowPositionSlopeWrite

            'keep writing second derivatives in column 8 for twice the estimated ring length
             Loop Until RowPositionSlopeWrite = PositionForRingLength + RingLength * 50

        Wend

        'Locate the start of the ring and the density at the start
        StartPosition = StopPosition ' This will be the first position of the current ring
        StartDensity = CurrentDensity ' This will be the density at the first position of the ring

        WhileCount = 0 ' reset whole ring length counter variable
        EWCount = 0 ' reset earlywood ring length counter variable
        LWCount = 0 ' reset latewood ring length counter variable

        'set a range of length rawposition minus positionforringlength to find min and max for 1st and
            2nd ‘derive slopes
```

```
    Set ThirdRange = Worksheets("1_1").Range(Cells(RowPositionInRaw, 7), _
Cells(PositionForRingLength, 7))

    Set FourthRange = Worksheets("1_1").Range(Cells(RowPositionInRaw, 8), _
Cells(PositionForRingLength, 8))

    'Find min and max first derivatives in the expected ring length
    With ThirdRange

      MaxFirst = Application.WorksheetFunction.Max(ThirdRange)
      MinFirst = Application.WorksheetFunction.Min(ThirdRange)

    End With

    'Find min and max second derivatives in the expected ring length
    With FourthRange

      Maxsecond = Application.WorksheetFunction.Max(FourthRange)
      MinSecond = Application.WorksheetFunction.Min(FourthRange)

    End With

    'reset active 1st and 2nd derivatives to RowPosition derivative from sheet
    Current2ndDer = Worksheets("1_1").Cells(RowPositionInRaw, 8).Value
    Current1stDer = Worksheets("1_1").Cells(RowPositionInRaw, 7).Value

    'walking through the raw data to find length and average density of latewood
    While Current2ndDer < Maxsecond / 20

      Do

       'StartPoint reached above is the first cell of the LW period
       StopPosition = Worksheets("1_1").Cells(RowPositionInRaw, 1).Value ' set the end of the
       ring to the current position

        CurrentDensity = Worksheets("1_1").Cells(RowPositionInRaw, 2).Value

        'needed two variables to average density, won't add to itself
        WholeRingDensity = CurrentDensity + RingDensityIntegration
        RingDensityIntegration = WholeRingDensity

        'index postion counters to be ready for the next loop
        WhileCount = WhileCount + 1
        LWCount = LWCount + 1
        RowPositionInRaw = RowPositionInRaw + 1

        'read the new 1st and 2nd derivative values to see if we are still in latewood
        Current2ndDer = Worksheets("1_1").Cells(RowPositionInRaw, 8).Value
        Current1stDer = Worksheets("1_1").Cells(RowPositionInRaw, 7).Value

        'debugging tool
        Worksheets("1_1").Cells(RowPositionInRaw, 12).Value = Maxsecond
        Worksheets("1_1").Cells(RowPositionInRaw, 13).Value = MinSecond
```

```
    'Loop to Do statement until these conditions are met ie left latewood
     Loop Until (Current2ndDer > Maxsecond / 20 And Current1stDer < (MinFirst / 2))

    'If we have left the preceeding loop, we are at the end of the latewood
    LWDensity = WholeRingDensity / LWCount

Wend

'When 2nd der passes back through 0, this is the inflection point
'Inflection point will be the first cell of the earlywood
StopPosition = Worksheets("1_1").Cells(RowPositionInRaw, 1).Value ' update stop position

CurrentDensity = Worksheets("1_1").Cells(RowPositionInRaw, 2).Value ' read new density

InflectionDensity = CurrentDensity

'debugging tool
Worksheets("1_1").Cells(RowPositionInRaw, 11).Value = InflectionDensity

InflectionPosition = StopPosition

WhileCount = 0

RingDensityIntegration = 0

'walk through the raw data to find end of ring and add up ew densities
While Current2ndDer > MinSecond / 20

    Do

        'debugging tool
        Worksheets("1_1").Cells(RowPositionInRaw, 12).Value = Maxsecond
        Worksheets("1_1").Cells(RowPositionInRaw, 13).Value = MinSecond

        'Update stopposition and current density to new row value
        StopPosition = Worksheets("1_1").Cells(RowPositionInRaw, 1).Value

        CurrentDensity = Worksheets("1_1").Cells(RowPositionInRaw, 2).Value

        WholeRingDensity = CurrentDensity + RingDensityIntegration

        RingDensityIntegration = WholeRingDensity

        WhileCount = WhileCount + 1

        RowPositionInRaw = RowPositionInRaw + 1

        EWCount = EWCount + 1

        'see if the next row is the same ring or not
        Current2ndDer = Worksheets("1_1").Cells(RowPositionInRaw, 8).Value
        Current1stDer = Worksheets("1_1").Cells(RowPositionInRaw, 7).Value

    'Loop to the Do statment until the following conditions are met ie leave earlywood
    Loop Until Current2ndDer < MinSecond / 10 And Current1stDer > MaxFirst / 4
```

```
        Wend

        'the current row position is out of the ring, calculate the new values below for the ring we just
left
        EWDensity = WholeRingDensity / WhileCount
        StopDensity = CurrentDensity
        RingLength = (EWCount + LWCount) * 0.02
        AverageDensity = ((LWCount * LWDensity) + (EWCount * EWDensity)) / (EWCount +
LWCount)
        Worksheets("1_1").Cells(RowPositionInRaw - 1, 10).Value = StopDensity

        Application.ScreenUpdating = True ' update the screen

        'print out all the values on the excel sheet in whatever RingCount row we are in
        Worksheets("1_1").Cells(RingCount + 1, 9).Value = RingCount
        Worksheets("1_1").Cells(RingCount + 1, 10).Value = StartPosition
        Worksheets("1_1").Cells(RingCount + 1, 11).Value = StartDensity
        Worksheets("1_1").Cells(RingCount + 1, 12).Value = InflectionPosition
        Worksheets("1_1").Cells(RingCount + 1, 13).Value = InflectionDensity
        Worksheets("1_1").Cells(RingCount + 1, 14).Value = LWDensity
        Worksheets("1_1").Cells(RingCount + 1, 15).Value = EWDensity
        Worksheets("1_1").Cells(RingCount + 1, 16).Value = StopPosition
        Worksheets("1_1").Cells(RingCount + 1, 17).Value = StopDensity
        Worksheets("1_1").Cells(RingCount + 1, 18).Value = LWCount * 0.02
        Worksheets("1_1").Cells(RingCount + 1, 19).Value = AverageDensity
        Worksheets("1_1").Cells(RingCount + 1, 20).Value = RingLength
        Worksheets("1_1").Cells(RingCount + 1, 21).Value = 100 * (LWCount * 0.02) / RingLength

        'Index RingCount variable and make sure Current1stDer and Current2ndDer are stored

        RingCount = RingCount + 1

        Current2ndDer = Worksheets("1_1").Cells(RowPositionInRaw, 8).Value

        Current1stDer = Worksheets("1_1").Cells(RowPositionInRaw, 7).Value

    'loop back to initial while statement as long as there is valid data for next ring
    Wend

End Sub
```

Appendix B
Polynomial method

Introduction

The polynomial inflection program reads raw densitometry data and reports ring characteristics based on the script at the end of the Appendix. This code was written to automate the process of calculating, identifying, and checking the transition point from earlywood to latewood as defined by the polynomial root method. The script uses raw data from the QTM-QTRX densitometer with annual rings identified using the inflection ring calculator to fit a sixth order polynomial to the raw annual ring data and the root of the second derivative of the polynomial that fits certain criteria. The criteria used for this method came from suggestions in Koubaa et al. 2002. The script also calculates earlywood and latewood densities, average density, ring length, and latewood proportion.

Method

Raw densitometer data with ring assignments from the Inflection ring method for one tree are imported on the clipboard and the Matlab file is executed. The script brings the raw data into a matrix and copies all of the density and position data of the first ring into a second matrix noting the start and stop position. When the script has pulled all data from the first ring into the second matrix, it calculates and stores the ring length, then fits a sixth order polynomial to the annual ring's data. It then calculates the second derivative of the polynomial and then identifies the roots of the second derivative. There are at most four roots of the second derivative of the polynomial, so the script must then determine which one meets the method criteria. The script finds the data point with the highest density (maximum density encountered in the annual ring), and chooses the roots which occurs closest to but after (from bark to pith) the maximum density, within 80% of the ring length, and the first derivative at that root is also negative.

The script then prints a graph on the screen to allow the user to check the root identification, an example is shown below. In the top graph, the current ring being analyzed is displayed with the density on the y-axis and the position from the raw densitometry data on the x-axis with circles

representing the individual data points of the annual ring. The root of the second derivative chosen for this ring is represented by the red X (position 10.1), and the line represents the sixth order polynomial fit to the ring. The bottom graph represents all of the rings analyzed thus far for this tree, again with X's at the earlywood/latewood inflection points determined by the script. These graphs were used to screen the results to ensure the script was functioning as expected.

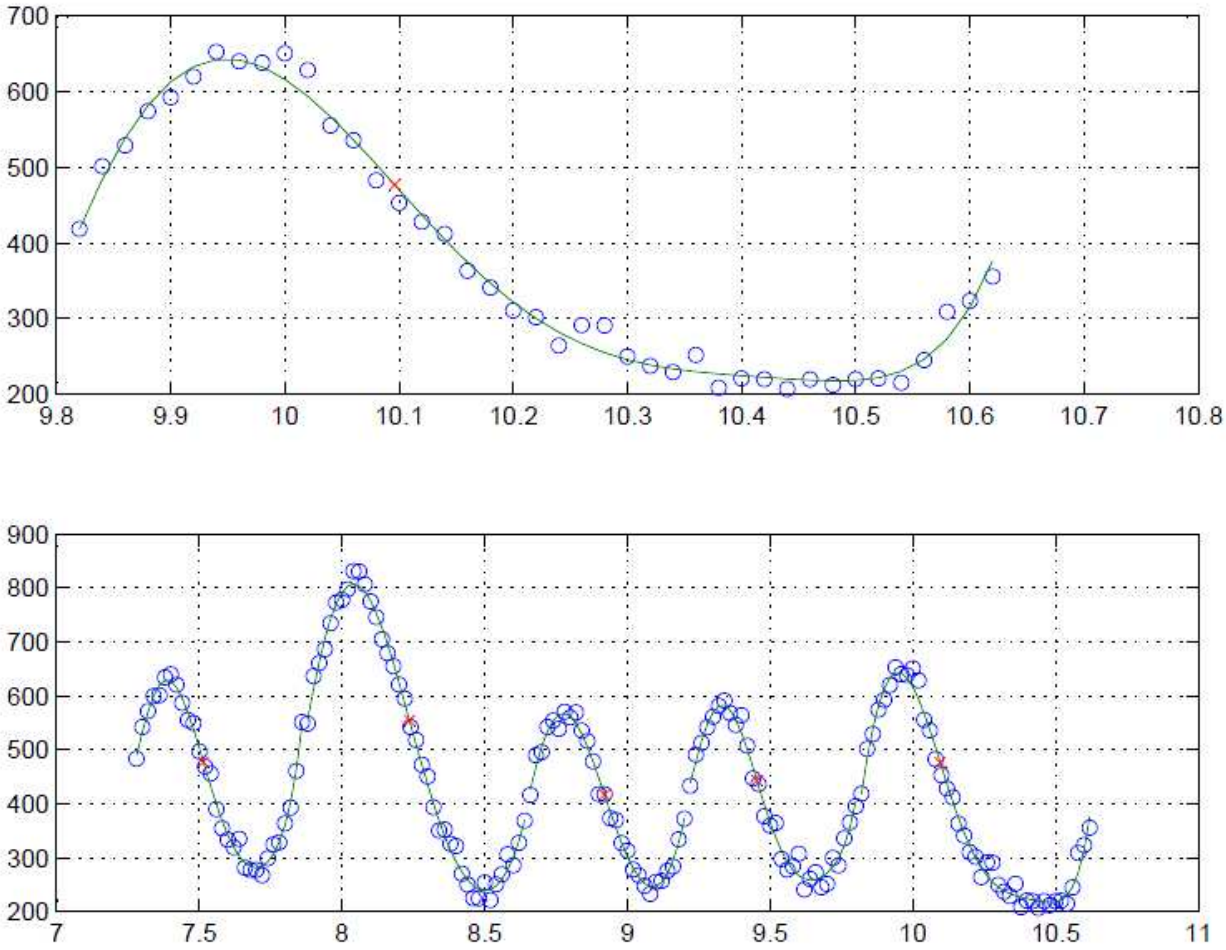

Figure B.1. Output graph from Matlab script to check assignment

Once the user is satisfied with the root determination, he presses a key and the script calculates the earlywood and latewood densities, percent latewood, and average density of the active ring, then records the results in a results matrix. The script also calculates earlywood and latewood densities

based on the integral of the polynomial, but this data was not used in the analysis. After recording all the ring characteristics, the script advances to the next ring and repeats the process until there are no remaining rings. The results matrix was then copied to Excel for use in the analysis.

Polynomial Method Instructions

Three columns of data for a tree are copied onto the clipboard from Excel. The first column should be the position, the second should be density, and the third should be the ring number assignment. This study used the ring assignment from the inflection ring calculator, but any ring assignment could be used. In Matlab, open the script below and run it. A graph similar to the one above will pop up, and the user will strike a key to advance the program to the next ring. Any rings with questionable assignments can be noted for additional assessment. Once all the rings contained on the clipboard have been analyzed, the matrix in Matlab named "OutputMatrix" can be saved as an Excel compatible file.

Polynomial Method Script

```
% This program is used to determine the EW/LW transition using Koubaa's  polynomial fit


%Pull in clipboard data and determine how many rings there are, reset counters
counter = 1;
Ring = [];
OutputMatrixRowCounter = 1
clipboarddatalength = length(clipboarddata)
clipboarddata(clipboarddatalength + 1,:) = 0
RingNumber=clipboarddata(counter, 3)
RingStartPosition = clipboarddata(counter, 1)
RingMatrixStart = counter
maxring = max(clipboarddata(:,3))


%While there is a valid ring to be read
while (RingNumber ~= 0)

        rcounter = 1
        Ring = []
        RingMatrixStart = rcounter
```

```
        RingStartPosition = clipboarddata(counter, 1)


        %While we are still in the same ring
        while ( RingNumber == clipboarddata(counter+1,3))

                %Copy the data from the clipboard to the Ring matrix, loop until ring number
                %changes
                Ring(rcounter, 1)=clipboarddata(counter, 1)
                Ring(rcounter, 2)=clipboarddata(counter, 2)
                counter = counter + 1
                rcounter = rcounter + 1

        end

Ring(rcounter, 1)=clipboarddata(counter, 1);
Ring(rcounter, 2)=clipboarddata(counter, 2);


%The current position is the end of the ring
RingStopPosition = clipboarddata(counter, 1)
RingMatrixStop = rcounter


%Calculate ring length
RingLength = RingStopPosition - RingStartPosition + .02

%Fit a 6th order polynomial to the ring data contained in Ring matrix
p = polyfit(Ring(RingMatrixStart:RingMatrixStop,1),Ring(RingMatrixStart:RingMatrixStop,2),6);

%Calculate and store 2nd derivative of polynomial as secondder
secondder = polyder(polyder(p))

%Find the roots of polynomial secondder and store in rootssecond
rootssecond = roots(secondder)

% Find the maximum density in the ring and identify the position as MaxPosition
MaxDensity = find(Ring(RingMatrixStart:RingMatrixStop,2) ==
Max(Ring(RingMatrixStart:RingMatrixStop,2)))
MaxPosition = max(Ring(MaxDensity,1))

%Criteria to determine which root of the second derivative is the best. As written below, find
%root which is pith side of the maximum density and within 80 percent of the ring length and
%the first derivative at that point is negative. Saved as integer (roots 1, 2, 3, 4) as “whichrootsecond”
whichrootsecond = max(find(MaxPosition < rootssecond & rootssecond < RingStartPosition +
.80*RingLength & polyval(polyder(p),rootssecond) < 0))

%Assign InflectionPoint as the root chosen above for this ring
InflectionPoint = rootssecond(whichrootsecond)

%Evaluate the polynomial at InflectionPoint to determine density at inflection point
InflectionDensity = polyval(p,InflectionPoint)
```

```
%Produce graphs for user
%1st graph of this ring raw data with polynomial and inflection point
x2 = Ring(RingMatrixStart:RingMatrixStop,1);
y2 = polyval(p,x2);

hold on

subplot(2,1,1);
plot(Ring(RingMatrixStart:RingMatrixStop,1),Ring(RingMatrixStart:RingMatrixStop,2),'o',x2,y2,
InflectionPoint, InflectionDensity, 'x');

grid on;

hold off

%Print second graph, just adds current graph to previous graphs of same tree
subplot (2,1,2);
plot(Ring(RingMatrixStart:RingMatrixStop,1),Ring(RingMatrixStart:RingMatrixStop,2),'o',x2,y2,
InflectionPoint, InflectionDensity, 'x');

grid on;

%Wait for user to hit key
pause

%Identify latewood data points and calculate the mean for latewood density
Latewoodpoints = find( Ring(RingMatrixStart:RingMatrixStop,1)< InflectionPoint)
LatewoodDensity = mean(Ring(Latewoodpoints,2))

%Identify earlywood points and calculate the mean for earlywood density
EarlywoodPoints = find( Ring(RingMatrixStart:RingMatrixStop,1)> InflectionPoint)
EarlywoodDensity = mean(Ring(EarlywoodPoints,2))

%Calculate latewood and earlywood width using number of points in each
LatewoodWidth = length(Latewoodpoints) * .02
EarlywoodWidth = length(EarlywoodPoints) * .02

%Calculate percent latewood using previously calculated values
PercentLatewood = 100*LatewoodWidth/RingLength

%Alternative measure of latewood and earlywood density using integral of polynomial over
%Earlywood and latewood regions
IntegratedLatewoodDensity = mean(polyval(p,RingStartPosition:.01:InflectionPoint))
IntegratedEarlywoodDensity = mean(polyval(p,InflectionPoint:.01:RingStopPosition))

%Calculate average density
AverageDensity = mean(Ring(:,2))

%Fill OutputMatrix with values for ring on the OutputMatrixRowCounter-th row
OutputMatrix(OutputMatrixRowCounter,:) = [RingNumber RingStartPosition InflectionPoint
RingStopPosition RingLength InflectionDensity LatewoodDensity IntegratedLatewoodDensity
PercentLatewood EarlywoodDensity IntegratedEarlywoodDensity AverageDensity]
```

```
%Index OutputMatrixRowCounter for next ring
OutputMatrixRowCounter = OutputMatrixRowCounter + 1

%Index counter to look at next ring and read next ring number –if none, exit while loop
counter = counter + 1
RingNumber=clipboarddata(counter, 3)

end
```

Appendix C
Repeated measures analysis

Background repeated measures

The study of serial data collected from the same individuals over time presents a unique set of challenges. Many of the more commonly used statistical tools require an assumption of independence between samples, in that the result of one sample has no correlation with the results of another sample. In addition, there is an assumption of constant variance between samples, which requires the degree of random variation to remain constant from sample to sample. In the study of annual rings of trees, the independence assumption would equate to the assumption that the events (e.g. climatic, cultural, or biological) in years past had no influence on this year's growth (covariance between years equals zero) or that the events of 100 years ago has the same influence as last year's event (covariance between years equals a constant). The assumption of constant variance would be interpreted to require that the random differences are constant through time and that all years would exhibit the same degree of dispersion (Fitzmaurice et al. 2011). A basic familiarity with tree growth and physiology would suggest that applying these assumptions to serial data would be spurious at best, or even misleading.

Violations of these assumptions using common analytical techniques can lead to interpretation issues regarding the significance of the effects being measured, but violations of these assumptions are often the norm in serial datasets (Oehlert 2000). Although it may be difficult to define the precise effects of assumption violations, some general patterns have been observed. Violations of the independence assumption lie in the fact that although our estimates of the treatment effect remain unbiased, our estimate of the variation about the averages of the treatments is no longer unbiased. Because the responses of each of our samples are correlated to one another, each additional sample no longer represents a "new" piece of information. The analysis may reveal that there is a numerically large difference between treatments, we are confident in that result, but we can't accurately assess the significance of that difference using standard practices. Depending on the

nature of the correlations, we may reject or accept the null hypothesis more frequently than we would expect using independent data.

In a similar vein, violations of the constant variance assumption lead to variation in the rates at which we reject or accept the null hypothesis and the departure from expected behavior increases with departures from balanced data sets and as the degree of differences in variance increases. Issues with nonconstant variance stem from the fact that we need to use the same estimate of error variance to test the significance of different groups, so when one small group has a very small associated error and a larger second group has a high degree of error, we overestimate the amount of error for the first group resulting in a conservative test, and underestimate the amount of error in the second group resulting in a liberal test. For dichotomous grouping with balanced data structure, nonconstant variance is less of an issue, but as more groups are compared and the degree of unbalance increases, these issues became more onerous (Oehlert 2000).

Repeated Measures methodologies provide a means to address the violations of independence and constant variance assumptions that are inherent in repeated measures of the same individuals over time. Put simply, repeated measures techniques use a much more complicated framework describing variation within (and in some cases between) individuals over time. By allowing observations close in time to be more similar and observations separated by more time to be less similar, repeated measures models can give a more valid estimation of the variation within the samples, and allows more accurate tests for significance. Likewise, allowing the variance within individuals to change through time permits more accurate assessments of significance. The use of these more complex models has a trade-off or penalty: for each additional parameter we estimate to develop a more accurate model of the sample's change through time, we lose parameters to estimate the final error variance, which requires larger differences between treatments to return a significant result. If accurately modeling the samples through time requires a lot of parameters (ie there is no general pattern or it is very complex), when we try to test the significance of elements of our model, we will

find that it takes a larger difference in treatments to register the same level of significant difference. There is no free lunch.

In basic ANOVA tests, the Independent Variables (IV) are considered fixed factors which, each in their own way, explain some of the variation in the whole dataset by assigning parameter estimates (means or slopes) associated with the levels (discrete IVs) or values (continuous IVs). The basic design of a single factor ANOVA is shown in Figure C.2, with groups representing different treatment levels. The basic test of significance for each of the IVs is whether or not the variation explained solely by the IV (Between groups in Figure C.2) being tested exceeds some ratio of the leftover variation(Within treatments in Figure C.2) once all the IVs have been accounted for. This ratio, called an F-value, is compared to a critical value for a given significance level and if it exceeds the critical value, we call the effect of the IV significant. If individuals in each group are clustered tightly around their respective group means, then the assignment of group means explains a lot of the total variation, and there will be little within-treatment variation. As the ratio of variance explained by treatment to error variation increases, the F-statistic will increase, and may reach a critical value at which we can call the treatment effect significant. All F-values in a simple ANOVA are calculated using the same denominator, an estimate of error which includes random variation, variation due to subjects, and measurement error.

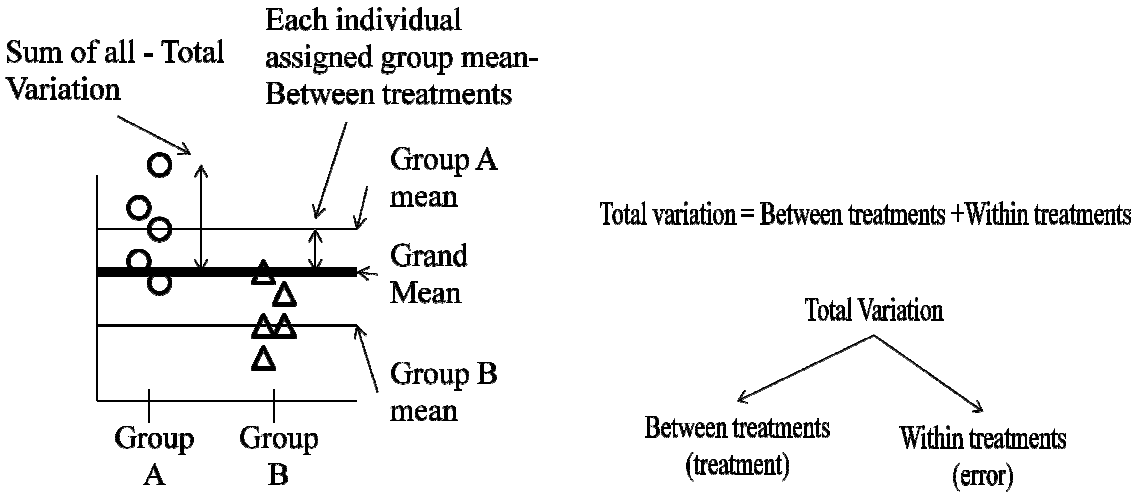

Figure C.1. Visualization of ANOVA

In the repeated measures models used here, the variation is split into two categories: between-subject and within-subject. Figure C.3 shows how variation is partitioned in a repeated measures design. The between-subject portion of the error is used to evaluate the treatments and other covariates that stay fixed through time. In basic ANOVA, all of the remaining error after accounting for IVs is used as the denominator for the F-test. In repeated measures designs, the error term for the between-subject F-test is really the amount of variation due to subjects within treatments. The F-test for the between-subject portion of the repeated measures analysis is really comparing the amount of variation explained by the treatments to the amount of variation within treatment groups without respect to time, or as an average across time. The between-subject component of the repeated measures analysis is identical to the ANOVA design depicted in Figure C.2 above. One can imagine that the more the groups converge on their respective groups averages, group means account for more variation and the random differences between individuals in the same group decreases, and the F-statistic for the test will increase.

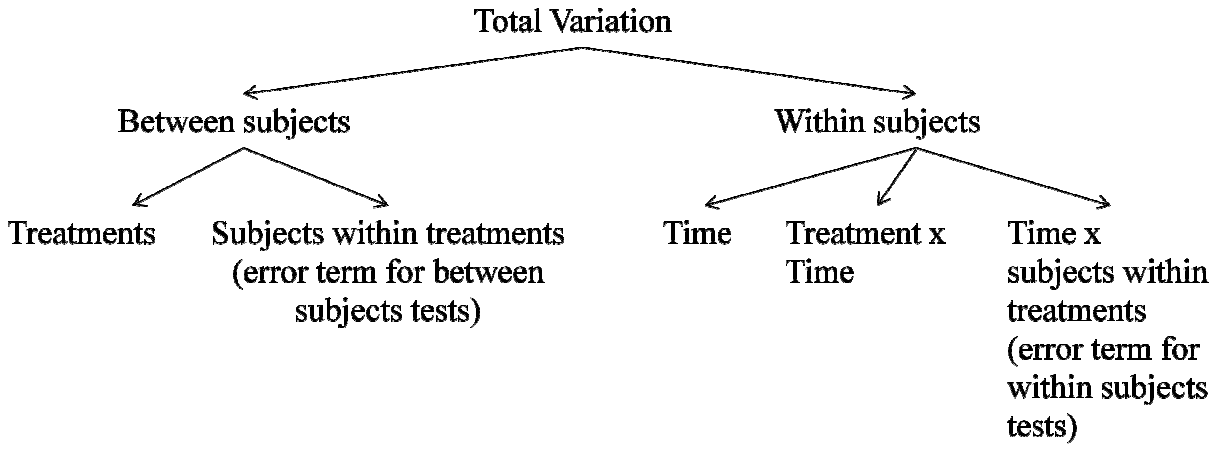

Figure C.2. Partitioning of variance in repeated measures

To assess the significance of IVs that vary (specifically time and interactions between treatments and time), a separate portion of the error variance is used, the within-subject portion. The within-subject portion of the variance assesses differences in individuals over time. Variance explained by time and interactions between time and treatments is pulled from the within-subject variance, and the remainder becomes the error term for within subject variables, and can be thought of as how individuals within treatments vary over time. Unlike simple ANOVA, where all treatments are tested against the same error term, repeated measures requires the use of different error terms depending on whether or not the IV being tested is constant or varies with time.

The mixed models used in this Chapter incorporate fixed effects such as treatments and covariates, but they also include random effects. Random effects are used as placeholders or explanatory variables for random differences that we can account for but may not want specific estimates of, as opposed to fixed effects, which are used to specifically measure the differences between things. A classic example takes place in a factory setting, where there are 3 machines, many operators, and some other IVs which are believed to affect some manufacturing outcome. We may be very interested in the effect of each machine or the other IVs, because for all practical purposes, they are the only ones available, or they are the things over which we have control. We may not be so

interested in the effect of operator because there are so many or we want to assess a population of operators. We account for the effect of operators in that we may estimate a range of likely deviations due to operators (or test whether or not operators impose a significant amount of variation) but typically do not estimate the effect of any one operator. The incorporation of random effects in a model provides a means to account for known or expected variation without specifically measuring the effect of every individual. The deviations that are attributable to the random effect are held separately, and do not contribute to the error term(s).

The model referenced in Equation 3 incorporates a random effect for tree: $(S\gamma)_{j(i)}$. This random effect is commonly referred to as a random intercept, and ideally would be thought of as accounting for random variation common to all trees. By using a random intercept, the model acknowledges that there are differences between trees, and we assume that those differences are normally distributed with a mean of zero and some variance. If we went back out to the field and sampled more trees, we would expect that the new trees sampled would be different than the originals, but we would expect their variations to be similarly distributed as the originals. Thus, when we use the model to estimate population parameters (making inferences across a large group of individuals), the random term essentially drops to zero in the same way that the residual variance drops to zero when estimating population parameters. Another way of thinking about the random intercept would be in the context of a regression for many individuals, and the y-intercept of each individual would be "allowed" to float, and the researcher would be interested therefore in how the slope with respect to the IV was able to account for remaining variance. The random intercept permits us to remove some of the variation common to all trees so that we can concentrate on measuring variation between and within treatments

One of the primary features of repeated measures analysis such as these is the use of a more complicated covariance matrix to explain residual errors through time. The covariance matrix is the

mathematical tool or matrix structure that is used to describe the variation of individuals at a given time (variance) and the relationships in errors between time periods (covariance). As stated previously, if a close approximation of the "true" covariance structure can be reached, with faithful representations of the variances and covariances within individuals through time, then the resulting measures of significance will be more accurate. In addition, some of that quantity that was considered random error in a simple ANOVA framework will be recognized as covariance, and reduce the random portion of the error. If you can accurately account for variation with a model, then the predictable portion of the variation is not really random.

For example, we can plot the average densities for all trees for two consecutive years, and we find there is some correlation there; that the trees that tended to have high density last year also have high density this year, and vice versa. Figure C.4a shows the average ring density of trees in the years 1976, and the average densities of the same trees in 1977. This correlation (or specifically this covariance) allows us to partition some of what we assumed was random error into covariance. Figure C.5 show how we can divide the within-subject error into four components: variation explained by Year, variation explained by the Treatment X Year interaction, the residual covariance between years, and finally the remaining error residuals that will form the error term for the analysis of the within-subject IVs. As mentioned previously, some covariance matrix models allow for different patterns of covariance within trees for different years, and different variances for different years. In Figure C.4b , the average densities in 1976 are fitted with the average densities in 2005. There was a dramatic reduction in the same tree correlation compared to 1977, and to accurately model the covariance patterns, the covariance should probably be allowed to decrease with time. The more closely we can model what is actually occurring in the data, the better our estimates of significance should be. As the covariance matrix become more complicated, we may be able to assign more of the error residuals term as covariance. As we make the covariance matrix more complicated, we also lose degrees of freedom from the error residual term, which may make it more

difficult to demonstrate significant differences later in the analysis. The trade-off is thus to determine the most parsimonious covariance matrix which does an adequate job of describing variance within years and covariance between years with the fewest possible number of parameters.

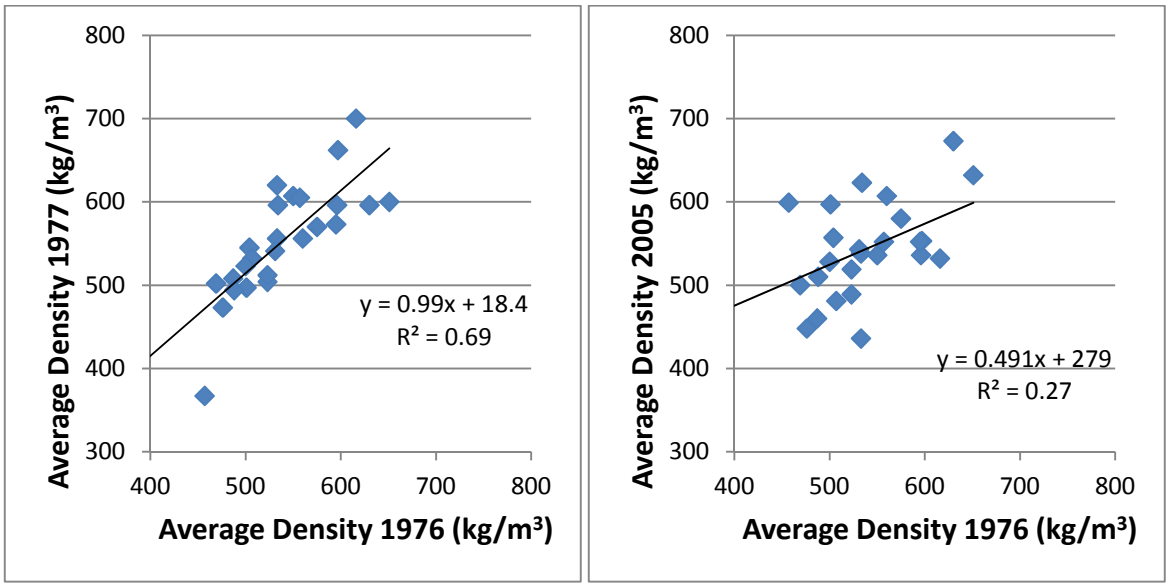

Figure C.3. Correlations between years. Correlations between 1976 and 1977 (a). Correlations between 1976 and 2005 (B).

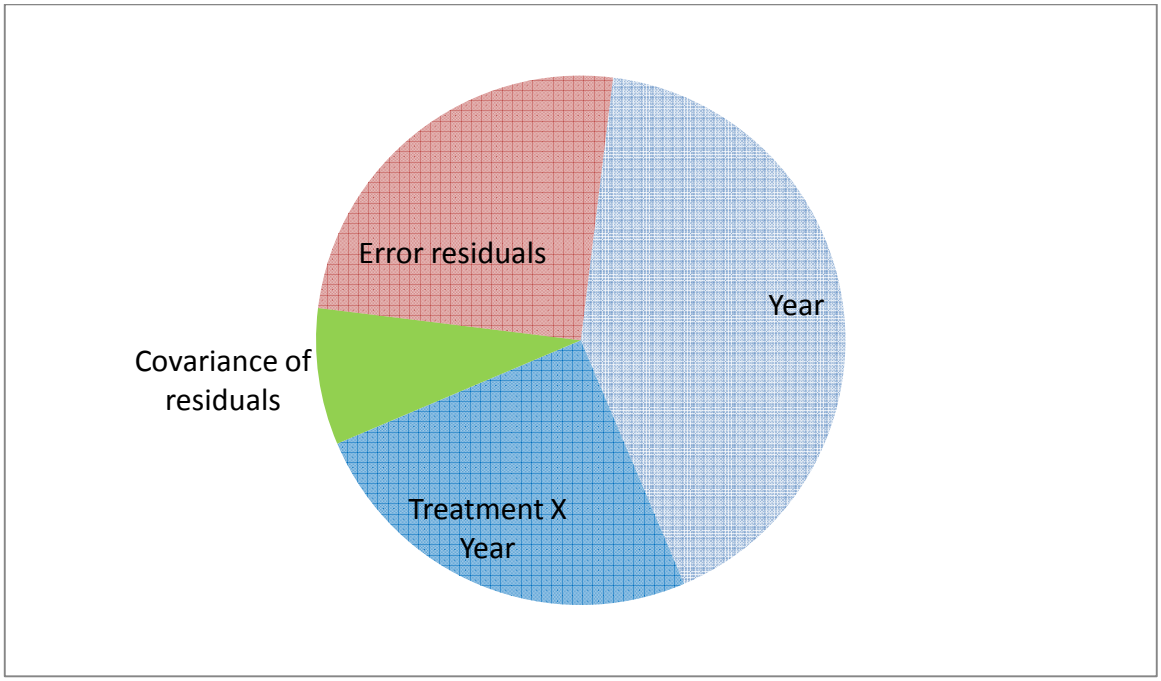

Figure C.4. Partitioning of within-tree error variance

Progression of analysis

The increment cores for the study were chosen randomly from the cores collected from the initial study performed in August of 2007. The only initial criteria were that the cambial age was at least 25 years in 1975, and that the cores were complete. The high and low SBD groups represented similar ranges of stand conditions, though not always with the same distribution. Figure C.6 shows histograms of some of the tree and stand blocking variables for the two SBD groups. Figure C.6 A shows the establishment year at breast height, and indicates that across many of the stands sampled, there was a major disturbance in the 1930's, after which, a great deal of ingrowth in the stands occurred. This same pattern was seen in the pool of original samples from which the trees for this study were drawn. In Figure C.6 B, the distribution of elevations for the sample trees suggests that the SBD groups cover approximately the same range, with the low SBD group exhibiting a slightly wider range. The clustering is a result of cross-sectional nature of the initial study to try and sample across a wide elevation gradient categories. Figure C.6 C shows the distribution of green canopy as a percent of total height, and shows that the two SBD groups encompassed a similar range of canopy lengths. Figure C.6 D shows the distribution of the specific gravities of the entire increment cores, from pith to bark. The member of the high SBD group exhibited a low whole tree specific gravity, but it was one of the youngest trees in the sample and presumably contained a high proportion of juvenile or core wood. The average densities from that tree used in the analysis were much closer to the mean of the high SBD group. Figure C.6 E shows the distribution of total tree heights, and Figure C.6 F shows the diameter distributions for the two SBD groups. In all, the distributions were similar to those found from which the samples were drawn from.

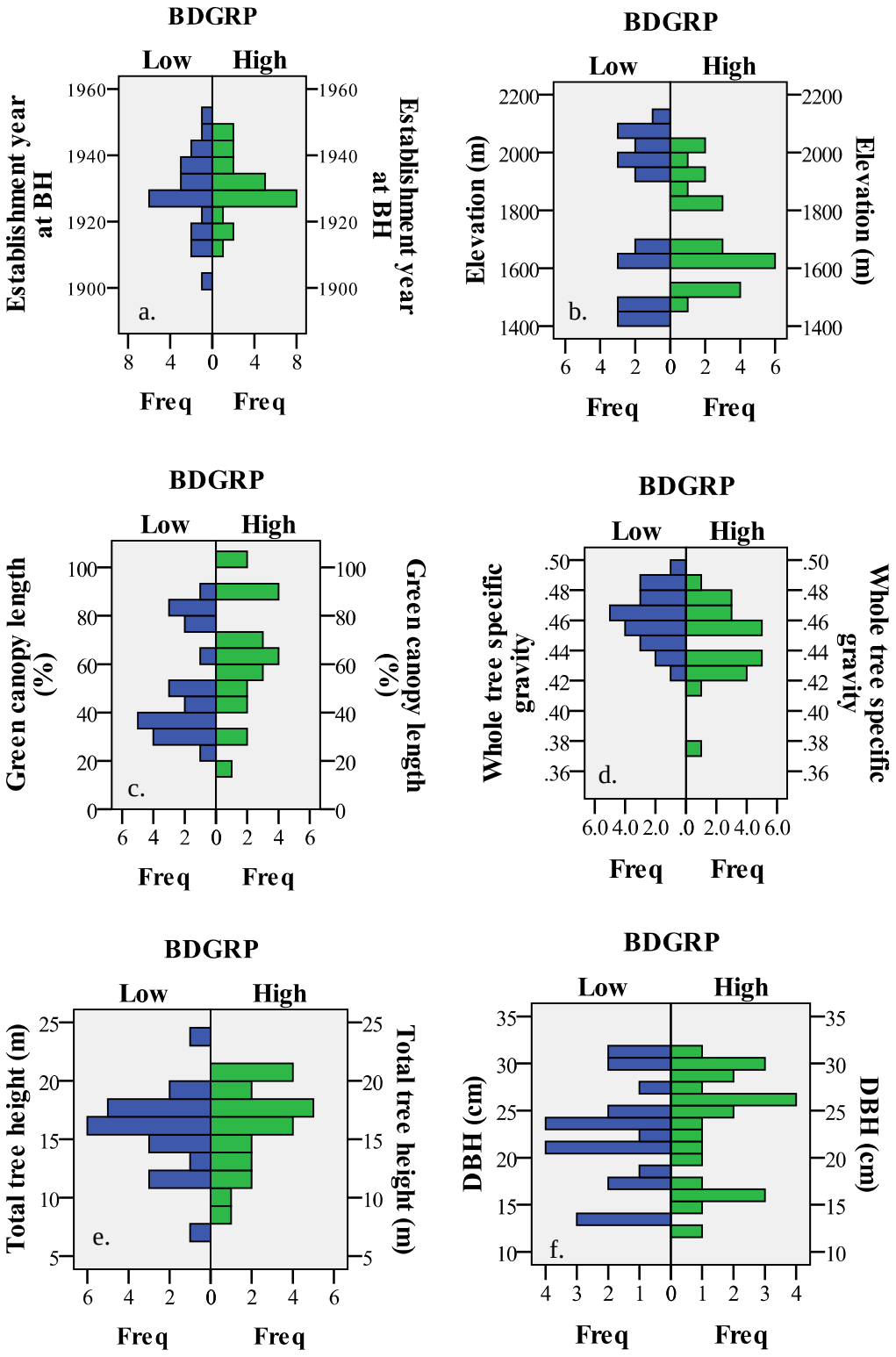

Figure C.5. Comparison of stand and tree characteristics between SBD groups: Establishment year(a), elevation(b), green canopy (c), whole tree SG (d), height (e), DBH (f).

The data set was split into a calibration set containing data from 1976-1985 and a test data set that contained data from 1986-2005. The intent was to use the calibration data set to determine the two most significant covariates to accompany Soil Bulk Density Group (BDGRP), Year, and BDGRP X Year. In addition, the calibration data was used to determine which covariance matrix model best fit the data by means of the Bayesian Information Criterion calculated in Proc Mixed in SAS.

The models were built using a top-down approach as outlined in West et al. in which the first step was to identify those variables that seemed to best explain variation in the ring characteristics of interest with no accommodations for the serial correlations in the data due to repeated sampling, and without random effects. The resulting model was likely overfit, but the goal was to explain as much systematic variation as possible using covariates (ie get the means as close as reasonably possible), leaving residuals that contained as little systematic error as possible. Next, models including the random effect (random intercept for this study) and potential residual covariance models were compared using the BIC value as a measure of parsimony. Once an appropriate random intercept and covariance combination were selected, the covariates in the model were reduced until the two most significant covariates remained along with BDGRP, YEAR, BDGRP X YEAR, and the random intercept.

To identify the best variables to accompany SBD, the first step was to use regression without accounting for repeated measures to see if any variables exhibited strong relationships across individuals and time with the ring characteristics being investigated in the calibration data set. The intent of the first step was to explore the relationships between variables, and determine if any interactions could be visually determined. All main effects and seemingly significant potential interactions were tested in the second phase.

The second phase of the analysis was to use a univariate ANOVA model in SPSS to reduce the number of variables in the model to a more reasonable subset. The models all included BDGRP, Year, and the BDGRP X Year interaction, but the other covariates were added to see which ones were best correlated to the ring characteristics. The univariate model still did not account for the repeated measures format of the analysis, but because all the variables being considered were between-tree factors, they all were tested against the same error term. The covariates that exhibited significance in the univariate ANOVA analysis were used for the final model building stage.

The final model building step was take those variables that exhibited significance in the univariate ANOVA and build a final model that accounted for the repeated measures structure of the data, possibly included the random effects, and used the most appropriate residual covariance matrix. The covariates that were significant in the prior step were added into PROC MIXED in SAS 9.1 with BDGRP, YEAR, BDGRP X YEAR, and executed with a script written to run all the potential combinations of random intercept and residual covariance matrices (as appropriate) in one pass. The Restricted Maximum Likelihood (REML) method was used to generate parameter estimates and the Kenward-Rogers method was used to approximate the denominator degrees of freedom. The covariance matrices tested were: diagonal, unstructured, first order autoregressive, heterogeneous autoregressive, compound symmetric, heterogeneous compound symmetric, toeplitz, and heterogeneous toeplitz. The final covariance matrix used was the one that registered the lowest BIC score, or in the case of a tie, the one that required the fewest parameters. Once the residual covariance matrix was chosen, the covariates were eliminated one by one based on their significance in the model until there were two covariates to accompany the treatment, time, treatment-time interaction, and random intercept. The final model was run on the calibration data to check residuals for normality and constant variance.

TLWP

After developing the models for the threshold, inflection, and polynomial models, an analysis of the residuals indicated that the assumption of constant variance across the predicted values may be violated in the calibration dataset. The graphs using the calibration dataset weren't definitive, but as a precaution, models for the log transformation of the three latewood measure were developed, and were the ones that were ultimately used. All the latewood measurements exhibited long right tails in their distributions and the smallest rings exhibited a greater variation than longer rings. The residuals for AVGDEN did not exhibit any patterns in the variance of the residuals in either the calibration or test dataset.

Figure C.7 shows the residuals from TLWP and LNTLWP, the consistency of the residuals over the range of predicted values showed a great deal of improvement using the transformed values. The two models used nearly the same covariates, the untransformed TLWP used LNAVGRL and ELEV, while LNTLWP used LNAVGRL and BHAGE, but ELEV was the last covariate removed (third best covariate). The BIC values from the covariance matrix fitting for LNTLWP are shown in Table C.1. The autoregressive model was essentially tied with the heterogeneous autoregressive model , and the autoregressive model was chosen. The results of the final model fitting for LNTLWP are shown in Table Y. The final covariates selected to model LNTLWP were: ELEV and LNAVGRL.

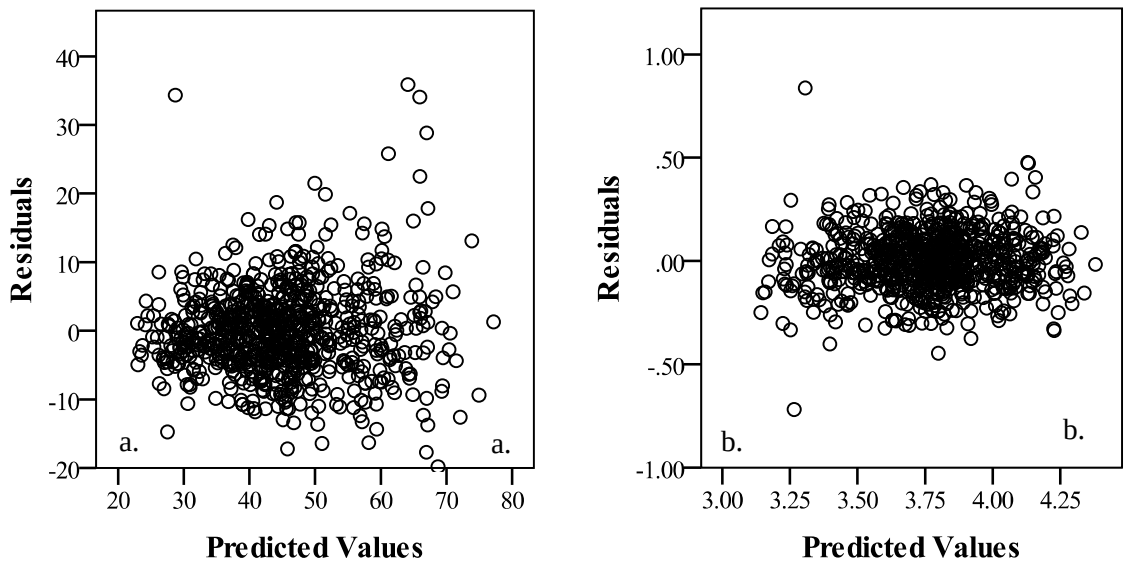

FigureC.6. Residuals plot of the calibration model for TLWP(a). Residual plot of the calibration model for LNTLWP(b).

Table C.1. BIC values for choice of covariance matrix for LNTLWP

Covariance Stucture	Random Intercept	BIC
Diagonal	No	271.3
Unstructured	Yes	189.6
Diagonal	Yes	112.4
Autoregressive	No	154.3
Autoregressive	**Yes**	**107.2**
Heterogenous Autoregressive	No	150.7
Heterogenous Autoregressive	Yes	106.9
Compound Symmetry	No	112.4
Compound Symmetry	Yes	112.9
Heterogenous Compound Symmetry	No	113.9
Toeplitz	Yes	123.3
Heterogenous Toeplitz	No	124.2

The model results are shown in the body of the Results section of the Chapter, but the analysis of the residuals is shown below. The distribution of the residuals for the low SBD group in Figure C.8a, and the high SBD group in the Figure C.8.b, the residuals for both appeared to be normal

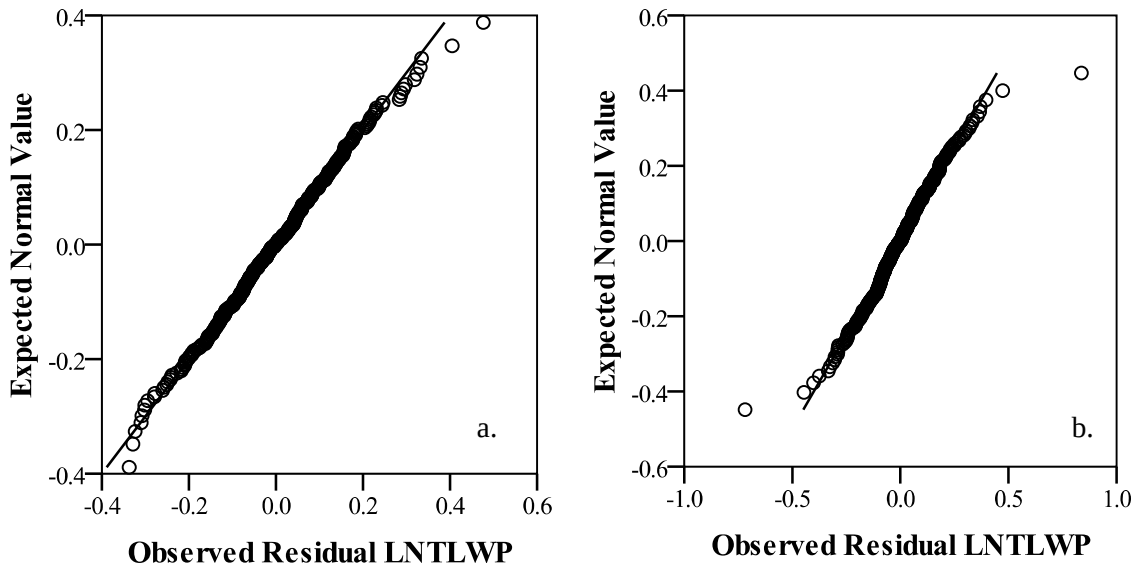

Figure C.7. Distribution of residuals for the final LNTLWP model, low SBD(a), high SBD (b)

The residuals for both of the covariates likewise seemed to be consistently distributed for both SBD groups across their respective ranges. Figure C.9 shows the distribution of residuals plotted across the range of LNAVGRL 86-05 and BHAGE

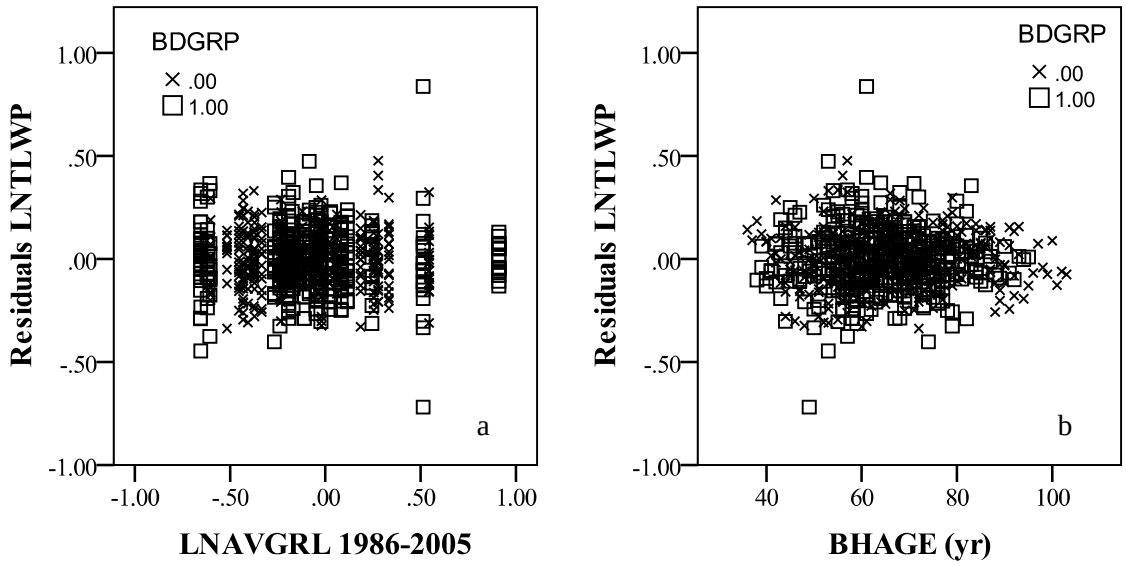

Figure C.8. Residuals from final model for LNTLWP plotted against LNAVGRL(a), BHAGE (b).

AVGDEN

The covariance selection process indicated that the autoregressive covariance model with a random intercept provided the best fit using the BIC values as a metric. The results of the covariance selection process are shown in Table C.2

Table C.2. BIC values for choice of covariance matrix for AVGDEN

Covariance Stucture	Random Intercept	BIC
Diagonal	No	4232
Unstructured	Yes	4005
Diagonal	Yes	3939
Autoregressive	No	3985
Autoregressive	**Yes**	**3928**
Heterogenous Autoregressive	No	3984
Heterogenous Autoregressive	Yes	3930
Compound Symmetry	No	3939
Heterogenous Compound Symmetry	Yes	3939
Heterogenous Compound Symmetry	No	3946
Toeplitz	No	3946
Heterogenous Toeplitz	No	3952

With the autoregressive covariance matix and the random intercept, the final two covariates chosen using the calibration data were ELEV and BHAGE.

The homogeneity of the variance across the predicted values of AVGDEN is shown in Figure C.10, and the normal distribution of the residuals for the low and high SBD groups are shown in Figures C.11.a and C.11.b. The distribution of residuals across the range of BHAGE and ELEV are shown in Figures C.12a and C.12b. All residuals appeared to be approximately normally distributed and showed no pattern to suggest differences in distribution across the ranges of any of the covariates.

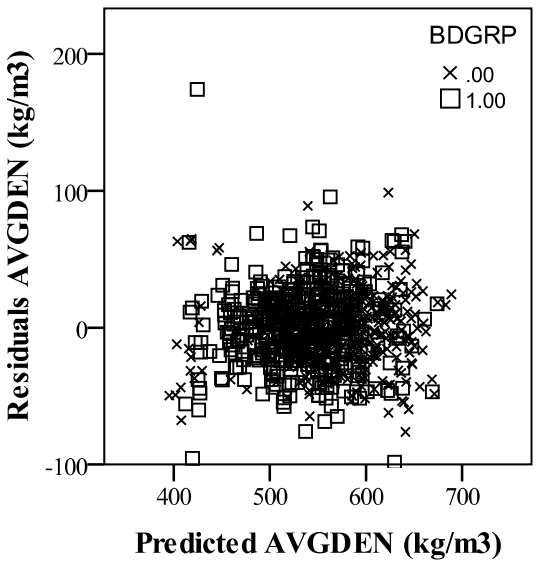

Figure C.9. Residual plot for final model of AVGDEN

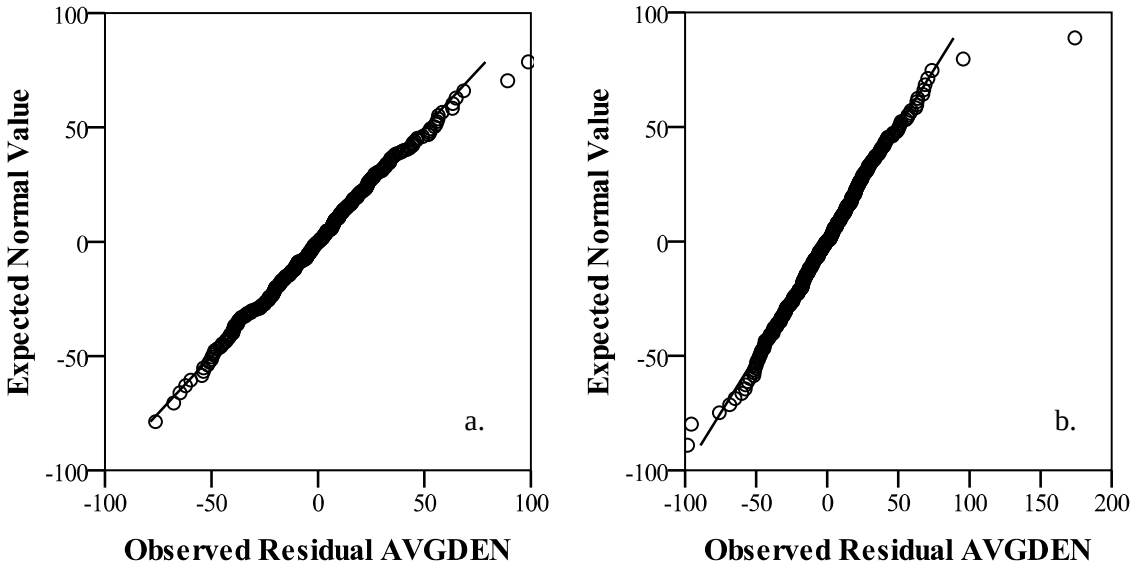

Figure C.10. Distribution of residuals from the final model for AVGDEN. Low SBD group (a), high SBD group (b).

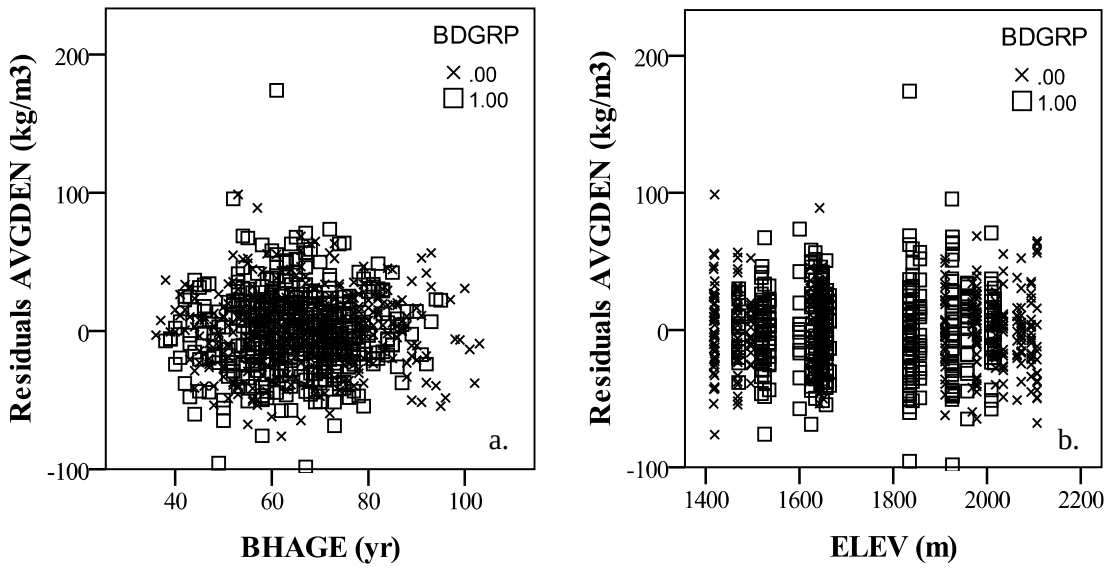

Figure C.11. Residuals from final model for AVGDEN plotted against BHAGE(a), ELEV (b).

LNINFLWP

The covariance selection process indicated that the autoregressive covariance model with a random intercept provided the best fit using the BIC values as a metric. The results of the covariance selection process are shown in Table C.3.

Table C.3. BIC values for choice of covariance matrix for LNINFLWP

Covariance Stucture	Random Intercept	BIC
Diagonal	No	63
Unstructured	Yes	94
Diagonal	Yes	-7
Autoregressive	No	11
Autoregressive	**Yes**	**-11**
Heterogenous Autoregressive	No	28
Heterogenous Autoregressive	Yes	8
Compound Symmetry	No	-7
Heterogenous Compound Symmetry	No	8
Toeplitz	No	0
Heterogenous Toeplitz	No	17

The final model selection in PROC MIXED is shown in Table BH. The final covariates chosen using the calibration dataset for LNINFLWP were BHAGE and LNAVGRL76_85 using the autoregressive covariance matrix and a random intercept term

The homogeneity of the variance across the predicted values for the test data set of LNINFLWP is shown in Figure C.13, and the normal distribution of the residuals for the low and high SBD groups are shown in Figures C.14a and C.14b. The distribution of residuals across the range of BHAGE and LNAVGRL are shown in Figures C.15a and C.15b. All residuals appeared to be approximately normally distributed and showed no pattern to suggest differences in distribution across the ranges of any of the covariates.

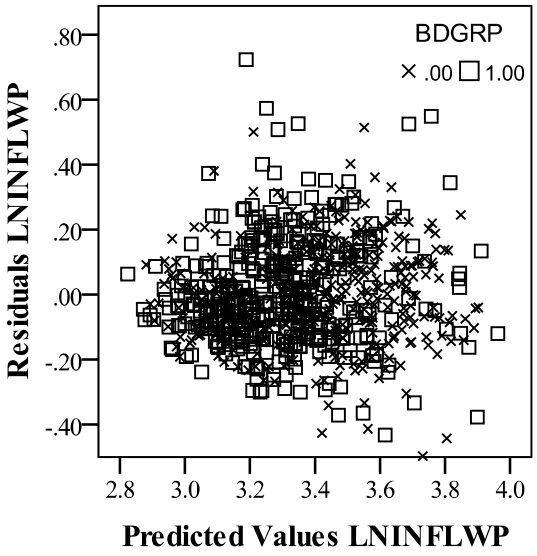

Figure C.12. Residual plot for final model of LNINFLWP

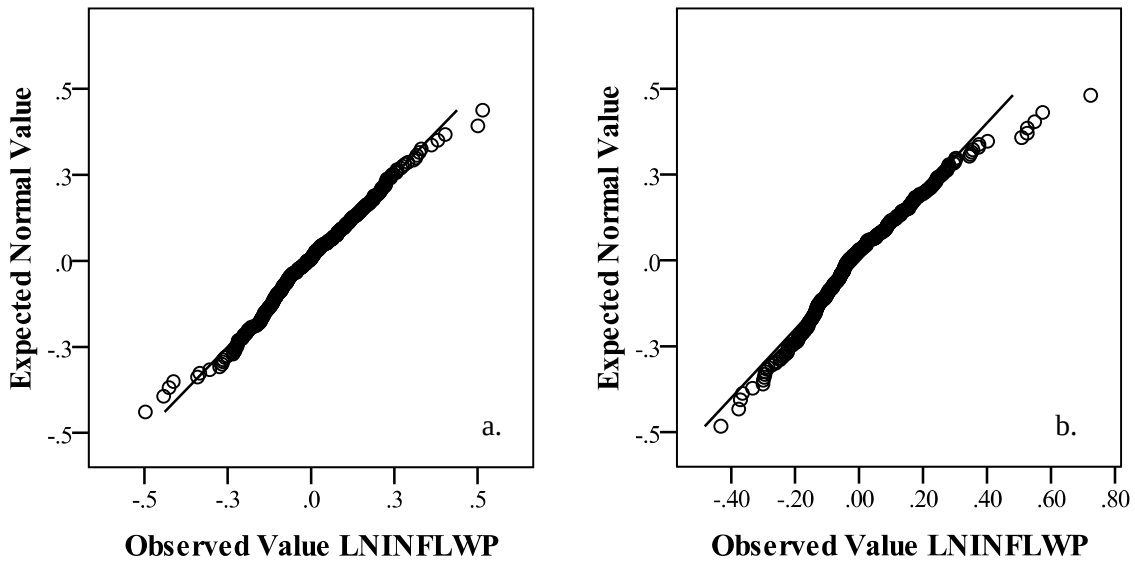

Figure C.13. Distribution of residuals from the final model for LNINFLWP. Low SBD group (a), high SBD group (b).

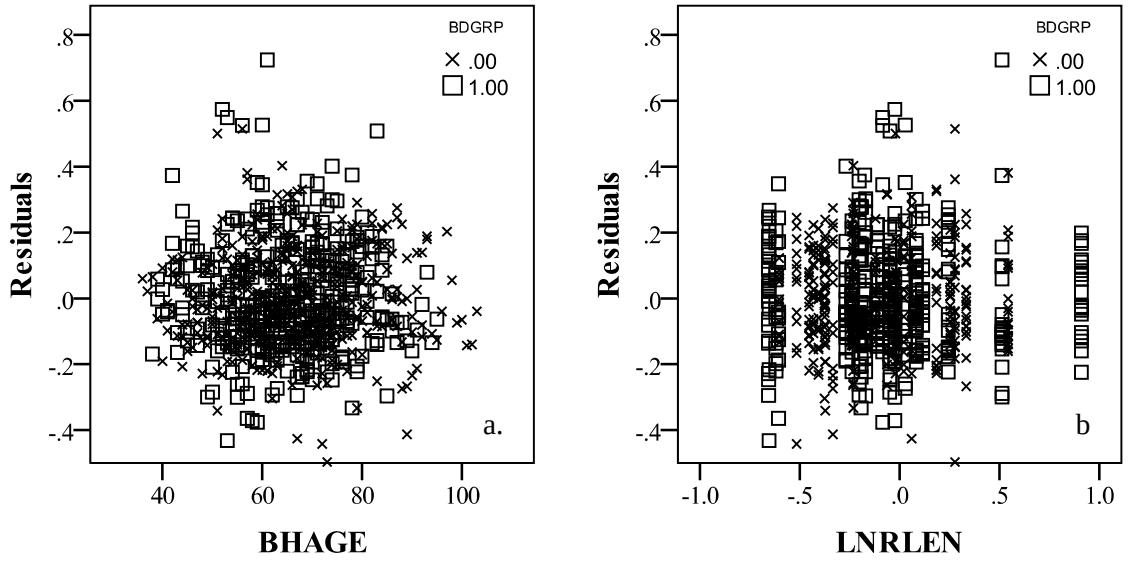

Figure C.14. Residuals from final model for LNINFLWP plotted against BHAGE (a), LNRLEN (b).

LNADJINFLWP

The covariance selection process indicated that while the heterogeneous compound symmetric covariance model without a random intercept provided the best fit using the BIC values as a metric, the autoregressive model was within 2 BIC points of the heterogeneous compound symmetric indicating near equivalency. In addition, the covariance parameters estimated by the unstructured matrix seemed to indicate a pattern more consistent with the autoregressive model with a few years with interspersed with higher covariance that did not fit the autoregressive pattern. The results of the covariance selection process are shown in Table C.4

Table C.4. BIC values for choice of covariance matrix for LNADJINFLWP.

Covariance Stucture	Random Intercept	BIC
Diagonal	No	407
Unstructured	Yes	363
Diagonal	Yes	282
Autoregressive	No	323
Autoregressive	**Yes**	**280**
Heterogeneous Autoregressive	No	307
Heterogeneous Autoregressive	Yes	283
Compound Symmetry	No	282
Heterogeneous Compound Symmetry	No	278
Toeplitz	No	289
Heterogeneous Toeplitz	No	286

The final covariates chosen using the calibration dataset for LNINFLWP were BHAGE and LNAVGRL76_85 using the autoregressive covariance matrix and a random intercept term.

The homogeneity of the variance across the predicted values for the test data set of LNADJINFLWP is shown in Figure C.16, and the normal distribution of the residuals for the low and high SBD groups are shown in Figures C.17a and C.17b. The distribution of residuals across the range of BHAGE and LNAVGRL86_05 are shown in Figures C.18a and C.18b. All residuals appeared to be

approximately normally distributed and showed no pattern to suggest differences in distribution across the ranges of any of the covariates.

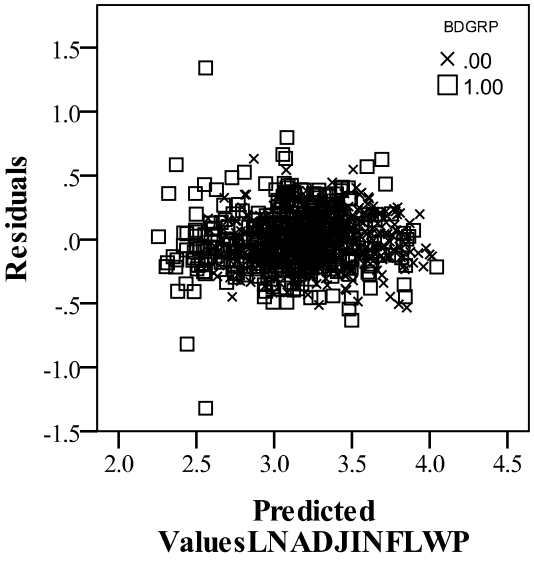

Figure C.15. Residual plot for final model of LNADJINFLWP

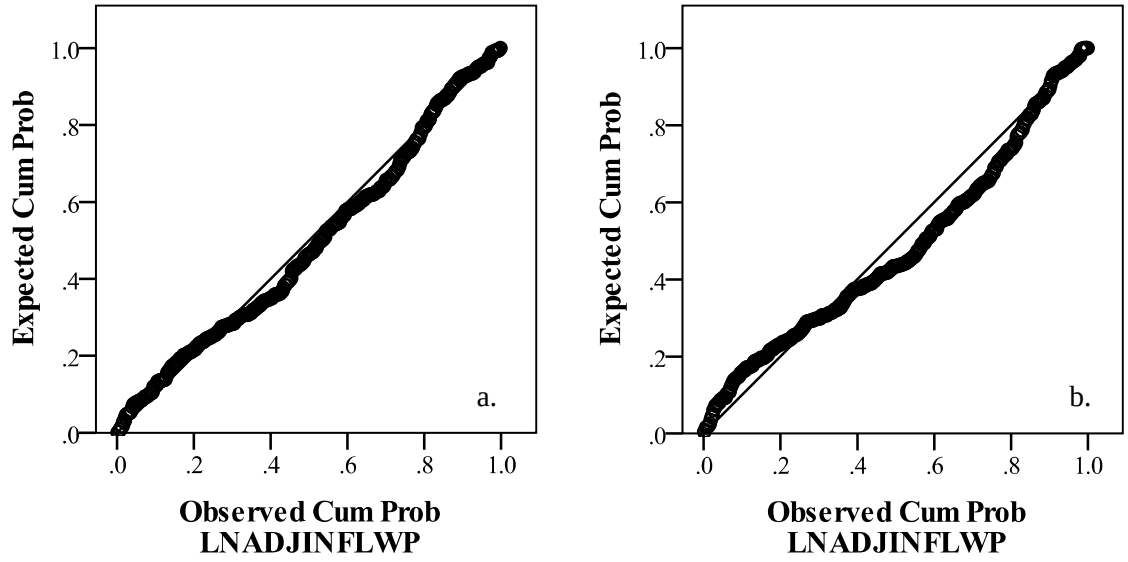

Figure C.16. Distribution of residuals from the final model for LNADJINFLWP. Low SBD group (a), high SBD group (b).

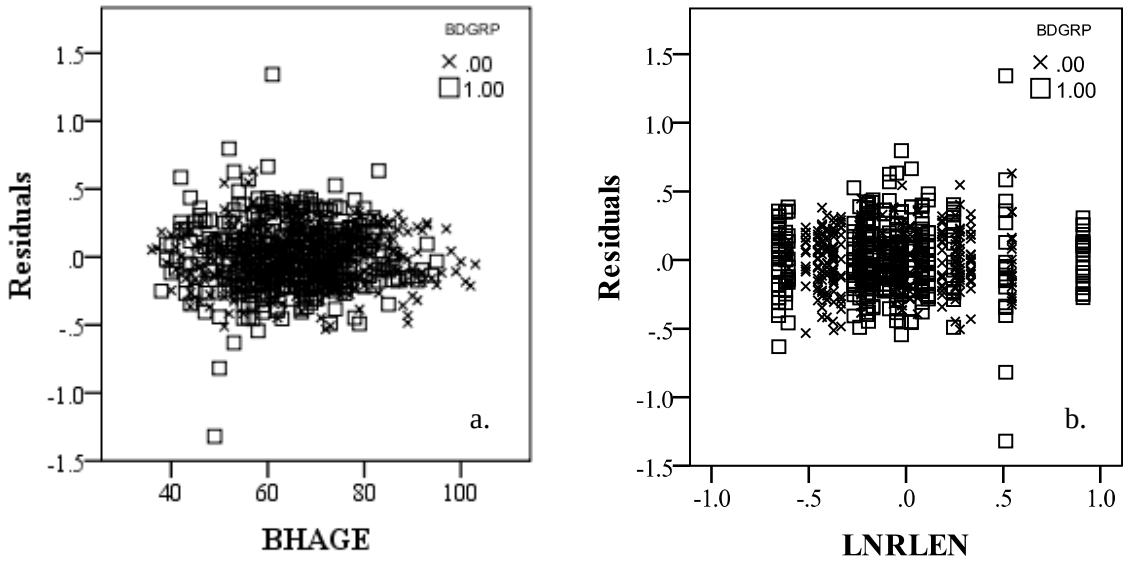

Figure C.17. Residuals from final model for LNADJINFLWP plotted against BHAGE (a), LNRLEN (b).

LNPLWP

The covariance selection process indicated that the autoregressive covariance model best fit the data..

The results of the covariance selection process are shown in Table C.5

Table C.5. BIC values for choice of covariance matrix for LNPLWP.

Covariance Stucture	Random Intercept	BIC
Diagonal	No	145
Unstructured	Yes	64
Diagonal	Yes	-28
Autoregressive	No	-12
Autoregressive	**Yes**	**-43**
Heterogeneous Autoregressive	No	-9.4
Heterogeneous Autoregressive	Yes	-19
Compound Symmetry	No	-28
Heterogeneous Compound Symmetry	No	-13
Toeplitz	No	-33
Heterogeneous Toeplitz	No	-16

The homogeneity of the variance across the predicted values for the test data set of LNPLWP is shown in Figure C.19, and the normal distribution of the residuals for the low and high SBD groups are shown in Figures C.20a and C.20b. The distribution of residuals across the range of PERGRN

and LNAVGRL86_05 are shown in Figures C.21a and C.21b. All residuals appeared to be approximately normally distributed and showed no pattern to suggest differences in distribution across the ranges of any of the covariates.

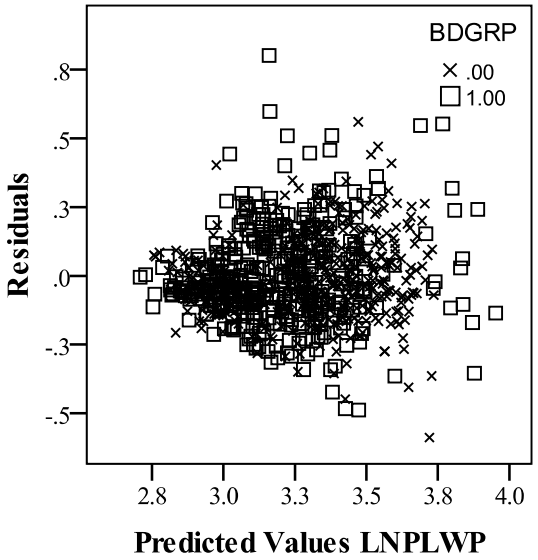

Figure C.18. Residual plot for final model of LNPLWP.

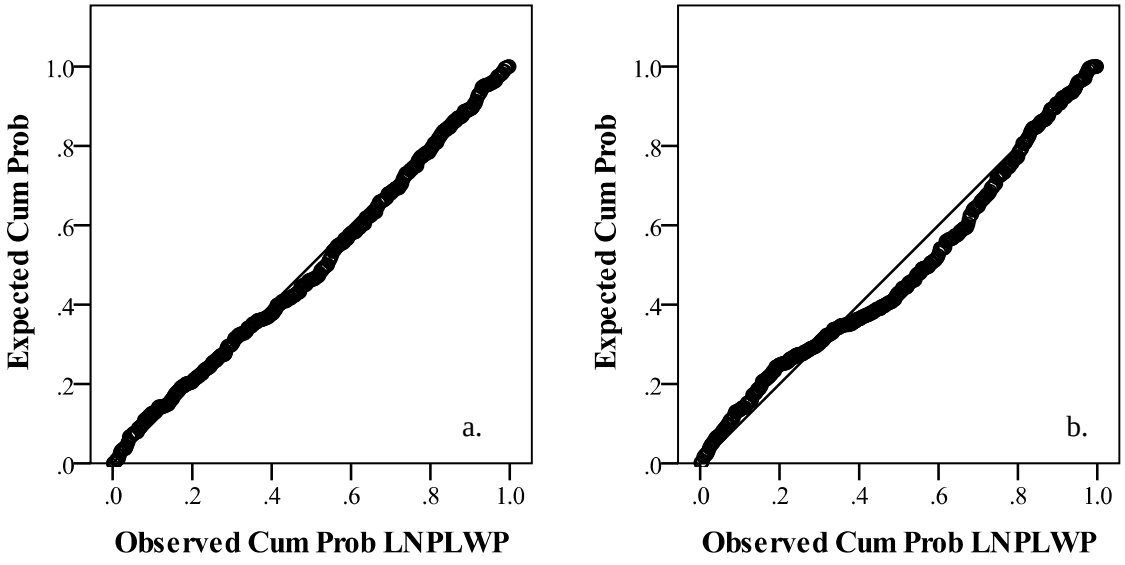

Figure C.19. Distribution of residuals from the final model for LNADJPLWP. Low SBD group (a), high SBD group (b).

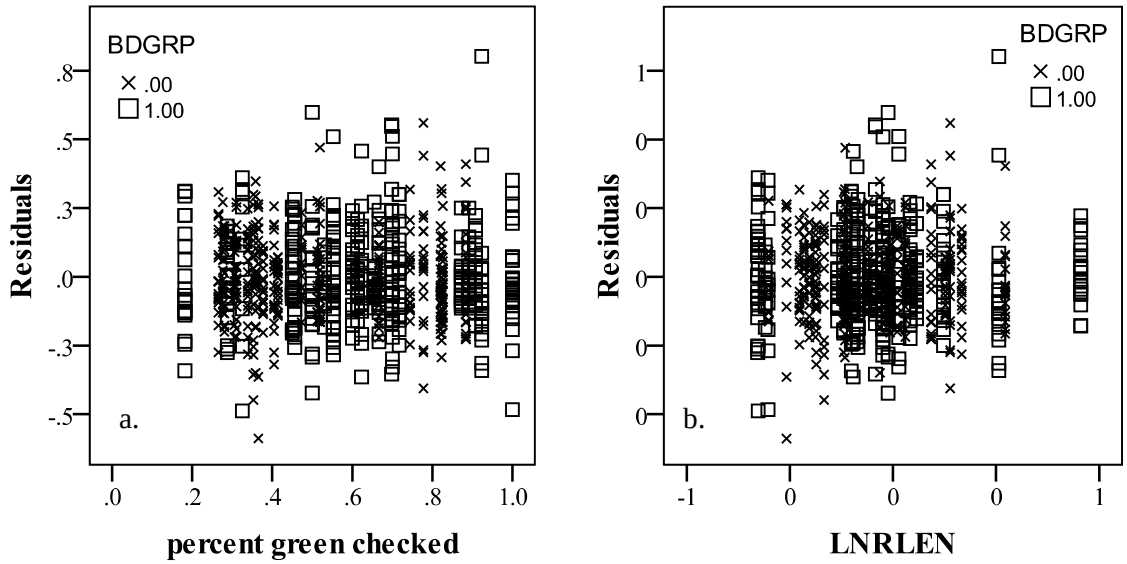

Figure C.20 Residuals from final model for LNPLWP plotted against PERGRN (a), LNRLEN (b).

LNADJPLWP

The covariance selection process indicated that the autoregressive covariance pattern provided the best fit. The results of the covariance selection process are shown in Table XD

Table C.6. BIC values for choice of covariance matrix for LNADJPLWP.

Covariance Stucture	Random Intercept	BIC
Diagonal	No	407
Unstructured	Yes	363
Diagonal	Yes	282
Autoregressive	No	323
Autoregressive	**Yes**	**280**
Heterogeneous Autoregressive	No	307
Heterogeneous Autoregressive	Yes	283
Compound Symmetry	No	282
Heterogeneous Compound Symmetry	No	278
Toeplitz	No	289
Heterogeneous Toeplitz	No	286

The final covariates chosen using the calibration dataset for LNINFLWP were BHAGE and LNAVGRL76_85 using the autoregressive covariance matrix and a random intercept term.

The homogeneity of the variance across the predicted values for the test data set of LNADJINFLWP is shown in Figure C.22, and the normal distribution of the residuals for the low and high SBD groups are shown in Figures C.23a and C.23b. The distribution of residuals across the range of BHAGE and LNAVGRL86_05 are shown in Figures C.24a and C.24b. All residuals appeared to be approximately normally distributed and showed no pattern to suggest differences in distribution across the ranges of any of the covariates.

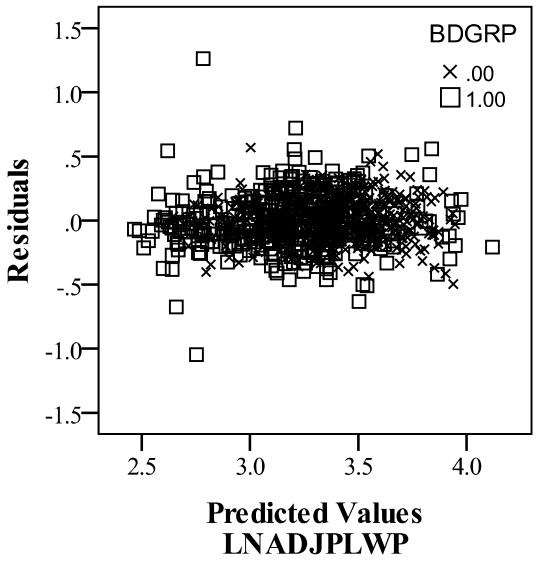

Figure C.21. Residual plot for final model of LNADJPLWP.

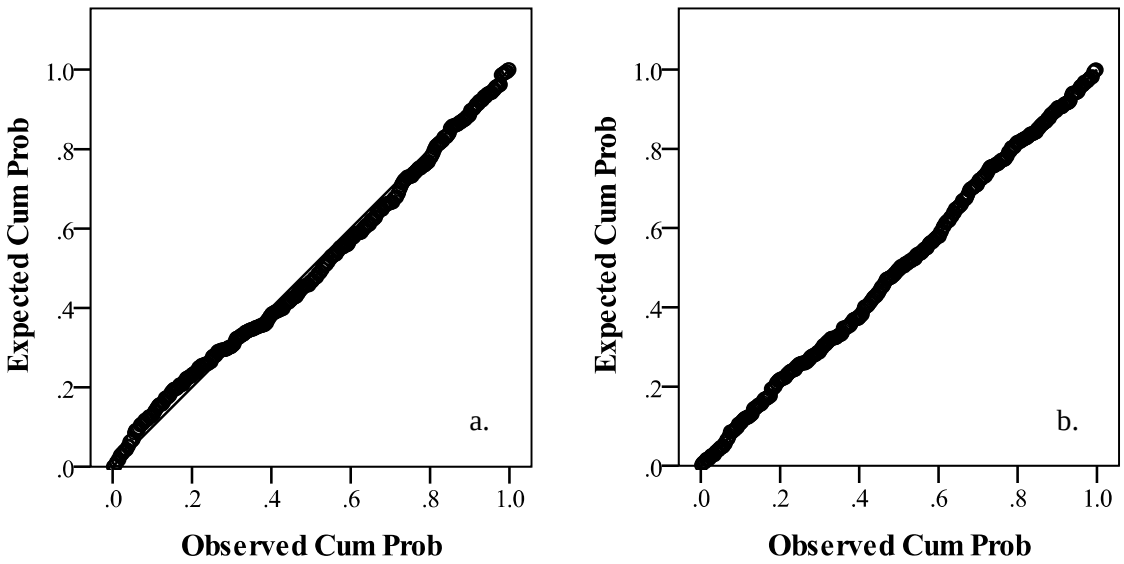

Figure C.22. Distribution of residuals from the final model for LNADJPLWP. Low SBD group (a), high SBD group (b).

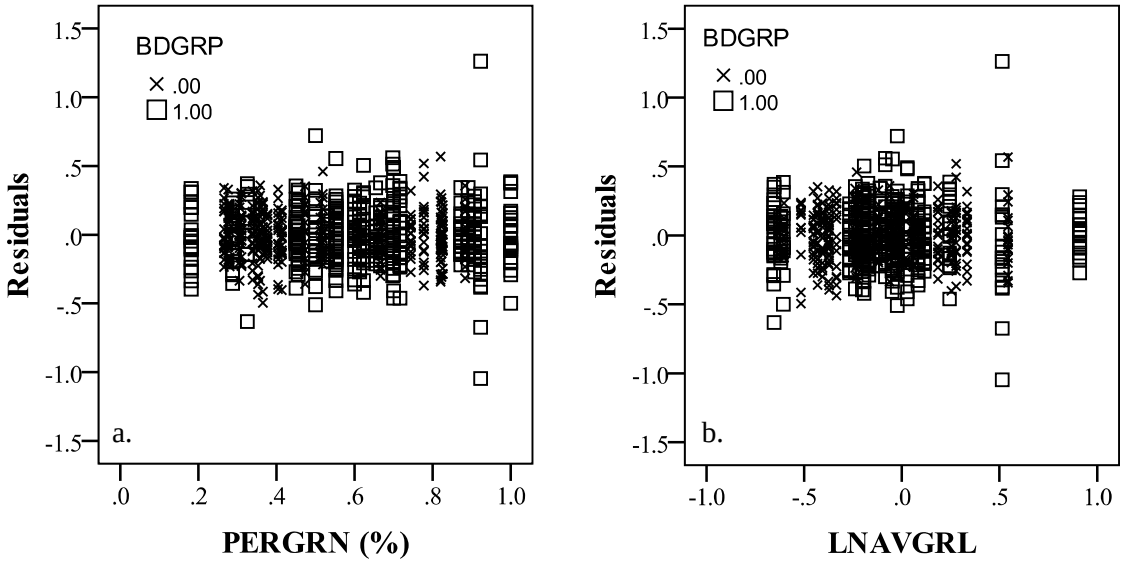

Figure C.23. Residuals from final model for LNADJPLWP plotted against PERGRN (a), LNAVGRL (b).

Appendix D
SAS Code

```
proc mixed data=fridaynight covtest method =
reml;/*autoregressive*/
class bsyrfix bdgrp tree;
model lntlwp = bdgrp bsyrfix bdgrp*bsyrfix bhage
lnavgrl86_05
/htype = 3 intercept ddfm=kr s outpred=predlntlwp;
random intercept/sub=tree(bdgrp);
repeated bsyrfix / sub=tree(bdgrp) type = ar(1);
lsmeans bdgrp bsyrfix*bdgrp / adjdfe=row slice= bsyrfix;
run;
proc mixed data=fridaynight covtest method =
reml;/*autoregressive*/
class bsyrfix bdgrp tree;
model ewden = bdgrp bsyrfix bdgrp*bsyrfix elevation
lnavgrl86_05
/htype = 3 intercept ddfm=kr s outpred=predewden;
random intercept/sub=tree(bdgrp);
repeated bsyrfix / sub=tree(bdgrp) type = ar(1);
lsmeans bdgrp bsyrfix*bdgrp / adjdfe=row slice= bsyrfix;
run;
proc mixed data=fridaynight covtest method =
reml;/*autoregressive*/
class bsyrfix bdgrp tree;
model lwden = bdgrp bsyrfix bdgrp*bsyrfix pcntgrnchecked
lnavgrl86_05
/htype = 3 intercept ddfm=kr s outpred=predlwden;

repeated bsyrfix / sub=tree(bdgrp) type = ar(1);
lsmeans bdgrp bsyrfix*bdgrp / adjdfe=row slice= bsyrfix;
run;
proc mixed data=fridaynight covtest method =
reml;/*autoregressive*/
class bsyrfix bdgrp tree;
model avgden = bdgrp bsyrfix bdgrp*bsyrfix bhage elevation
/htype = 3 intercept ddfm=kr s outpred=predavgden;
random intercept/sub=tree(bdgrp);
repeated bsyrfix / sub=tree(bdgrp) type = ar(1);
lsmeans bdgrp bsyrfix*bdgrp / adjdfe=row slice= bsyrfix;
run;
proc mixed data=fridaynight covtest method =
reml;/*autoregressive*/
class bsyrfix bdgrp tree;
model lnmtplwnew = bdgrp bsyrfix bdgrp*bsyrfix
pcntgrnchecked lnavgrl86_05
```

```
/htype = 3 intercept ddfm=kr s outpred=predlnmtplwnew;
random intercept/sub=tree(bdgrp);
repeated bsyrfix / sub=tree(bdgrp) type = ar(1);
lsmeans bdgrp bsyrfix*bdgrp / adjdfe=row slice= bsyrfix;
run;
proc mixed data=fridaynight covtest method =
reml;/*autoregressive*/
class bsyrfix bdgrp tree;
model lncorrectedmtplw = bdgrp bsyrfix bdgrp*bsyrfix
pcntgrnchecked lnavgrl86_05
/htype = 3 intercept ddfm=kr s
outpred=predlncorrectedmtplw;
random intercept/sub=tree(bdgrp);
repeated bsyrfix / sub=tree(bdgrp) type = ar(1);
lsmeans bdgrp bsyrfix*bdgrp / adjdfe=row slice= bsyrfix;
run;
proc mixed data=fridaynight covtest method =
reml;/*autoregressive*/
class bsyrfix bdgrp tree;
model lninflwp = bdgrp bsyrfix bdgrp*bsyrfix bhage
lnavgrl86_05
/htype = 3 intercept ddfm=kr s outpred=predlninflwp;
random intercept/sub=tree(bdgrp);
repeated bsyrfix / sub=tree(bdgrp) type = ar(1);
lsmeans bdgrp bsyrfix*bdgrp / adjdfe=row slice= bsyrfix;
run;
proc mixed data=fridaynight covtest method =
reml;/*autoregressive*/
class bsyrfix bdgrp tree;
model correctedlninflwp = bdgrp bsyrfix bdgrp*bsyrfix bhage
lnavgrl86_05
/htype = 3 intercept ddfm=kr s
outpred=predcorrectedlninflwp;
random intercept/sub=tree(bdgrp);
repeated bsyrfix / sub=tree(bdgrp) type = ar(1);
lsmeans bdgrp bsyrfix*bdgrp / adjdfe=row slice= bsyrfix;
run;
```